SYNTHESIS, CHARACTERIZATION AND REACTIVITY OF SOME PERMETHYLTANTALOCENE ALKYLIDENES AND UNUSUALLY STABLE METALLAOXETANES

Thesis by

LeRoy L. Whinnery, Jr.

In Partial Fulfillment of the Requirements

for the degree of

Doctor of Philosophy

California Institute of Technology

Pasadena, California

1991

(Submitted September 20, 1990)

Acknowledgements

Obviously, this is the time when I have to thank all of the people that have played significant roles throughout my graduate career, previous schooling and other aspects of my life. I'll apologize in advance if these acknowledgements get a little on the mushy side. But, this is where you are supposed to tell it like it is. Besides that, it's my acknowledgement and I'll write what I want.

As many before have already discovered, there is no better advisor than John Bercaw. Not only do I have a tremendous amount of respect for his knowledge of chemistry and incredible chemical intuition, I also consider him one of the best friends I have made at Caltech. Thanks, John.

Throughout my nine years of higher education many of the professors I've had along the way played important roles as teachers and friends. Glenn Vogel is responsible for getting me interested in science. I will always be thankful to him for that. Glenn also opened many doors for me, resulting in my working at Cornell and Air Products, my "senior sebatical" at Penn State and my decision to come to Caltech. Thanks for all of the clippings too. Go Nittany Lions!!!

Several other educators from my pre-Caltech days who I learned as much from scientifically as non-scientifically include: Larry Que, Heinz and Judy Koch, John Marsella and Greg Geoffroy.

I have to give a special thanks to Mike Margolin for his true friendship over the years and for not letting me become a complete geek at IC.

Ahhh the Bercaw Group. I'll start by thanking all of the past and present Bercaw group members for all of the science I have learned from them and the memories of dancing on tables and singing "New York, New York" down at the Ath. There are few people I enjoy talking science with as much as Mark "the quiet one" Trimmer. Barb, Van, Ray, Helmut, Ged, Trim and Trudy helped to keep life interesting. Although the group has changed *a lot since I joined*,

sometimes change is good. I must thank Bryan (who I have faith can bring the group back to the gutter where it belongs) for taking over as coach of the HOGS before it drove me nuts. Donnie also deserves special mention for organizing several of the group activities, putting up with my whines about the computers (when it was usually operator error) and for being a good friend. My only words of wisdom for you, Donnie, are to keep your head up when you're hiking.

I was told before I even applied to Caltech that it is a unique place in many aspects. The most significant of which was that Caltech is very interactive and the faculty are very accessible and friendly. I have definitely found this to be the case and have enjoyed the friendship of several professors here (and I'm not just saying that because some of them are on my committee).

I have enjoyed many hiking trips, squals in San Gabriel and long "sessions" down at the Ath with Jim and Dave (and look forward to many more hikes). Dave, I really am sorry about your boots, but it does make for a good story and I know how much you love to tell stories.

Several other non-Bercaw group people that I have enjoyed hiking trips, drinking beers or learing to Lambada with include: Gail Ryba, Reggie Penner, Teri Longin, Bill Tumas, Mike Hampson, the whole Bio crowd and city league softball team, Pat Kearny, Dom McGrath, Bruce Tufts, Amit Kumar and Alison McCurdy.

Finally, I have to thank my parents for encouraging me to think independently, to do everything (no matter how seeming insignificant) to the best of my ability and for supporting me emotionally over the last third of my life while I was doing something they really didn't understand. I'm not sure I always understood why I wanted a Ph.D., but I think I do now. Thanks to all of those mentioned above (and many more who are not) for their support and friendship.

Abstract

Several tantalaoxetanes have been prepared and the X-ray crystal structure of O-*exo*-Cp_2*Ta($OCHPhCH_2$)CH_3 is reported (Cp* = η^5-C_5Me_5). The kinetic products of the reactions of Cp_2*Ta(=CH_2)CH_3 with paraformaldehyde or benzaldehyde are O-*endo*-Cp_2*Ta(CH_2CH_2O)CH_3 and O-*endo*-Cp_2*Ta(CH_2CHPhO)CH_3, respectively. These tantalaoxetanes undergo an acid and base-catalyzed isomerization to O-*exo*-Cp_2*Ta(OCH_2CH_2)CH_3 and O-*exo*-Cp_2*Ta($OCHPhCH_2$)CH_3 followed by thermal decomposition to Cp_2*Ta(=O)CH_3 and the appropriate olefin. Cp_2*Ta(=CH_2)H deoxygenates epoxides to form Cp_2*Ta(=O)CH_3 and olefin. No intermediates are observed in this deoxygenation under conditions where the appropriate tantalaoxetanes are stable and would have been spectroscopically observed. Stereolabeled epoxides were deoxygenated to probe the mechanism for the possible intermediacy of a 1,4-biradical. Retention of stereochemistry of the resulting olefin was observed and is indicative of a concerted mechanism. These results and their implications for the mechanism of olefin epoxidation are discussed.

Treatment of $Cp^*_2TaCl_2$ with a variety of substituted benzyl potassium reagents affords an equilibrium mixture of Cp^*_2Ta(=CHC_6H_5)H, **1**, and Cp^*_2Ta(o-$CH_2C_6H_4$)H, **2**, which interconvert presumably *via* the unstable 16 electron intermediate [Cp^*_2Ta($CH_2C_6H_5$)]. Several derivatives substituted at the phenyl ring have been prepared to explore the effect of both sterics and electronics on the α-hydrogen migration equilibrium. Trapping of the benzyl intermediate by methylenetrialkylphosphoranes results in methylene transfer to give Cp^*_2Ta(=CH_2)$CH_2C_6H_5$. The substituted benzyl derivatives have provided a system to determine the influence of phenyl substituents on migratory aptitude of the benzyl group.

Table of Contents

CHAPTER 1

Metallaoxetanes of Permethyltantalocene: Synthesis, Investigation of Their Decomposition to Olefin and $Cp^*_2Ta(O)CH_3$ and Possible Intermediacy in the Deoxygenation of Epoxides

Abstract: Several tantalaoxetanes have been prepared and the X-ray crystal structure of O-*exo*-Cp_2*Ta($OCHPhCH_2$)CH_3 is reported (Cp^* = η^5-C_5Me_5). The kinetic products of the reactions of Cp_2*Ta(=CH_2)CH_3 with paraformaldehyde or benzaldehyde are O-*endo*-Cp_2*Ta(CH_2CH_2O)CH_3 and O-*endo*-Cp_2*Ta(CH_2CHPhO)CH_3, respectively. These tantalaoxetanes undergo an acid and base-catalyzed isomerization to O-*exo*-Cp_2*Ta(OCH_2CH_2)CH_3 and O-*exo*-Cp_2*Ta($OCHPhCH_2$)CH_3 followed by thermal decomposition to Cp_2*Ta(=O)CH_3 and the appropriate olefin. Cp_2*Ta(=CH_2)H deoxygenates epoxides to form Cp_2*Ta(=O)CH_3 and olefin. No intermediates are observed in this deoxygenation under conditions where the appropriate tantalaoxetanes are stable and would have been spectroscopically observed. Stereolabeled epoxides were deoxygenated to probe the mechanism for the possible intermediacy of a 1,4-biradical. Retention of stereochemistry of the resulting olefin was observed and is indicative of a concerted mechanism. These results and their implications for the mechanism of olefin epoxidation are discussed.

INTRODUCTION

The mechanism of epoxide deoxygenation by an unsaturated metal center (and its microscopic reverse, olefin epoxidation by a metal-oxo complex) has been debated in the literature for quite some time.[1] Although a metallaoxetane has never been observed for the reaction of an epoxide and a metal complex or for the reaction of an olefin and a metal-oxo, metallaoxetanes have been proposed by many investigators as intermediates for these reactions (Eqn 1). Other mechanisms that have been proposed for these reactions involve the intermediacy of a 1,4-biradical, a radical cation and a concerted mechanism.

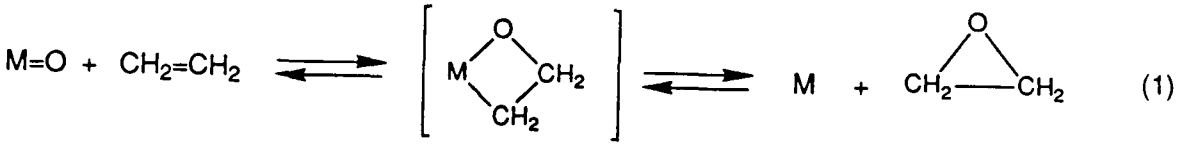

(1)

Sharpless[1a] has proposed metallaoxetanes as possible intermediates in olefin epoxidation by chromyl chloride, epoxide deoxygenation by W(IV) and olefin dihydroxylation with OsO_4; however, investigators in this area have looked for evidence of metallacycle formation without success. Rappé and Goddard[2] have performed theoretical studies on the classic chromyl chloride epoxidation of epoxides and concluded that a metallaoxetane was a likely intermediate. Goddard's results have been seriously questioned. As Nugent and Mayer[3] have pointed out, it is not clear that reasonable comparisons were made in obtaining bond strength and heats of formation. Recently some elegant mechanistic studies by Groves have argued against metallaoxetane formation in cytochrome P450 model systems.[1b-e] Groves and co-workers concluded that the isomerization of chiral epoxides by ruthenium(II) porphyrin complexes proceeds *via* a radical intermediate. Although homolysis of the Ru-C bond of a metallaoxetane intermediate is also consistent with their results, no evidence for a metallacyclic intermediate has been observed. This development has seemed to spur further theoretical

investigation with the general consensus that metallaoxetanes are probably not intermediates in the porphyrin-based systems.[4] In the conclusion of Sharpless' 1977 paper in which he first suggests metallaoxetanes as intermediates in these reactions, he states "...we have as yet no evidence which cannot also be rationalized by direct attack of the olefin on the (oxo) ligands."[1a]

Although there are many examples of metallaoxetanes stabilized with electron withdrawing groups on the oxetane ring (*e.g.*, $L_2Pt(TCNEO)$, $L_2(CO)IrX(TCNEO)$; L=R_3P and R_3As; TCNE = tetracyano ethylene), unstabilized metallaoxetanes are quite rare. Late transition metal examples of isolated unstabilized metallaoxetanes include $(C_8H_{12}O)Ir(P_3O_9)^{2-}$,[5] $Cp^*Ir(PMe_3)(OC(CH_3)_2CH_2)$[6] and $(Me_3P)_4Ru(CH_2CCH_3C_6H_5O)$.[7] The low temperature glass matrix FTIR spectrum of the reaction of gas phase iron atoms and ethyleneoxide showed two small peaks (with respect to the rest of the spectrum) which Margrave and co-workers[8] assigned as the metallaoxetane. Examples of metallaoxetanes with early transition metals are $Cp_2Ti(CPh_2C{=}CH_2O)$[9] and the structurally characterized $M[CH(C(CH_3)_3)CHC_6F_5O](N\text{-}2,6\text{-}C(CH_3)_3C_6H_3)(OC(CH_3)_3)_2$ (M = Mo and W).[10] Both of these examples may be considered to be "partially stabilized," since relatively high energy allene would be the product olefin from cleavage of the oxatitanacyclobutane to $(Cp_2TiO)_n$. The metallaoxetanes of molybdenum and tungsten are stabilized by electron withdrawing pentafluorophenyl groups.

We have previously shown the permethyltantalocene fragment to be very versatile and capable of stabilizing a variety of intermediates.[11] This system has allowed us to observe equilibria, to separate out ground state and transition state effects[12] and in general is very well suited to mechanistic investigation.[13] In this chapter we report the synthesis, characterization and decomposition kinetics of several unstabilized tantalaoxetanes and the X-ray crystal structure of O-*exo*-$Cp^*_2Ta(CH_2CHC_6H_5O)CH_3$, as well as a proposed mechanism of epoxide deoxygenation by 16-electron permethyltantalocene alkyls.

RESULTS AND DISCUSSION

Synthesis and Characterization of Tantalaoxetanes. Several synthetic strategies were employed in our efforts to isolate a metallaoxetane. We felt the most successful route to a metallaoxetane in our system would be through methylene transfer (Wittig-type chemistry).[9,14] We have previously reported the synthesis of $Cp^*_2Ta(=CH_2)H$[11] which seemed an obvious first choice to attempt the methylene-transfer chemistry. Although we had also shown that this alkylidene hydride species undergoes a fast and reversible α-migratory insertion/elimination at room temperature, we expected the aldehyde to react in a 2+2 fashion with the alkylidene rather than trap the 16-electron alkyl species. However, when paraformaldehyde or benzaldehyde react with $Cp^*_2Ta(=CH_2)H$ only the aldehyde adducts, $Cp^*_2Ta(CH_2O)CH_3$ and $Cp^*_2Ta(C_6H_5CHO)CH_3$, are observed (Scheme I). The exact regioisomer assignment (O-*exo* or O-*endo*) has not been made at this time.

Scheme I

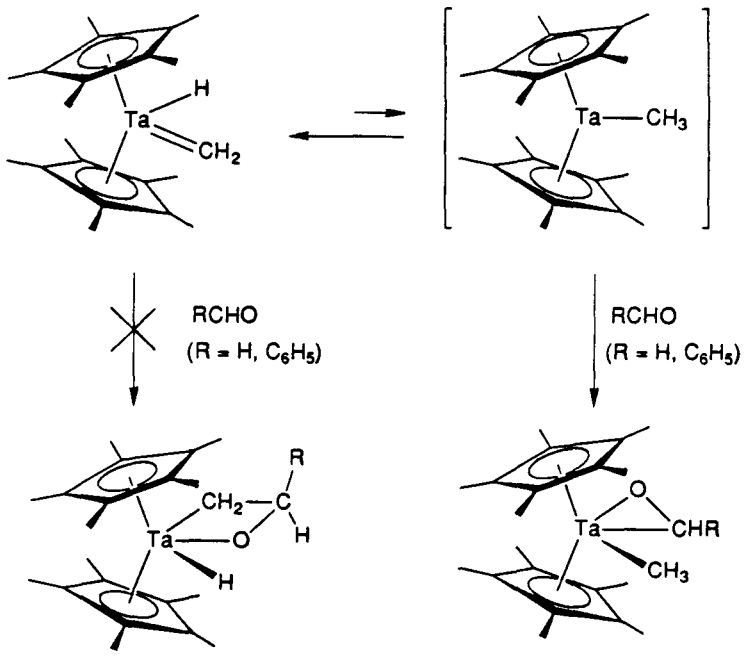

An alkylidene complex which has a slower (and irreversible) α-migratory insertion pathway available is $Cp^*_2Ta(=CH_2)CH_3$. The reaction of paraformaldehyde and substituted benzaldehydes with $Cp^*_2Ta(=CH_2)CH_3$ does indeed yield O-*endo*-$Cp^*_2Ta(CH_2CH_2O)CH_3$ and O-*endo*-$Cp^*_2Ta(CH_2CH(C_6H_4$-*p*-X)O)CH_3, (where X = H, CH_3, Cl, CF_3, CN, NO_2), respectively, as shown in Scheme II. The O-*endo* isomer has the oxygen atom in the center of the wedge and the O-*exo* isomer has the oxygen atom in the outer portion of the wedge. We subsequently established that the O-*endo* isomers rearrange to the O-*exo* isomers, which upon heating (>80 °C) decompose to $Cp^*_2Ta(=O)CH_3$ and the olefin (Scheme II).

Scheme II

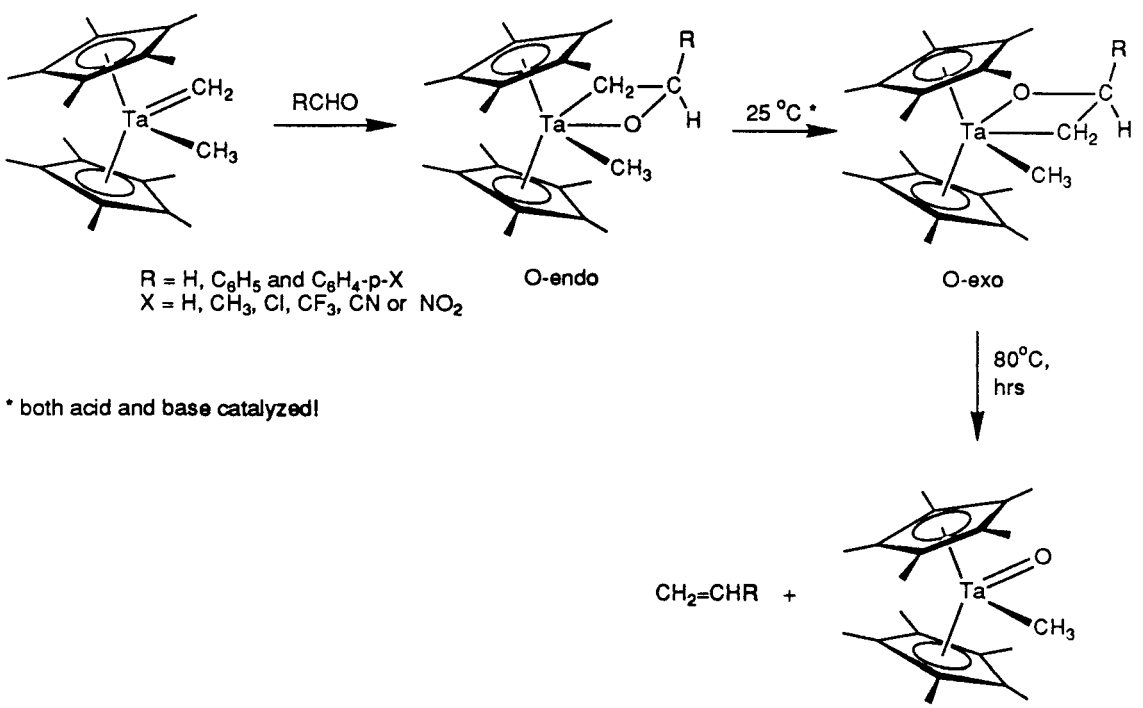

The O-*endo* and O-*exo* tantalaoxetanes have been characterized by ^{1}H-NMR, ^{13}C-NMR (Table 5) and elemental analysis. The Thermodynamically most stable metallaoxetane, the O-*exo*-3-phenyltantalaoxetane, has been characterized by X-ray crystallography. The ORTEP

drawing is shown in Figure 1, and selected distances and angles are listed in Table 1. This crystal was obtained from a cooled acetone solution of the second, thermodynamic isomer of the 3-phenyltantalaoxetane. The crystal structure resulted in the assignment of O-*endo* as the kinetic isomer and O-*exo* as the thermodynamic isomer.

As shown in Figure 2, the tantalaoxetane ring is slightly puckered. All four atoms of the ring are within ±0.16Å of being coplanar. The sum of the internal angles of the tantalaoxetane is 353.3°. Titanium and molybdenum metallaoxetanes have both been shown to be puckered by ^{1}H NMR and X-ray crystallography, respectively. The puckering of the oxatitanacyclobutane ring was attributed to the lone pair on the oxygen donating to the otherwise 16-electron titanium.[9] Whereas the oxamolybdenacyclobutane[10] ring might be puckered to increase lone pair donation to the metal, this is not necessary for the metal to achieve an 18-electron configuration. Further support for the non-donation of the oxygen lone pairs is the comparison to other structurally characterized group 6 metallacyclobutanes (which are also puckered) as well as the Mo-O bond length consistent with a Mo-O single bond without lonepair donation. In comparison, the tantalaoxetanes reported here are 18-electron complexes without lone pair donation. The Ta-O single bond distance is 2.057(9)Å. We suggest the tantalaoxetane ring is slightly puckered as a result of steric interactions between the Cp* methyl groups and the phenyl ring. Also in support of this theory is the observation that we have not been able to freeze out a puckered conformation for the unsubstituted O-*endo*-$Cp^*_2Ta(OCH_2CH_2)CH_3$ or O-*exo*-$Cp^*_2Ta(CH_2CH_2O)CH_3$ on the ^{1}H NMR timescale.

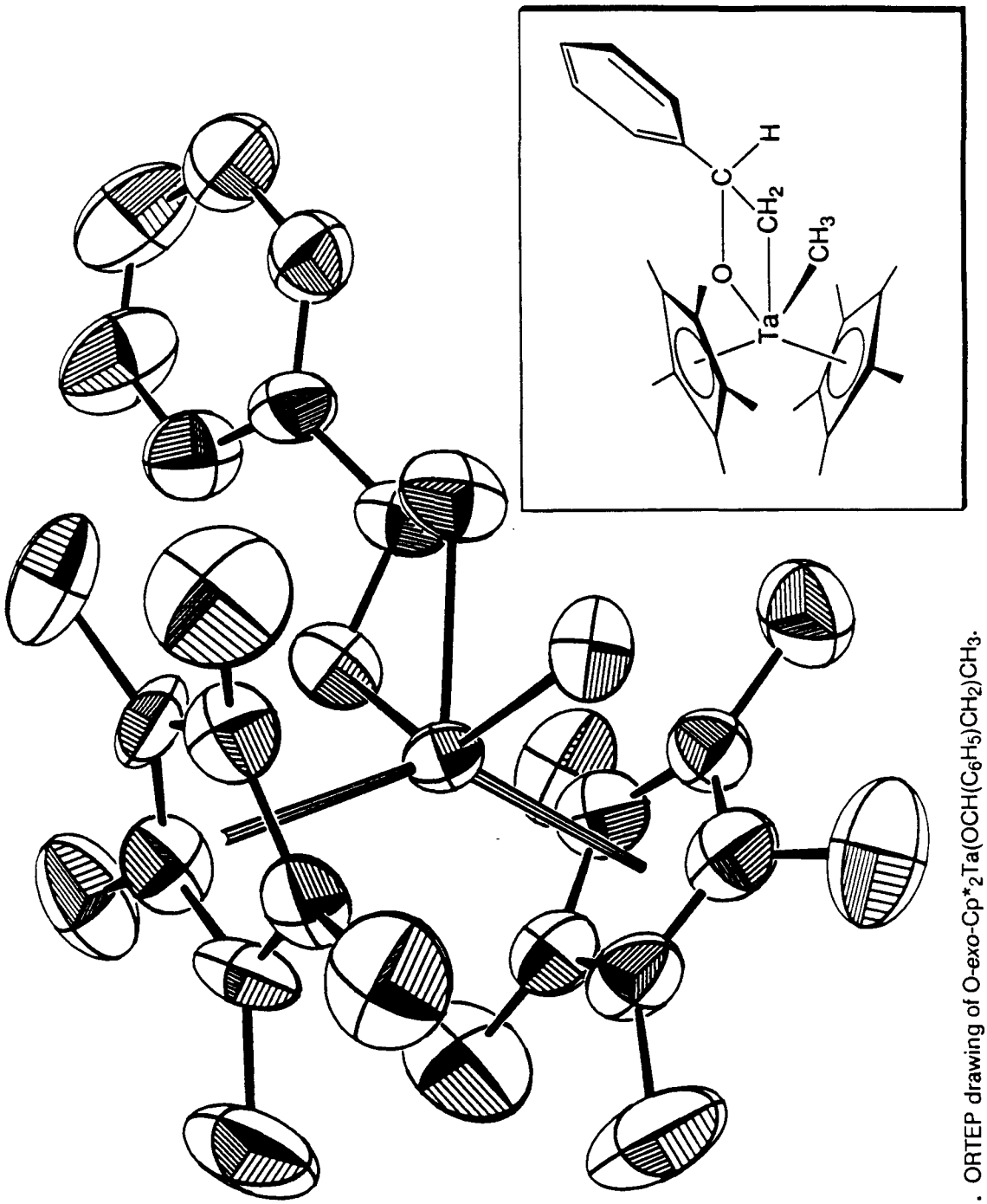

Figure 1. ORTEP drawing of O-exo-$Cp^*_2Ta(OCH(C_6H_5)CH_2)CH_3$.

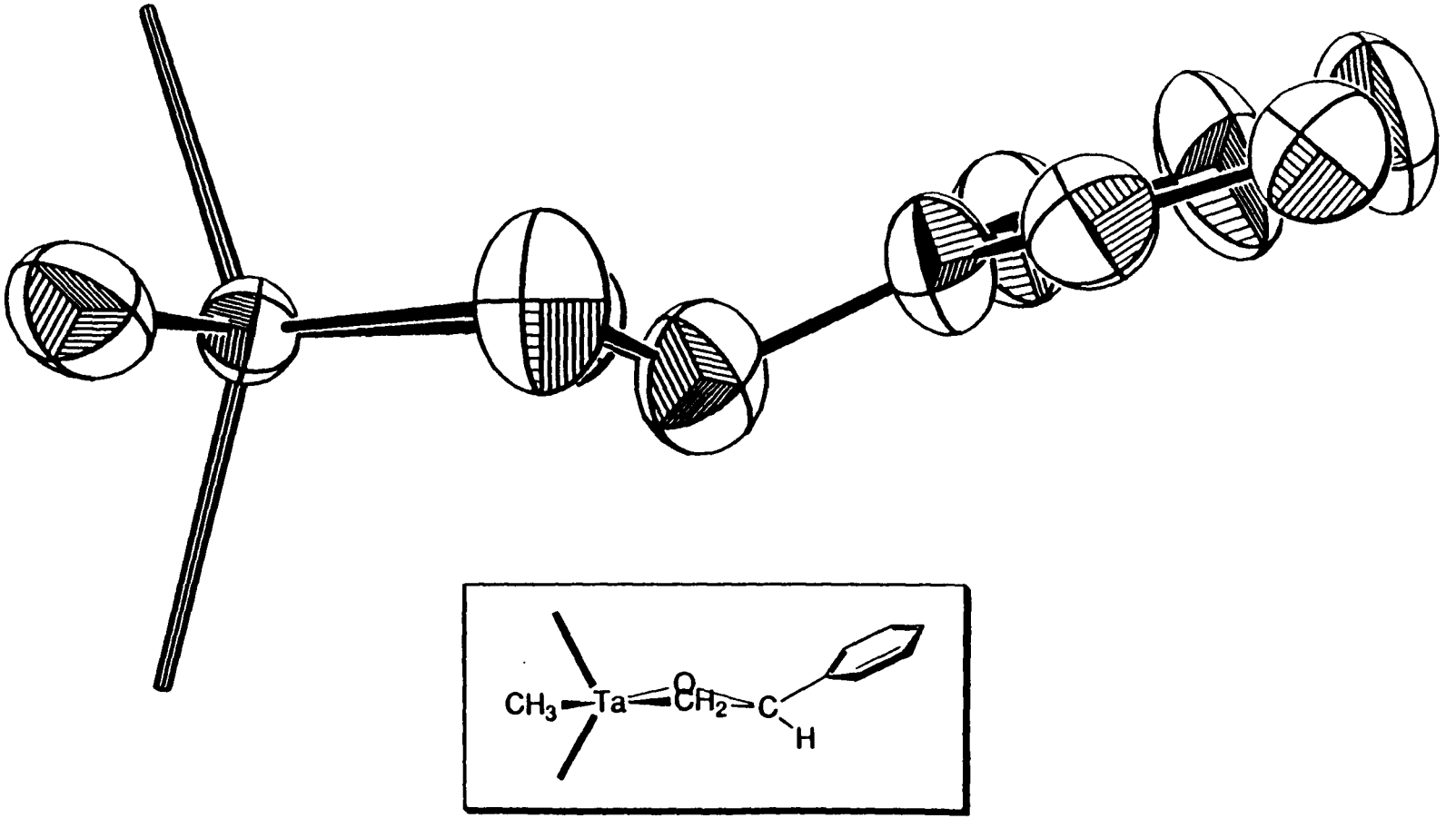

Figure 2. ORTEP drawing showing slight puckering of the tantalaoxetane ring of O-*exo*-$Cp^*_2Ta(OCH(C_6H_5)CH_2)CH_3$.

Table 1. Selected distances and angles from the X-ray crystal structure of O-*exo*-$Cp^*_2Ta(OCH(C_6H_5)CH_2)CH_3$.

	Distance(Å)		Angle(°)
Ta –C1	2.271(12)	Ta –C2 –C3	91.1(9)
Ta –C2	2.236(14)	C2 –C3 –O	99.2(11)
Ta –O	2.053(8)	C3 –O –Ta	100.9(7)
Ta –CpA	2.198	O –Ta –C2	62.8(4)
Ta –CpB	2.220	CpA –Ta –CpB	135.8
O –C3	1.436(17)	CpA –Ta –C1	99.2
C2 –C3	1.506(20)	CpA –Ta –C2	113.0
		CpA –Ta –O	98.0
		CpB –Ta –C1	96.4
		CpB –Ta –C2	111.2
		CpB –Ta –O	100.1
		C1 –Ta –C2	71.4(5)
		O –Ta –C1	134.2(4)

Acetaldehyde also reacts with $Cp^*_2Ta(=CH_2)CH_3$ to yield a metallaoxetane, although the reaction is not as clean as paraformaldehyde or benzaldehyde reactions. The reaction of ketones with [Cp^*_2Ta-R] is not clean and many products are observed.

We have also previously reported that alcohols react with $Cp^*_2Ta(=CH_2)H$ to afford 16-electron alkoxides (with loss of methane), which subsequently undergo a reversible β-hydrogen elimination/insertion to form stable aldehyde hydride species.[11b] Alcohols that have γ-hydrogens available as well as β-hydrogens react with $Cp^*_2Ta(=CH_2)H$ to give only the β-hydrogen elimination product, assuming other steric factors do not preclude aldehyde adduct formation. Treatment of $Cp^*_2Ta(=CH_2)H$ with phenethyl alcohol results in a fairly clean reaction (^1H NMR) to yield the phenethylaldehyde hydride complex (Scheme III). The reaction shown in Scheme IV reveals the role sterics play in this system. A slight excess of *sec*-phenethyl alcohol reacts with $Cp^*_2Ta(=CH_2)H$ to give the oxatantalabenzocyclopentene hydride complex shown in Equation 3. The β-hydride elimination product would have both the methyl and phenyl groups directed at the Cp* ligands. The oxametallacyclobutane (from γ-hydride elimination) and the oxametallabenzocyclopentene each have only one (non-hydrogen) group directed at the Cp*'s. There are several possible reasons why the *ortho*-metallated tautomer is observed. Five-membered rings are less strained than 3- or 4-membered rings. The observed product is further stabilized by the placement of the least sterically demanding substituent at the β-carbon, *i.e.*, the methyl group, directed at a Cp* ring, and by the formation of a strong Ta-phenyl bond.

Scheme III

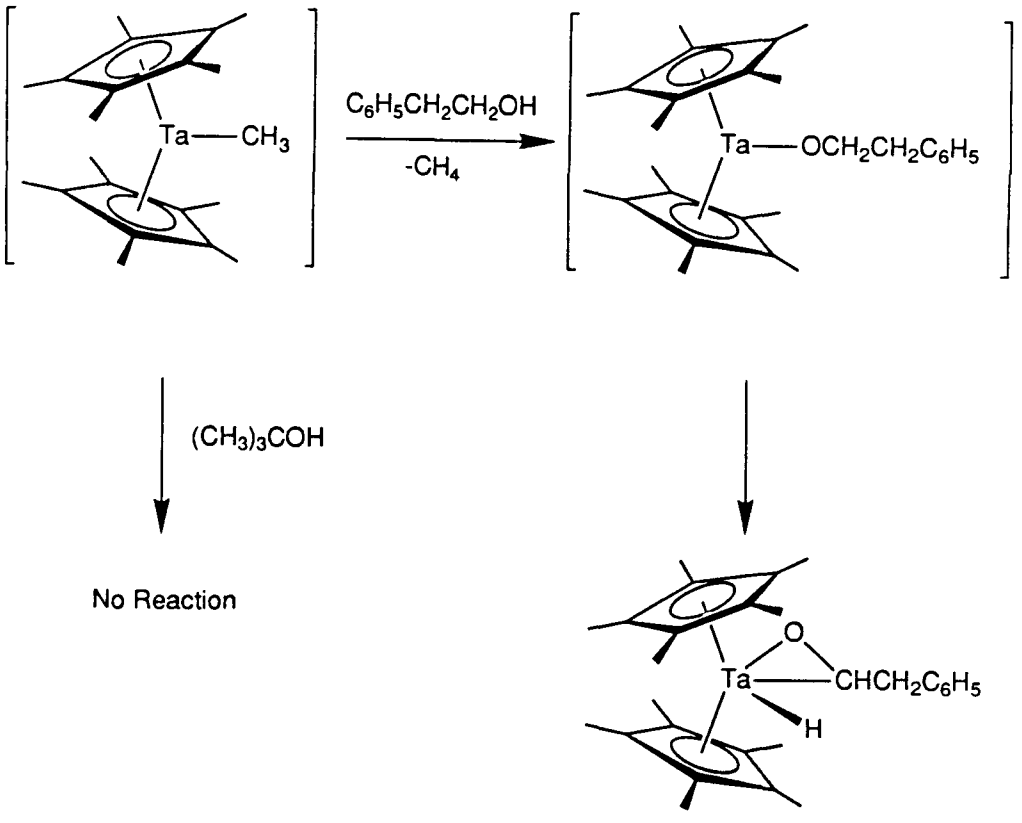
Ta—CH3
C6H5CH2CH2OH
-CH4
Ta—OCH2CH2C6H5
(CH3)3COH
No Reaction
O
Ta—CHCH2C6H5
H

Scheme IV

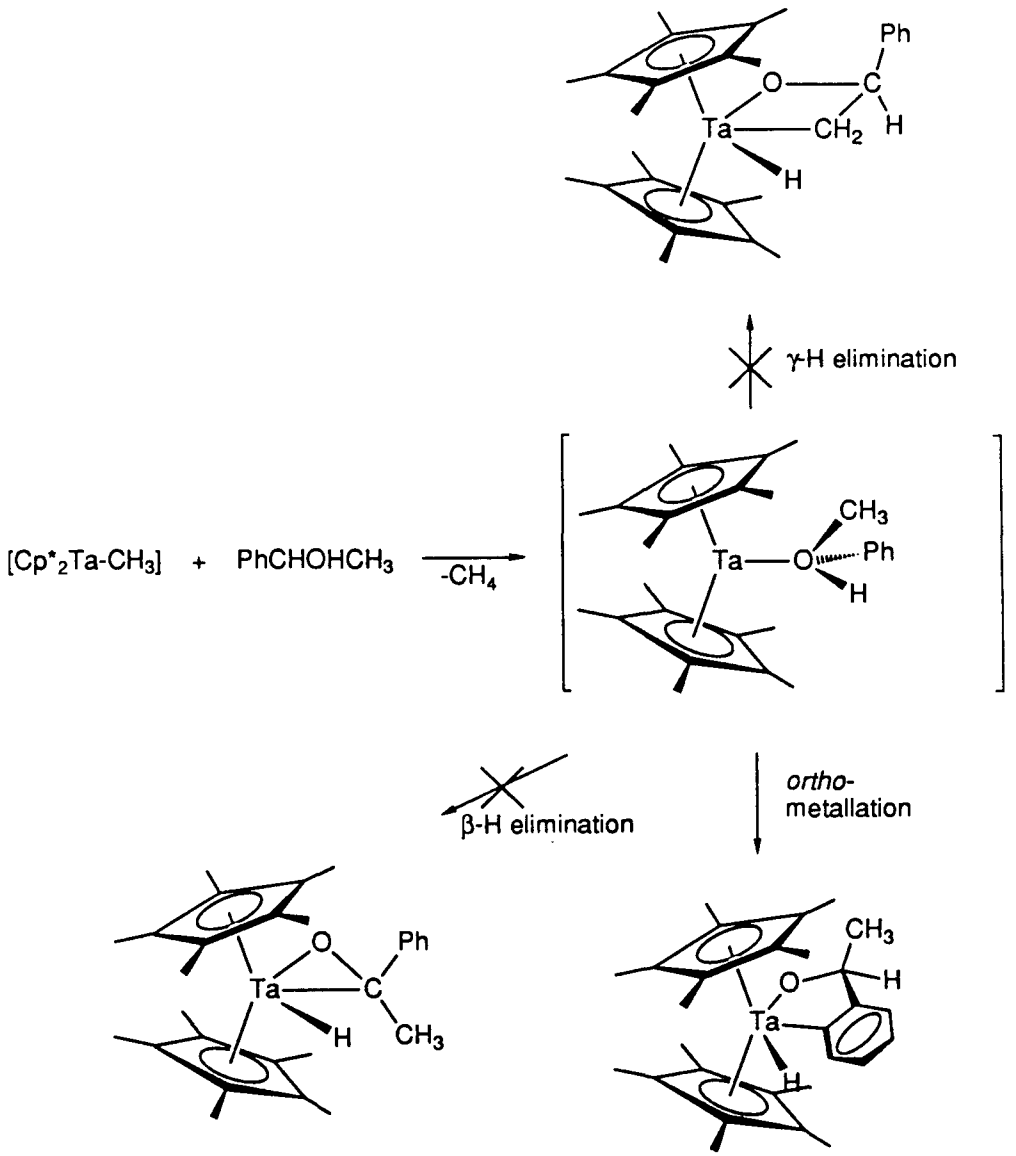

When the β-hydrogen positions are completely blocked with methyl groups (*i.e.*, *tert*-butyl alcohol) no reaction was observed with $Cp^*_2Ta(=CH_2)H$, presumably due to sterics or the pK value of 19 for $(CH_3)_3COH$.

O-*endo* to O-*exo* Isomerization of Tantalaoxetanes. The mechanism associated with the isomerization of the tantalaoxetane from O-*endo* to O-*exo*, shown in Scheme II, was

investigated. The O-*endo* to O-*exo* isomerization spontaneously proceeds in the opposite direction of that observed for early transition metal acyls, where the O-*exo* isomer is the kinetic product and the O-*endo* isomer is the thermodynamic product.[15] Acid and base catalysis of the O-*endo* to O-*exo* isomerization prevented us from obtaining an accurate $\Delta S^{\ddagger}$ for the isomerization which may have been very helpful in determining the mechanism. From the slowest observed rate of isomerization we can put a lower limit on $\Delta G^{\ddagger}_{25\,^{\circ}C}$ of 23 kcal · mol^{-1}.

Dissociation and recoordination of the aldehyde to the outer portion of the wedge could lead to the second isomer. This hypothesis was easily tested by addition of a labeled aldehyde to the first isomer of the tantalaoxetane. No incorporation of the substituted aldehyde was observed in the first isomer, second isomer or the styrene produced when paramethylbenzaldehyde or paracyanobenzaldehyde were reacted with O-*endo*-Cp*$_2$Ta(CH$_2$CHC$_6$H$_5$O)CH$_3$, indicating that once the C-C bond forms it remains intact upon isomerization (Scheme V). We have also shown, by independent synthesis, that if formed the substituted phenyl metallaoxetanes would be stable under the reaction conditions. We have not pursued the detailed mechanism of this isomerization further.

Scheme V

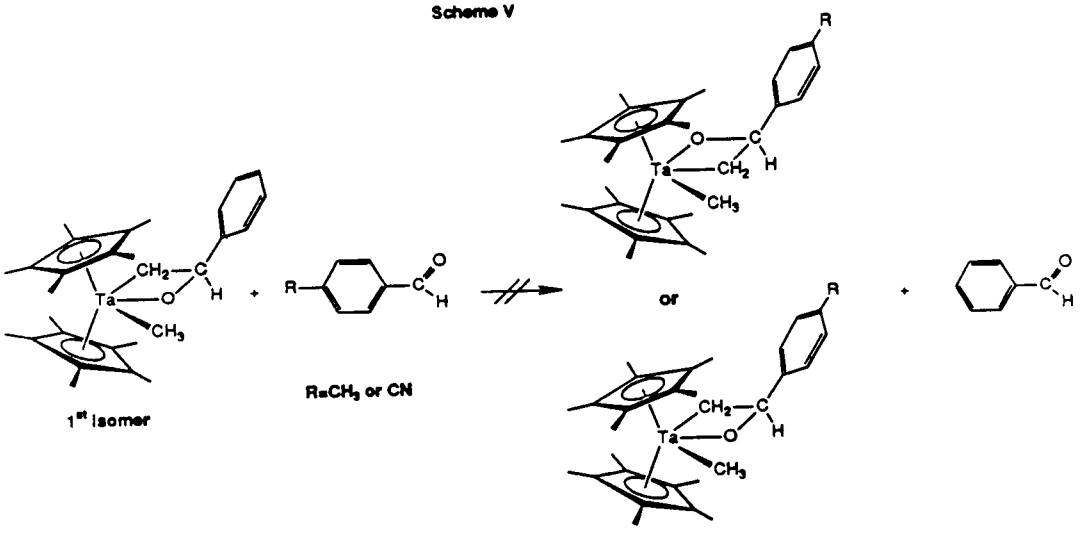

The theory of microscopic reversibility implies that if the O-*endo* tantalaoxetane were to undergo a retro 2+2, it would go back to starting materials, but instead it isomerizes to the O-*exo* tantalaoxetane (Scheme VI). This O-*exo* tantalaoxetane then does a retro 2+2 elimination to products from the center of the wedge, which is the reverse of the way the O-*endo* isomer was formed.

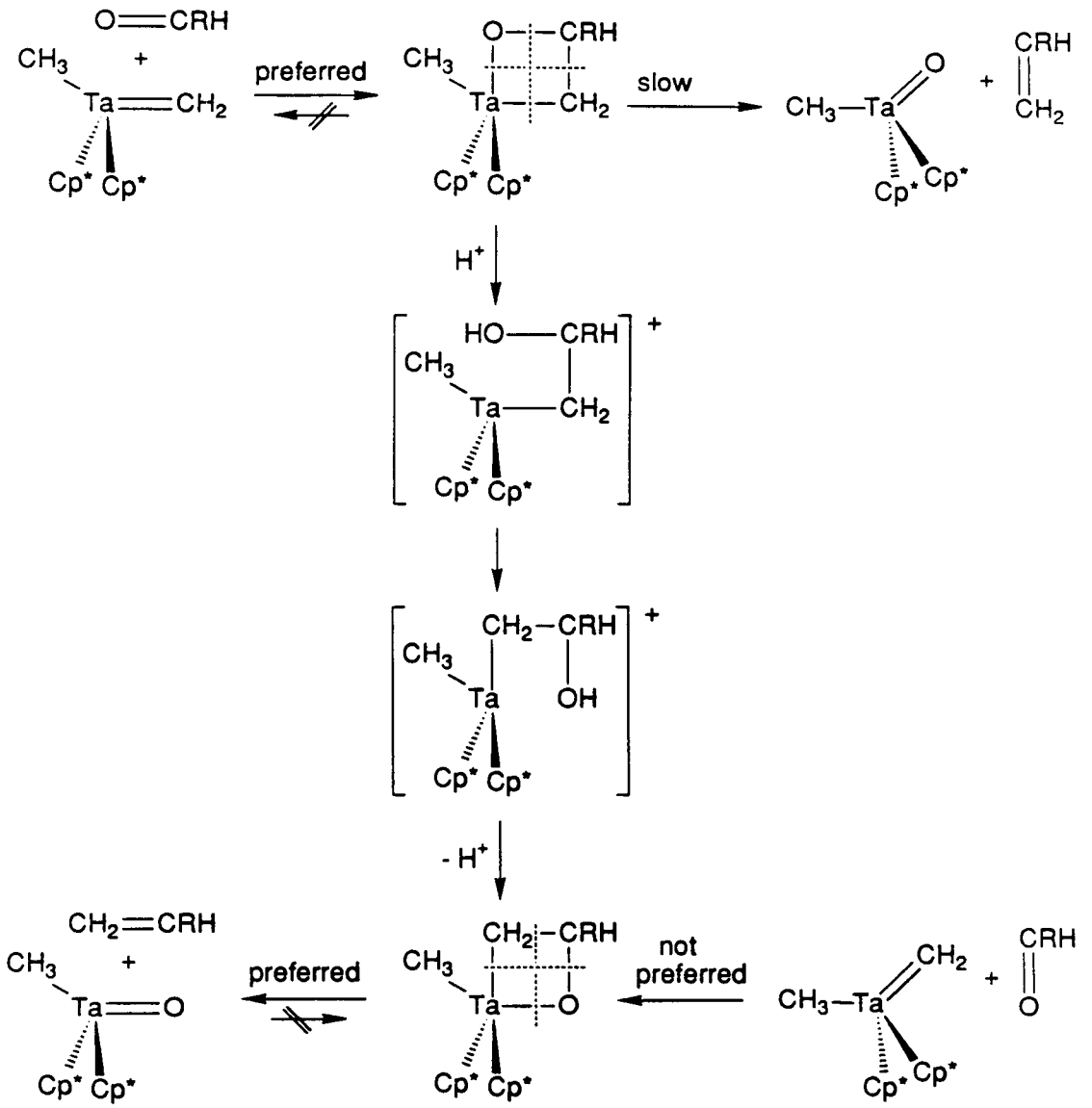

Decomposition of Tantalaoxetanes. The decomposition of the O-*exo*-tantalaoxetane to $Cp^*_2Ta(=O)CH_3$ and olefin was probed by examining its sensitivity to added acids and bases, kinetics at various temperatures, solvent polarity, and the effect of varying the electronics of the oxetane substituent at the three position.

Before looking at the kinetics of this decomposition, the extent to which the reaction is acid and base catalyzed had to be established. If the reaction proved to be both acid and base catalyzed, the observed rate would be a lower limit because acidic or basic impurities present in solution or on the walls of the nmr tube used to measure the kinetics would contribute to the observed rate.

Rate constants at 79°C for the decomposition of the O-*exo*-tantalaoxetane were obtained with as much as one equivalent of various acids and bases added to the benzene-d_6 solution (Table 2). No trend in rates was apparent. A factor of only three was observed between the fastest and slowest rates at 79°C. We consider this factor of three to be a fairly modest effect. Any study that relies on kinetics to determine the result of changes made to the system will have to have a rate that lies outside the rates obtained for the reactions with acids and bases added.

Table 2. Kinetics for the decomposition of O-*exo*-$Cp^*_2Ta(CH_2CHC_6H_5O)CH_3$ at 79°C with acids and bases added.

Acids and Bases Added	Ratex10^5(sec^{-1})
Acid washed NMR tube	1.85(5)
Base washed NMR tube	2.16(5)
1,8-bis(dimethylamino)naphthalene (Proton Sponge)	2.93(5)
1,8-Diazabicyclo[5.4.0]undec-7-ene (DBU)	3.14(5)
Nothing added-1	3.33(5)
Nothing added-2	3.50(5)
10% MeOH	3.51(5)
10% 2,6-Lutidine	5.52(5)
10% $C_6H_5CO_2H$	5.72(5)
Ph_3PCH_2	6.21(5)

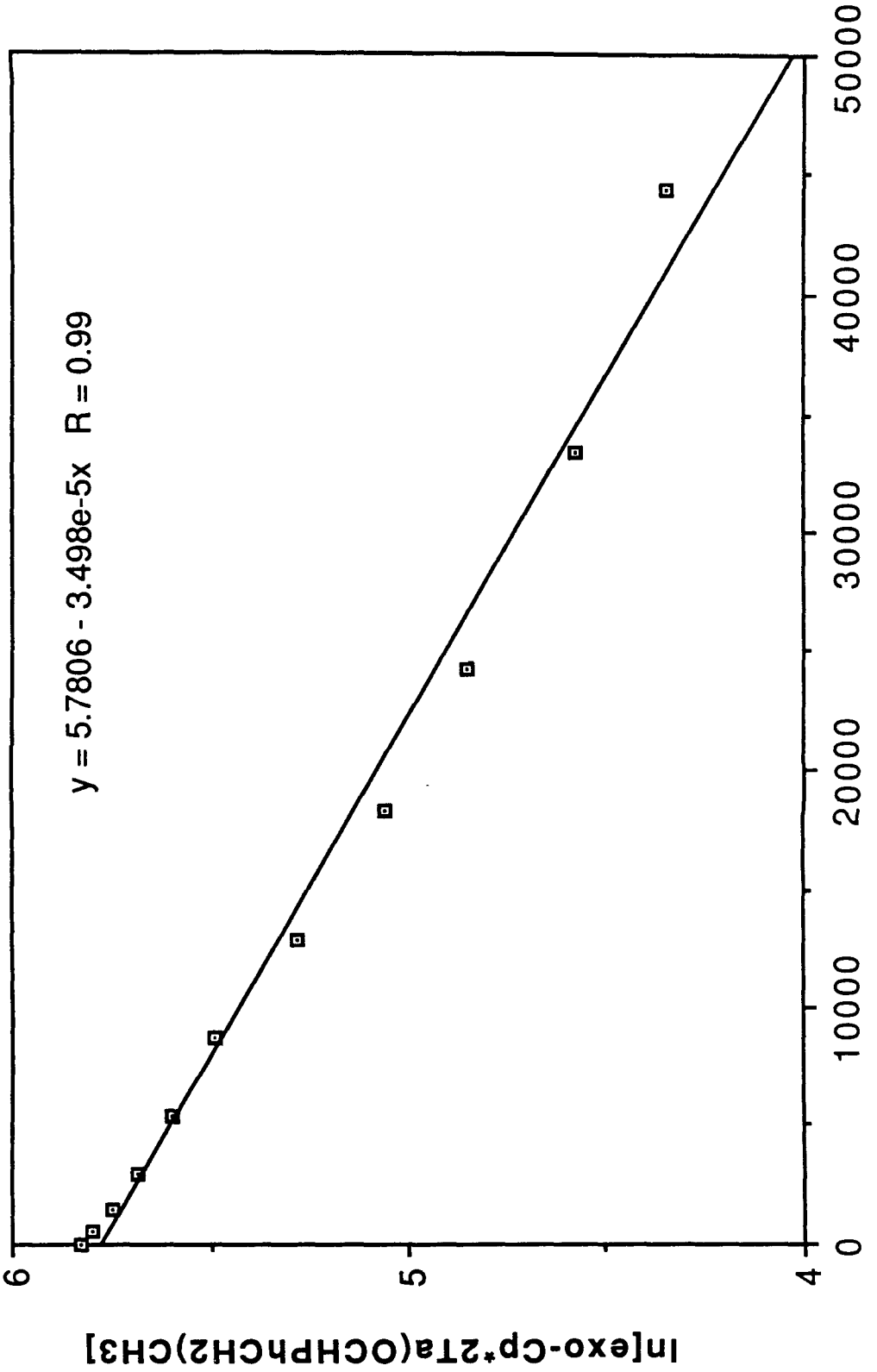

Figure 3. First order decomposition kinetics of O-exo-Cp*2Ta(OCHPhCH2)CH3 at 79°C.

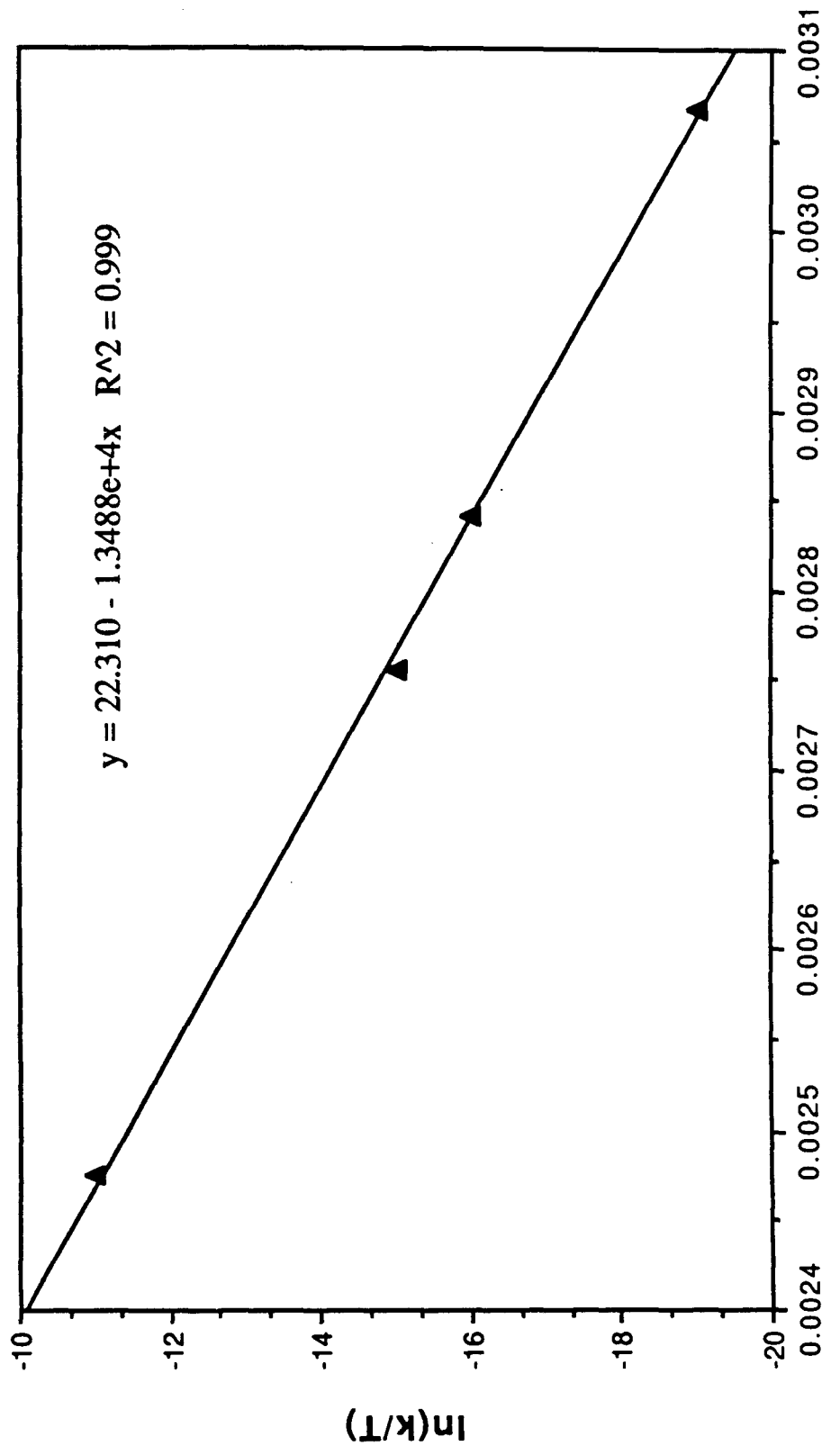

Figure 4. Eyring plot for decomposition of O-exo-Cp*2Ta(OCHPhCH2)CH3.

The decomposition of O-*exo*-$Cp^*_2Ta(CH_2CHC_6H_5O)CH_3$ exhibits well behaved first order kinetics (Figure 3). Rate constants were obtained for this decomposition over a fairly wide temperature range (53-131 °C) and an Eyring plot (Figure 4) resulted in $\Delta H^{\ddagger}$ = 27.8 kcal · mol^{-1}, $\Delta S^{\ddagger}$ = 0 e.u. and $\Delta G^{\ddagger}_{25\,^{\circ}C}$ = 28 kcal · mol^{-1}. The $\Delta S^{\ddagger}$ of 0 e.u. is consistent with bonding in the transition state that is not very different than it is in the reactant which might be expected for a four membered ring that is already strained.[16] The small value for the entropy is in accord with that for cleavage of $Cp_2Ti(CH_2CH(CMe_3)CH_2)$ ($\Delta S^{\ddagger}$ = 9 e.u.),[17] *trans*-$Mo[CH(CMe_3)CH(C_6F_5)O](NAr)(OCMe_3)_2$ ($\Delta S^{\ddagger}$ = -16 e.u.)[10] and *trans*-$W[CH(CMe_3)CH(C_6F_5)O](NAr)(OCMe_3)_2$ ($\Delta S^{\ddagger}$ = -7 e.u.).[10]

The combination of these thermodynamic and kinetic parameters has resulted in the energy surface mapped out in Figure 5. There are no observable equilibria along this reaction coordinate indicating each of the energy wells shown are at least 3 kcal · mol^{-1} lower in energy than the previous well.

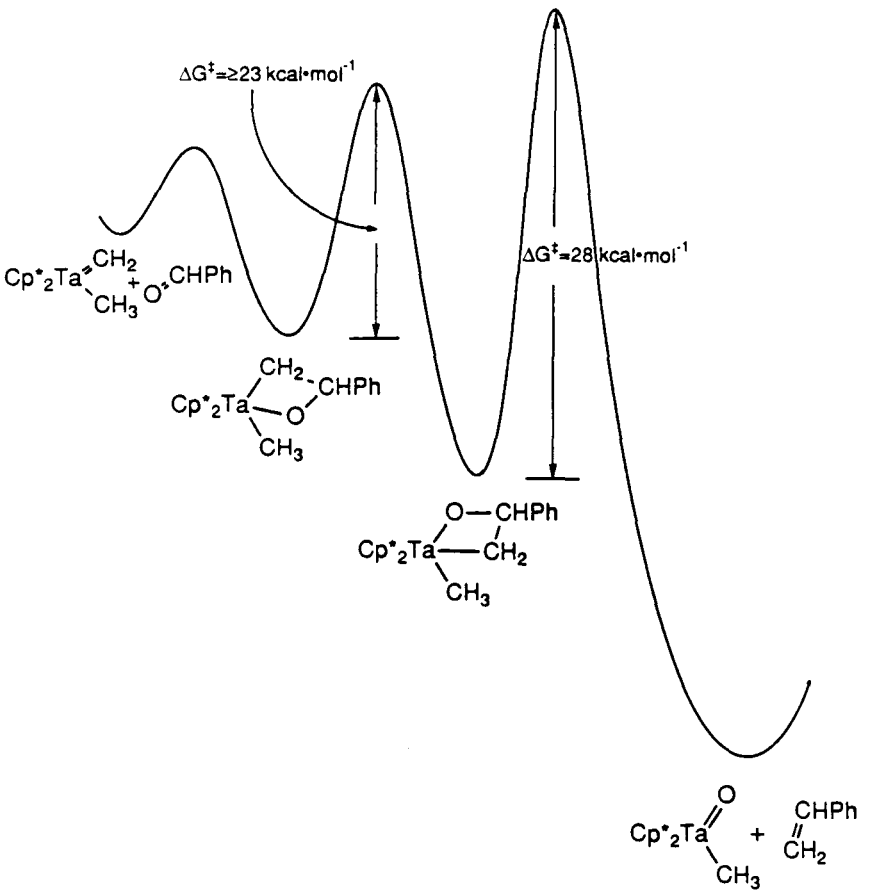

Figure 5. Tantalaoxetane Energy Surface

The effect of solvent polarity has been investigated to determine if there is any charge development in the transition state. The solvents chosen for this study include acetone-d_6, acetonitrile-d_3, benzene-d_6, dioxane-d_8, methylene chloride-d_2, and chloroform-d_1. The respective rates are shown in Table 3. The same products ($Cp^*_2Ta(=O)CH_3$ and styrene) are observed in all of these solvents. The rates of decomposition of O-*exo*-$Cp^*_2Ta(CH_2CHC_6H_5O)CH_3$ at 79°C in the first four solvents listed (acetone-d_6, acetonitrile-d_3, benzene-d_6, and dioxane-d_8) are essentially the same despite rather disparate solvent dielectric constants (ϵ = 20.7, 36.2, 2.28 and 2.21). The rates for the decomposition in

methylene chloride-d_2 and chloroform-d_1 are roughly 13 and 100 times, respectively, faster than in the non-chlorinated solvents. As shown in Table 3, the addition of nitrosobenzene (radical trap) slows the rate of decomposition in chloroform-d_1 by a factor of thirty, indicating that an unknown radical chain mechanism is likely responsible for the observed rate acceleration in chlorinated solvents. We conclude from lack of a substantial effect on the rate of decomposition in solvents of different polarity that there is little if any charge buildup in the transition state for loss of olefin.

Table 3. Decomposition of O-*exo*-$Cp^*_2Ta(CH_2CHC_6H_5O)CH_3$ at 79°C in various solvents.

Solvent	Ratex10^5(sec^{-1})
Acetone-d_6	2.91
Acetonitrile-d_3	3.07
Benzene-d_6	3.50
Dioxane-d_8	3.67
Chloroform-d_1 + Nitrosobenzene	9.91
Methylene Chloride-d_2	42.4
Chloroform-d_1	291

The effect of varying the electronics at the three position of the 3-phenyltantalaoxetane ring (by changing substituents in the para position of the phenyl ring) on the rate of decomposition has been examined. The rate constants for decomposition of O-*exo*-$Cp^*_2Ta(CH_2CH(C_6H_4$-*p*-X)O)CH_3 (X = H, Cl, CF_3, CN, and NO_2) at 79°C to $Cp^*_2Ta(=O)CH_3$ and $CH_2=CHC_6H_4$-*p*-X are listed in Table 4. A Hammett plot (Figure 6) of this data shows that electron-withdrawing substituents on the phenyl ring (slightly) accelerate the rate of olefin elimination. This effect is very small, however, and does not correlate well with σ or σ^+.

Table 4. Rate constants and sigma values for substituted 3-phenyltantalaoxetane decomposition at 79°C (see Figure 6).

Substituent	σ	Ratex10^5(sec^{-1})
H	0.00	3.33
H	0.00	3.51
p-Cl	0.23	4.19
p-CF_3	0.54	1.55
p-CN	0.63	0.66
p-NO_2	0.78	1.18

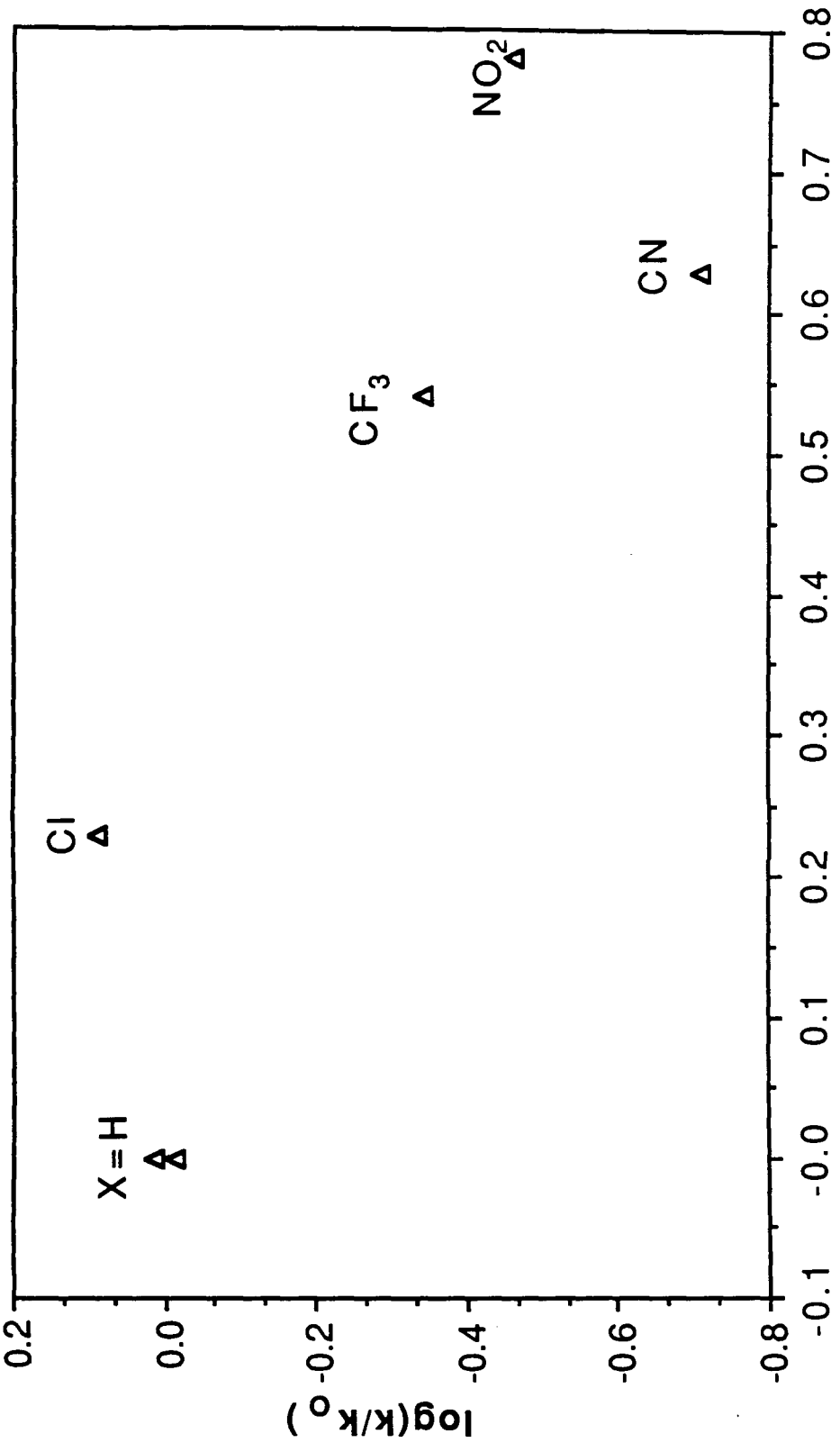

Figure 6. Substituent effects on decomposition rate of phenyl tantalaoxetanes at 79C.

Mechanism of the Deoxygenation of Epoxides. The decomposition of the tantalaoxetanes to $Cp^*_2Ta(=O)CH_3$ and olefin indicated we would not have much success in preparing a metallaoxetane by the reaction of a Ta=O complex and an olefin. Moreover, the preferential pathway leading to olefin and tantalum-oxo rather than reductive elimination of epoxide and $[Cp^*_2TaCH_3]$, does not offer the possibility of olefin epoxidation with these tantalum-oxo derivatives. However, the microscopic reverse reaction, epoxide deoxygenation by the unsaturated tantalum center, $[Cp^*_2TaCH_3]$, did appear likely to occur.

Indeed, the reaction of epoxides with $Cp^*_2Ta(=CH_2)H$ (which is in fast and reversible equilibrium with $[Cp^*_2TaCH_3]$) very cleanly produces $Cp^*_2Ta(=O)CH_3$ and olefin, as shown in Equation 2. Since we have shown that tantalaoxetanes with Cp* and CH_3 coligands are moderately stable, we expected to observe them in the deoxygenation of epoxides, if these mediated epoxide deoxygenation. No intermediates were observed when the reaction of ethylene oxide with $Cp^*_2Ta(=CH_2)H$ was monitored by ^{1}H-NMR at room temperature in benzene-d_6 or at -50 °C in THF-d_8.

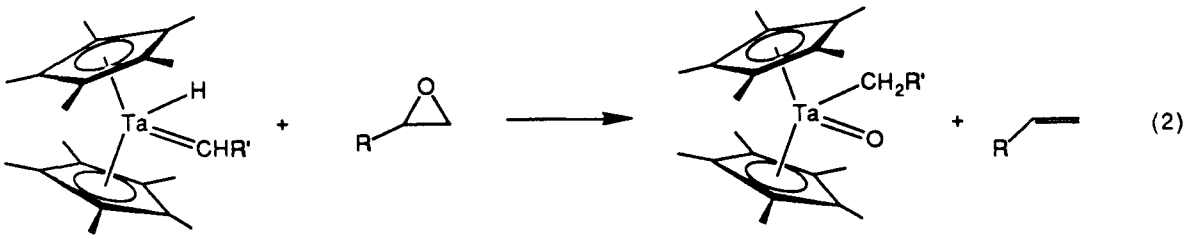

(2)

The appropriate control reaction was performed to ensure that the metallaoxetane would have been stable under the reaction conditions for this deoxygenation. Monosubstituted epoxides, such as styreneoxide, have four possible isomers (Figure 7) depending on which C-O

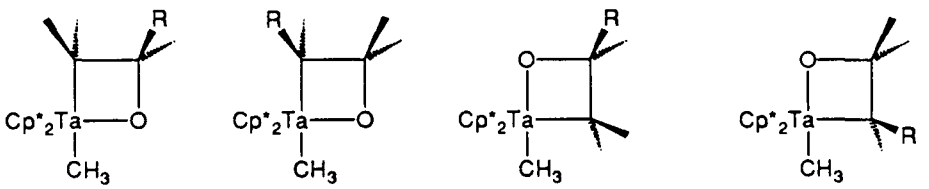

Figure 7. Four possible isomers of mono-substituted metallaoxetanes.

bond is broken. The synthetic route we employed to make the tantalaoxetanes produces only two of the phenyl substituted isomers (O-*exo*-3-phenyl and O-*endo*-3-phenyl). Since the parent tantalaoxetane which only has two possible isomers (*endo* and *exo*), thee control was carried out with 15 equivalents of ethylene oxide and O-*endo*-$Cp^*_2Ta(CH_2CH_2O)CH_3$. Isomerization and decomposition were monitored by ^{1}H-NMR, and the kinetics for isomerization and decomposition at 79 °C were found to be the same, within experimental error, as in the absence of excess ethylene oxide. Thus, ethylene oxide does not promote rapid decomposition of tantalaoxetane, ruling out its intermediacy in the deoxygenation of ethylene oxide by $[Cp^*_2TaCH_3]$.

Having established that deoxygenation of epoxides by permethyltantalocene alkyls clearly does not involve a metallaoxetane, the next obvious question is: What is the mechanism of epoxide deoxygenation? We chose to examine the stereochemistry associated with this reaction to determine if a significantly long-lived 1,4-biradical intermediate is involved.

Two research groups have independently investigated the deoxygenation of epoxides by "titanocene." Schobert[18] used chemically generated "titanocene" (from the reaction of titanocene dichloride and magnesium metal at room temperature in THF solvent) while Wheeler

and Grubbs[19] used a photochemically generated "titanocene" (from photolysis of $Cp_2Ti(CH_2CH(CMe_3)CH_2)$. Some significant differences were observed in these two studies. Schobert observed complete retention of stereochemistry in the deoxygenation of *trans*-epoxides and high retention of stereochemistry for *cis*- epoxides. Wheeler and Grubbs observed 1:1 mixtures of *cis*- and *trans*- olefins upon deoxygenation of *cis*- or *trans*- epoxides. This scrambling of stereochemistry was taken as evidence for a 1,4-biradical intermediate in the deoxygenation of epoxides. As pointed out by Wheeler there are several possible explanations for this observed difference in reactivity. (1) The Mg^0, $MgCl_2$ or MgO may not play an innocent role in the chemically generated case. (2) Schobert only reports the deoxygenation of alkyl and aryl disubstituted epoxides which could have considerable steric interactions.

Initially *trans*-d_1-styreneoxide[20] was chosen as the epoxide, since we reasoned that the weaker benzyl carbon-oxygen bond would be expected to homolize resulting in a 1,4-biradical with one of the unpaired electrons on the Ta atom and the other on the benzylic carbon. We expected this benzyl stabilization would result in a longer lived 1,4-biradical allowing more time for rotation about the C-C bond, as compared to an alkyl substituted 1,4-biradical. The reaction of $Cp^*_2Ta(=CH_2)H$ with *trans*-d_1-styreneoxide produced only $(\eta^5\text{-}C_5Me_5)_2Ta(=O)CH_3$ and *trans*-d_1-styrene (^{1}H NMR). This retention of stereochemistry for the product is indicative of a concerted mechanism.

Investigation of the organic literature[21] reveals that the rate of C_1-C_2 bond rotation decreases as the number of alkyl substituents is increased. To the best of our knowledge, analogous systems with aryl substituents have not been studied. Thus, it is not clear whether the expected benzyl stabilization would be sufficient to allow C-C bond rotation to compete with decomposition to products for the putative, very crowded 1,4-biradical $[Cp^*_2Ta(CH_3)(OCH_2CHPh)]$.

We have prepared both *cis*- and *trans*-ethylene oxide-d_2 to determine if steric interactions are responsible for the observed retention of stereochemistry in the deoxygenation of *trans*-styrene oxide-d_1. The deoxygenation of ethylene oxide-d_2 should have the lowest barrier to C-C bond rotation (2-3 kcal $\cdot$ mol^{-1})[22] in the 1,4-biradical intermediate. Due to the importance of preparing these labeled epoxides in high purity (specifically, very high isomeric purity), the absence of such a synthetic route in the literature and ambiguities in the spectral properties of these compounds, their synthesis will be briefly discussed. The following synthetic outline (Scheme VII) has an obvious organometallic bias,[23] but each step is high yield with known stereochemistry, and the organic products are white crystalline solids until final epoxide is produced in the last step.

Scheme VII.

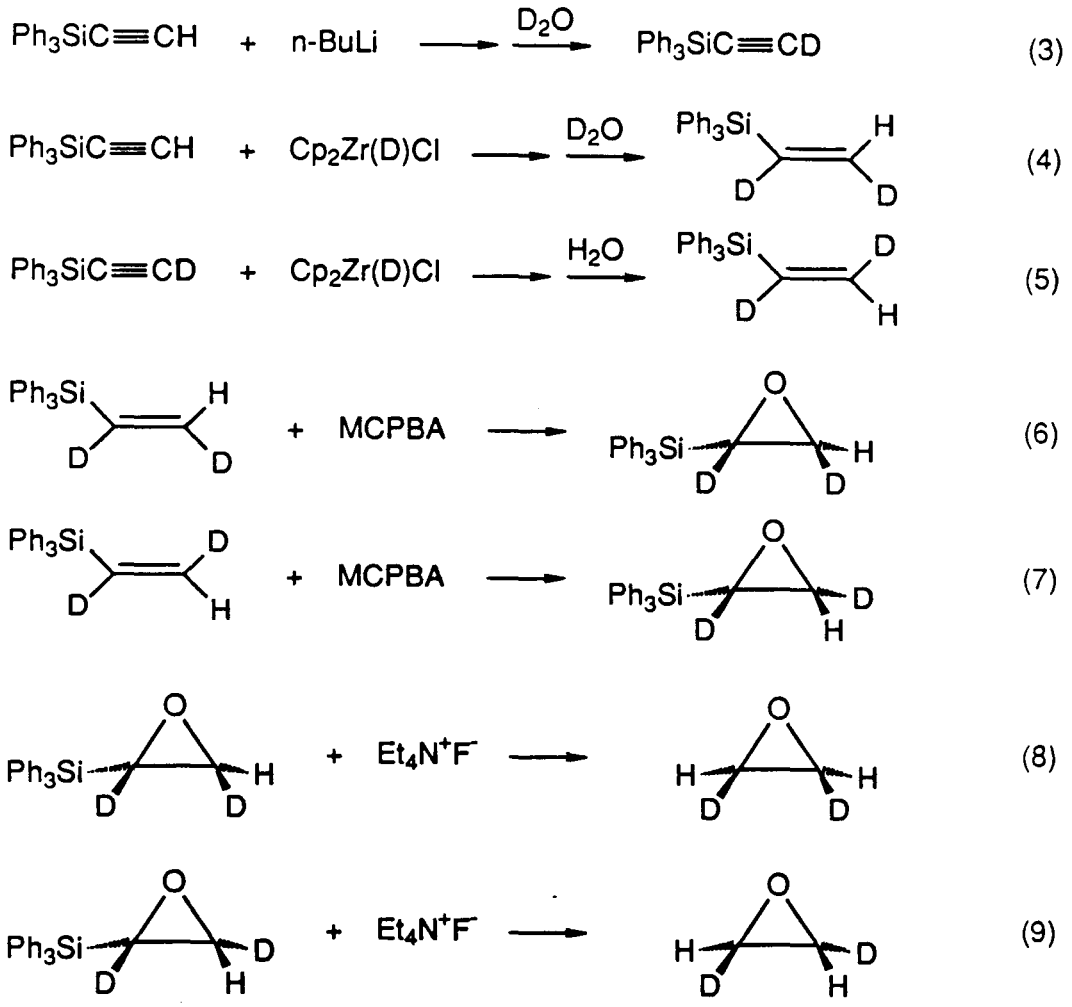

All of the steps illustrated in Scheme VII are well precedented in the literature (not necessarily for the labeled compounds used here), although we are not aware of their application to the preparation of labeled ethylene oxides. Deuterozirconation[24] of triphenylsilylacetylene followed by deutorolysis yields triphenylsilyl-*cis*-dideuteroethylene (Eqn.

4). It is important to use triphenylsilyl, not trimethylsilyl, throughout this procedure for two reasons: (1) the triphenylsilyl derivatives are white crystalline solids instead of high boiling oils and (2) trimethylsilylfluoride boils within 2°C of ethylene oxide making it very difficult to separate in the final step. Triphenylsilyl-*trans*-dideuteroethylene is obtained by deuterozirconation of triphenylsilylacetylene-d_1 (from deprotonation of triphenylsilylacetylene then deuterolysis, Eqn. 3) followed by hydrolysis (Eqn. 5). Epoxidation of the silylethylenes (Eqns. 6 and 7) with *meta*-chloroperoxybenzoic acid (MCPBA)[25] proceeds stereospecifically to the triphenylsilylepoxides. Cleavage of the silyl group by F^-[26] in the final step (Eqns. 8 and 9) gives the appropriately labeled dideuteroethyleneoxides in high yield and isotopic purity. The product gases were collected by Toepler pump through two -78°C traps and analyzed by mass spectrometry, ^{1}H NMR, IR spectroscopies.

The solution IR spectra for *cis*- and *trans*-ethylene oxide-d_2 in CCl_4 have been reported in the literature.[27] Comparison of our spectra to the literature values in the same solvent revealed several significant differences. Several of the literature values for the epoxide stretching frequencies would be completely masked by the solvent, making us skeptical about the reliability of the other values. There are clean regions in each epoxide gas phase spectrum where greater than 1-2% of the other isomer would have been observed, if present. Gas-phase IR analysis of the labeled ethylenes (from the deoxygenation of the epoxides with [Cp^*_2TaR]) was equally diagnostic and were compared to commercially available samples.

The IR spectra of the ethylenes produced in the deoxygenation of *cis*- and *trans*-ethylene oxide-d_2 by [$Cp^*_2TaCH_2C_6H_5$] (Figure 8) show greater than 95% retention of stereochemistry, consistent with the reaction proceeding *via* a concerted mechanism. However, we do not understand why a small amount (less than 2-5%) of isomerization is observed for the *cis* isomer. The small amount of isomerization is variable and indicates there

may be an impurity present in the *cis*-ethylene oxide-d_2, but not in the *trans*-ethylene oxide-d_2, that is responsible for the observed isomerization.[28]

The treatment of $Cp^*_2Ta(=CH_2)H$ with 2-methylaziridine yielded the previously known $Cp^*_2Ta(=NH)CH_3$ and propene. The mechanism for this reaction was not examined. No reactivity was observed between $Cp^*_2Ta(=CH_2)CH_3$ and benzylidene-N-methylamine, possibly for steric reasons.

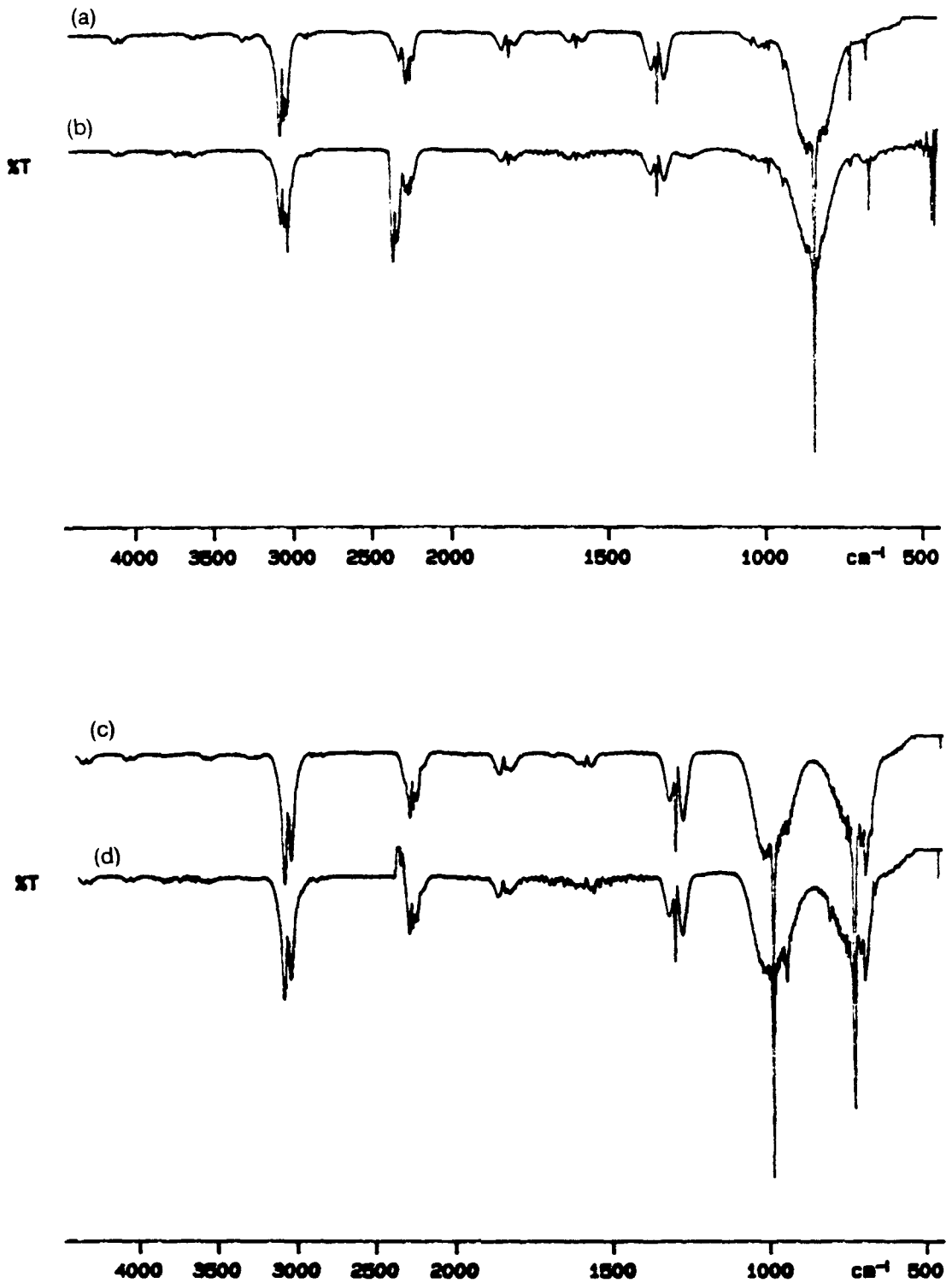

Figure 8. IR spectra of dideuteroethylenes. (a) *cis*-ethylene-d_2 from CIL. (b) product ethylene from [Cp*$_2$Ta($CH_2C_6H_5$)] + *cis*-ethyleneoxide-d_2. (c) *trans*-ethylene-d_2 from CIL. (d) product ethylene from [Cp*$_2$Ta($CH_2C_6H_5$)] + *trans*-ethyleneoxide-d_2.

Scheme VIII

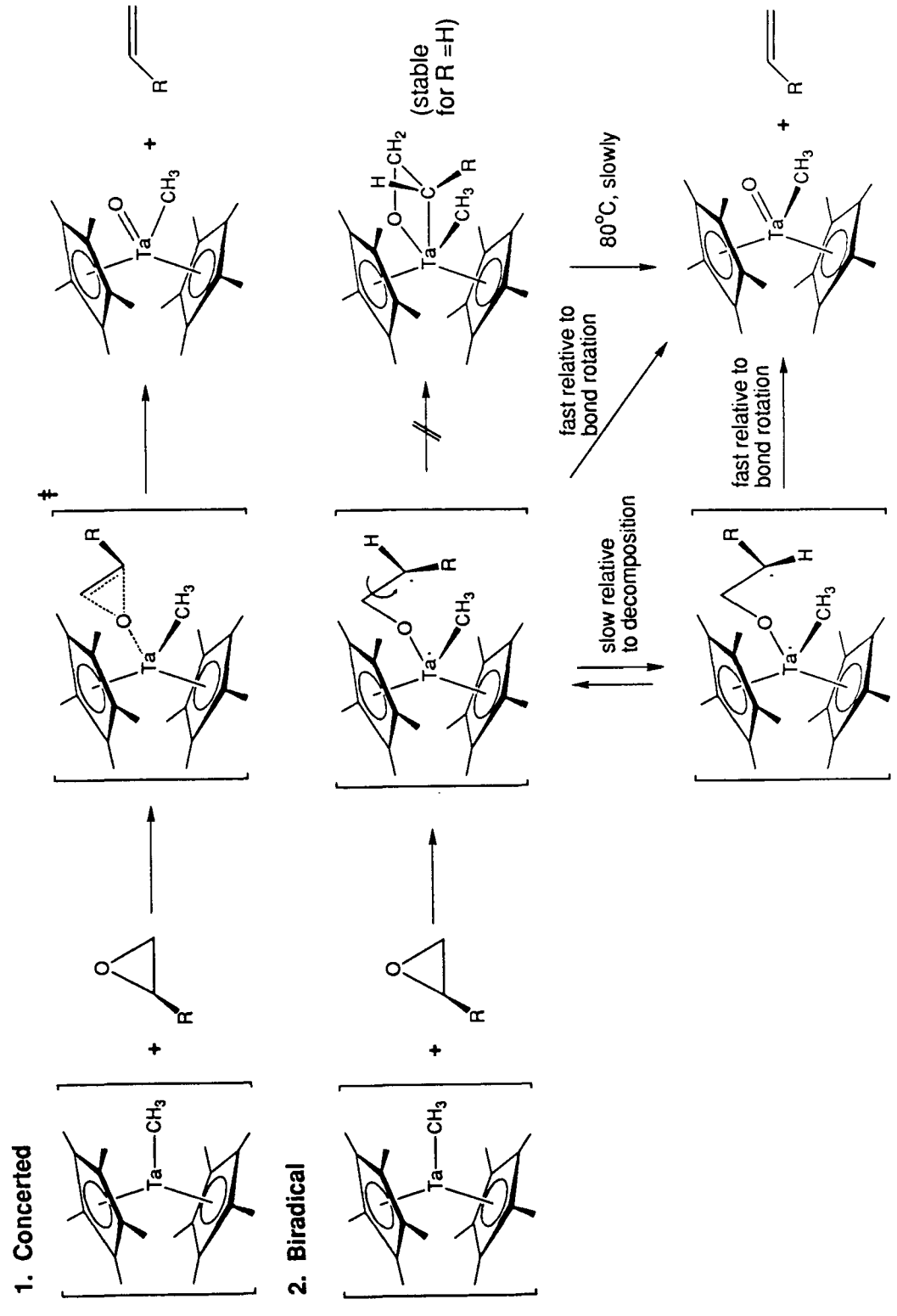
1. Concerted
2. Biradical
(stable for R =H)
fast relative to bond rotation
80°C, slowly
slow relative to decomposition
fast relative to bond rotation

The summary of the mechanism of epoxide deoxygenation by 16-electron permethyltantalocene alkyls is shown in Scheme VIII. We envision the concerted mechanism with a symmetrical transition state and no tantalum-carbon interaction. An asymmetrical transition state would resemble a metallaoxetane which would have been observed, if formed. If a 1,4-biradical is along the reaction coordinate, it must eliminate to products faster than C-C bond rotation **and** faster than collapse to a tantalaoxetane. We feel the mechanism is adequately described as concerted.[29]

CONCLUSION

We have shown that unstabilized early transition metal metallaoxetanes can be prepared and isolated. Although sufficiently stable to be isolated and fully characterized, the tantalaoxetanes decompose smoothly to $Cp^*_2Ta(=O)CH_3$ and olefin above 60°C. We have been able to discount tantalaoxetanes as intermediates in the deoxygenation of epoxides by permethyltantalocene alkyls. Our mechanistic investigation of this deoxygenation reaction concluded that if a 1,4-biradical is involved it must be **very** short-lived, and thus, a concerted mechanism seems to be operating. This is the first system, as far as we are aware, in which it can be conclusively demonstrated that a metallaoxetane is **not** on the reaction surface of epoxide deoxygenation. It must be stressed however, that our conclusions cannot necessarily be applied to epoxide deoxygenation (or olefin epoxidation) in other systems. The potential existence of the metallaoxetane or biradical intermediates discussed in this chapter will depend on the particular metal and its oxidation state as well as the ligand arrangement. The most significant implication from this mechanistic investigation is that the deoxygenation of epoxides by an unsaturated metal center (and by microscopic reversibility, olefin epoxidation by a metal-oxo) can occur without metal-carbon interaction.

Philosophically speaking. We are to the point in this mechanistic investigation where the only question that appears to remain is: when is a dip a well? There is most likely a dip (maybe many dips) in the energy surface we have been investigating. We have designed and performed the best possible experiments to obtain evidence for the expected biradical intermediate without success. At this time the story has come to an end, at least until technology advances a little further and someone comes up with a better way to determine when a dip becomes a well.

Table 5. ^{1}H and ^{13}C NMR data. Spectra were recorded on a JOEL GX400Q (^{1}H, 399.78 MHz; ^{13}C, 100.38 MHz) spectrometer in benzene-d_6 and referenced to residual benzene-d_5 at 7.15 ppm, unless otherwise noted.

Compound	assignments	^{1}H(ppm)	^{13}C(ppm)	$^{1}J_{CH}$ (Hz)
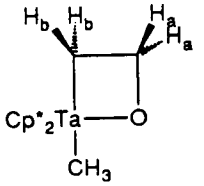	[a]$C_5(CH_3)_5$	1.67(s)		
	CH_a	5.56(t) J_{ab}=7Hz		
	CH_b	0.78(t)		
	CH_3	-0.19(s)		
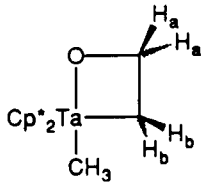	[a]$C_5(CH_3)_5$	1.64(s)	[b]11.0(q)	127
	$C_5(CH_3)_5$		114.7(s)	
	CH_a	5.48(t)	20.3(t)	132
	CH_b	0.09(t)	75.4	134
		J_{ab}=7Hz		
	CH_3	-0.45(s)	37.0(q)	125
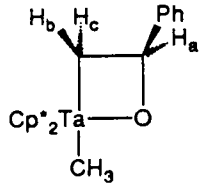	[a]$C_5(CH_3)_5$	1.64(s)	[b,c]11.9(q)	127
	$C_5(CH_3)_5$	1.55(s)	11.3(q)	127
	$C_5(CH_3)_5$		113.3(s)	
	$C_5(CH_3)_5$		112.6(s)	
	H_a	5.56(dd)		
	[d]H_b	1.12(dd)		
	H_c	0.67(dd)		
	$^{2}J_{ab}$=9Hz, $^{2}J_{ac}$=6Hz, $^{2}J_{bc}$=12Hz			
	CH_2	[e]		
	$CHPh$		81.7	138
	CH_3	0.01(s)	43.6	124
	C_6H_5: H_o	7.77(d)	127.3(d)	158
	H_m	7.34(t)	124.0(d)	158
	H_p	[e]	124.5(d)	160
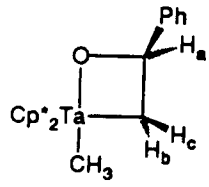	$C_5(CH_3)_5$	1.61(s)	11.8(q)	127
	$C_5(CH_3)_5$	1.57(s)	10.3(q)	127
	$C_5(CH_3)_5$		114.9(s)	
	$C_5(CH_3)_5$		113.4(s)	
	H_a	5.31(dd)		
	[d]H_b	0.51(dd)		
	H_c	0.17(dd)		
	$^{2}J_{ab}$=9Hz, $^{2}J_{ac}$=6Hz, $^{2}J_{bc}$=13Hz			
	CH_2		30.0	132
	$CHPh$		81.2	138
	CH_3	0.01(s)	35.6	120
	C_6H_5: H_o	7.70(d)	127.5(d)	157
	H_m	7.37(t)	124.4(d)	158
	H_p	[e]	124.9(d)	155

	$C_5(CH_3)_5$	1.62(s)
	$C_5(CH_3)_5$	1.52(s)
	H_a	5.45(m)
	[d]H_b	1.00(m)
O-*endo*-Ph-Cl	H_c	0.59(m)
	CH_3	0.00(s)
	C_6H_4	7.42(d)
		7.29(d)
	[f]$C_5(CH_3)_5$	1.59(s)
	$C_5(CH_3)_5$	1.52(s)
	H_a	5.17(m)
	H_b	[g]
O-*exo*-Ph-Cl	H_c	[g]
	CH_3	-0.31(s)
	C_6H_4	6.5-7.5[h]
	[f]$C_5(CH_3)_5$	1.63(s)
	$C_5(CH_3)_5$	1.50(s)
	H_a	5.47(m)
	H_b	[g]
O-*endo*-Ph-CF_3	H_c	[g]
	CH_3	0.00(s)
	C_6H_4	6.5-7.5[h]
	$C_5(CH_3)_5$	1.63(s)
	$C_5(CH_3)_5$	1.55(s)
	H_a	5.20(m)
	[d]H_b	1.05(m)
O-*exo*-Ph-CF_3	H_c	0.27(m)
	CH_3	-0.33(s)
	C_6H_4	6.5-7.5[h]
	$C_5(CH_3)_5$	1.59(s)
	$C_5(CH_3)_5$	1.47(s)
	H_a	5.35(m)
	[d]H_b	0.88(m)
O-*endo*-Ph-CN	H_c	0.50(m)
	CH_3	-0.04(s)
	C_6H_4	6.5-7.5[h]
	[f]$C_5(CH_3)_5$	1.60(s)
	$C_5(CH_3)_5$	1.50(s)
	H_a	[g]
	H_b	[g]
O-*exo*-Ph-CN	H_c	[g]
	CH_3	-0.30(s)
	C_6H_4	6.5-7.5[h]

	[f]$C_5(CH_3)_5$	1.60(s)	
	$C_5(CH_3)_5$	1.50(s)	
	H_a	[g]	
	H_b	[g]	
O-*endo*-Ph-NO_2	H_c	[g]	
	CH_3	0.00(s)	
	C_6H_4	6.5-7.5[ref]	
	$C_5(CH_3)_5$	1.58(s)	
	$C_5(CH_3)_5$	1.50(s)	
	H_a	5.10(dd)	
	H_b	[g]	
O-*exo*-Ph-NO_2	H_c	[g]	
	CH_3	-0.35(s)	
	C_6H_4	8.15(d)	
		7.48(d)	
	$C_5(CH_3)_5$	1.56(s)	
$Cp^*_2Ta(OCH_2)CH_3$	CH_2	1.90(s)	
	CH_3	-0.07(s)	
	$C_5(CH_3)_5$	1.57(s)	
	$C_5(CH_3)_5$	1.40(s)	
$Cp^*_2Ta(OCHPh)CH_3$	CH	2.79(s)	
	CH_3	0.07(s)	
	C_6H_5	6.5-7.5[h]	
	$C_5(CH_3)_5$	1.43(s)	
$Cp^*_2Ta(OCH_2)Ph$	CH_2	[g]	
	[i]C_6H_5	8.92(d)	
		7.58(t)	
		7.53(d)	
		7.32(t)	
	$C_5(CH_3)_5$	1.69(s)	
	$C_5(CH_3)_5$	1.67(s)	
$Cp^*_2Ta(o\text{-}C_6H_4CHCH_3O)H$	CH	5.14(q)	J=6.5Hz
	CH_3	1.65(d)	
	H	[g]	
	C_6H_4	8.16(d)	
		[e]	

[a]toluene-d_8. [b]THF-d_8. [c]-20°C. [d]H_b and H_c assignment based in coupling to H_a. [e]obscured by solvent. [f]recorded on EM390 spectrometer. [g]not assigned. [h]complex. [i]the fifth phenyl resonacne is obscured by solvent.

EXPERIMENTAL

General Considerations. All manipulations of air-sensitive were carried out glovebox, high vacuum or Schlenk line techniques. Solvents were dried over $LiAlH_4$ or sodium/benzophenone and stored over "titanocene." Benzene-d_6 and toluene-d_8 were dried over activated 4Å molecular sieves and stored over "titanocene." 1,4-Dioxane-d_8 and acetonitrile-d_3 were also dried over 4Å molecular sieves but stored over sodium/benzophenone. Acetone-d_6 was both dried and stored over activated 4Å molecular sieves. Chloroform-d_1 and methylene chloride-d_2 were washed with an aqueous KOH solution, dried over anhydrous magnesium sulfate, activated 4Å molecular sieves, and stored over sodium/benzophenone. Argon was purified by passage over MnO on vermiculite and activated molecular sieves.

NMR spectra were recorded on Varian EM-390 (^1H, 90MHz), JOEL FX90Q (^1H, 89.56MHz; ^{13}C, 22.50MHz), and JOEL GX400Q (^1H, 399.78MHz; ^{13}C, 100.38MHz) spectrometers. Infrared spectra were recorded on a Perkin-Elmer 1600 Series FTIR. All elemental analyses were conducted by either Lawrence Henling or Fenton Harvey of the Caltech Analytical Laboratory.

Starting Materials. Paraformaldehyde, *p*-dimethylaminobenzaldehyde, *p*-methylbenzaldehyde, *p*-chlorobenzaldehyde, *p*-methoxybenzaldehyde, *p*-cyanobenzaldehyde, potassium hydride, silver hexafluorophosphate, benzophenone, styreneoxide, benzylidenemethylamine, *sec* -phenethyl alcohol, phenethyl alcohol, α,α,α-trifluoro-*p*-tolualdehyde, 2-methylaziridene, triphenylsilylacetylene, n-butyl lithium, deuterium oxide, Cp_2ZrCl_2, tetraethylammonium fluoride, trimethylphosphine and nitrosobenzene were used as obtained from Aldrich without further purification. Benzaldehyde (Spectrum or MC/B) and *p*-nitrobenzaldehyde (Matheson), acetaldehyde (Baker) were used as obtained from the companies indicated without further purification. Ethyleneoxide (Matheson) was taken through at least two freeze/pump/thaw cycles directly prior to use.

The *trans*-styreneoxide-d_1 was a generous gift from Dr. Dave Wheeler and was prepared from the reaction of *trans*-styrene-d_1 with *m*-chloroperbenzoic acid according to literature methods.[25]

$Cp^*_2TaCl_2$,[11a] $Cp^*_2Ta(=CH_2)H$,[11b] $Cp^*_2Ta(=CH_2)CH_3$,[11b] $Cp^*_2Ta(C_6H_4)H$[30] and "$Cp^*_2Ta(=CHC_6H_5)H$"[31] were prepared by literature methods developed in our laboratory.

$LiAlD_4$ was purified by dissolving the soluble part of the commercially available (Aldrich) gray powder in dry diethylether. Filtering off the insoluble impurities followed by removal of the solvent under vacuum results in a nice white powder of $LiAlD_4$. Using diethylether soluble $LiAlD_4$ makes the filtrations in the hydrozirconation much easier. $Cp_2Zr(D)Cl$ was prepared by the modified procedure described by Buchwald.

Cis- and *trans*-ethylene-d_2 were obtained, for comparison purposes, from Cambridge Isotope Laboratories. Mass spectra of *cis*- and *trans*-ethyleneoxide-d_2 were obtained by Rich Kondrat of the U.C. Riverside Mass Spectroscopy Facility.

O-*endo*-$Cp^*_2Ta(CH_2CH_2O)CH_3$ and O-*exo*-$Cp^*_2Ta(OCH_2CH_2)CH_3$. The thermal instability of these compounds made their isolation difficult. They were therefore characterized spectroscopically. Treatment of $Cp^*_2Ta(=CH_2)CH_3$ (15 mg, 0.03 mmoles) with excess paraformaldehyde (40 mg, 1 mmole) in C_6D_6 resulted in clean conversion to O-*endo*-$Cp^*_2Ta(CH_2CH_2O)CH_3$ in approximately 10 minutes. The isomerization to O-*exo*-$Cp^*_2Ta(OCH_2CH_2)CH_3$ was observed over several hours at room temperature.

O-*endo*-$Cp^*_2Ta(CH_2CHC_6H_5O)CH_3$. A slurry of $Cp^*_2Ta(=CH_2)CH_3$ (480 mg, 1 mmole) and 10 equivalents of benzaldehyde (1 mL, 10 mmoles) in ≈10 mL of toluene was stirred in a Schlenk tube at room temperature for 1 hour. The solvent and excess benzaldehyde were removed under vacuum. Toluene was transfered onto the oily solid, stirred and removed again under vacuum. This process was repeated twice more to help remove all of the benzaldehyde.

The solid was dissolved in the minimum amount of toluene and petroleum ether was added. Cooling the solution to -78°C and removal of the mother liquor *via* cannula resulted in a light brown precipitate. The remaining volatiles were removed under vacuum and the solid was washed several times with cold petroleum ether and pumped on one last time to give 330 mg (56% yield, 1st crop) of O-*endo*-$Cp^*_2Ta(CH_2CHC_6H_5O)CH_3$. Anal Calcd. for $C_{29}H_{41}OTa$ (MW=586.7): C, 59.37; H, 7.06. Found: C, 59.63; H, 6.73.

O-*exo*-$Cp^*_2Ta(OCH_2CHC_6H_5)CH_3$. Gentle warming (50°C) of a Schlenk flask containing a solution of $Cp^*_2Ta(=CH_2)CH_3$ (250 mg, 0.5 mmoles) and 10 equivalents of benzaldehyde (0.5 mL, 5 mmoles) in ≈10 mL of toluene for 4 hours, followed by a workup similar to that described above for the *endo* isomer resulted in isomerically pure O-*exo*-$Cp^*_2Ta(OCH_2CHC_6H_5)CH_3$ (115 mg 1st crop, 40% yield). Anal Calcd. for $C_{29}H_{41}OTa$ (MW=586.7): C, 59.37; H, 7.06. Found: C, 59.15; H, 6.91.

The substituted phenyl derivatives were prepared by procedures directly analogous to those above. The isomer assignments were based on comparison to the parent 3-phenyltantalaoxetane where the thermodynamic isomer was shown to be the O-*exo* isomer by X-ray crystallography.

X-ray crystal structure determination of O-*exo*-$Cp^*_2Ta(OCH_2CHC_6H_5)CH_3$. The ORTEP drawing of O-*exo*-bis(pentamethylcyclopentadienyl)-3-phenyl-1,2-tantalaoxetane, O-*exo*-$Cp^*_2Ta(CH_2CHC_6H_5O)CH_3$, is shown in Figure 3. Important angles and distances are shown in Table 1. A colorless crystal was mounted in a greased capillary. Oscillation and Weissenberg photographs showed the crystal to be twinned, with a maximum difference in orientation of nearly two degrees. The crystal was then centered on a CAD-4 diffractometer. Unit cell parameters and an orientation matrix were obtained by a least squares calculation from the setting angles of 24 reflections with $10° < 2\theta < 25°$. One data set out to a 2θ of 40° was collected by an ω scan of $(1.8 + 0.35\tan\theta)°$ width. The data were corrected for absorption and a

slight decay, and adjusted by Lorentz and polarization factors. Systematic absences in the diffractometer data led to the choice of space group $P2_1/c$. Coordinates of the tantalum atom were obtained from a Patterson map; locations of the other non-hydrogen atoms were determined from successive structure factor-Fourier calculations. Hydrogen atom positions were determined from difference maps for the methyl group coordinated to the metal atom and by calculation for the remaining atoms. The methyl groups with calculated positions were modelled by six half-weight hydrogen atoms. All hydrogen atoms were given isotropic B values 20% greater than that of the attached atom. No hydrogen parameters were refined. The complete least squares full matrix, consisting of spatial and anisotropic and isotropic thermal parameters for the non-hydrogen atoms and a scale factor, contained 200 parameters. A final difference Fourier map showed deviations ranging from -0.85 $e\text{Å}^{-3}$ to +2.13 $e\text{Å}^{-3}$. The larger peaks are near the tantalum atom and indicate imperfectly applied absorption corrections. The refinement converged with an R-factor of 0.0580 (0.0406 for $F_o^2 > 3\sigma(F_o^2)$) and a goodness of fit of 1.55 for all 2368 reflections. The final parameters are listed in Appendix 1.

Calculations were done with programs of the CRYM Crystallographic Computing System and ORTEP. Scattering factors and corrections for anomalous scattering were taken from a standard reference[32]. $R = \Sigma||F_o|-|F_c||/\Sigma F_o$, for only $F_o^2 > 0$, and goodness of fit = $[\Sigma w(F_o^2-F_c^2)^2/(n-p)]^{1/2}$, where n is the number of data and p the number of parameters refined. The function minimized in least squares was $\Sigma w(F_o^2-F_o^2)^2$, where $w = 1/\sigma^2(F_o^2)$. Variances of the individual reflections were assigned based on counting statistics plus an additional term, $0.014I^2$. Variances of the merged reflections were determined by standard propagation of error plus another additional term, $0.014\langle I\rangle^2$. The absorption correction was done by Gaussian integration over an 8 X 8 X 8 grid. Transmission factors varied from 0.240 to 0.486.

The permethylcyclopentadienyl rings are bound normally to the tantalum atom with the metal to ring centroid distances of 2.200 and 2.217 Å and a ring centroid-tantalum-ring centroid

angle of 135.9°. In the wedge between these rings lie the methyl group and the tantalaoxetane ring. The Ta-O and Ta-C distances in the oxetane are 2.057(9)Å and 2.236(15)Å, respectively. The O-Ta-C angle is only 62.6(5)°. The oxetane is slightly puckered; the four atoms are within ±0.16Å of being coplanar and the sum of the internal angles is 353.3°. The methyl group, 2.269(13)Å from the tantalum, is also in the wedge. It is nearest the carbon of the oxetane, with a C-Ta-C angle of 71.4(5)°. The remaining distances and angles are normal. There are no significant interactions between molecules.

$Cp^*_2Ta(OCH_2)CH_3$. Treatment of $Cp^*_2Ta(=CH_2)H$ (20 mg, 0.04 mmoles) with an excess of paraformaldehyde (5 mg, 0.15 mmoles) in C_6D_6 (0.5 mL) resulted in clean conversion (^1H NMR) to the aldehyde adduct $Cp^*_2Ta(OCH_2)CH_3$ within 15 minutes at room temperature. An exact isomer assignment was not made.

$Cp^*_2Ta(OCHPh)CH_3$. A very clean reaction was observed (by ^1H NMR) when 1 equivalent of benzaldehyde (4 μl, 0.04 mmoles) was added *via* syringe to a benzene-d_6 solution containing $Cp^*_2Ta(=CH_2)H$ (17 mg, 0.04 mmoles). The reaction was complete after 10 minutes at room temperature.

$Cp^*_2Ta(OCH_2)C_6H_5$. Monitoring the reaction of $Cp^*_2Ta(C_6H_4)H$ (20 mg, 0.04 mmoles) with excess paraformaldehyde (3 mg, 0.1 mmole) over two days at room temperature resulted in trapping the phenyl intermediate as $Cp^*_2Ta(OCH_2)C_6H_5$. Based on other trapping studies of $[Cp^*_2TaC_6H_5]$ where there is an apparent correlation between the shift of the ^1H NMR resonance of the *ortho* proton of the phenyl ring directed toward the center of the wedge and the size of the trapping ligand,[30] we believe the O-*exo* isomer is formed in this reaction.

$Cp^*_2Ta(o\text{-}C_6H_4CHCH_3O)H$. Addition of *sec*-phenethyl alcohol (6 μl, 0.05 mmoles) *via* syringe to a solution of $Cp^*_2Ta(=CH_2)H$ (21 mg, 0.05 mmoles) in C_6D_6 resulted in slow (12 hours), but clean (^1H NMR), formation of $Cp^*_2Ta(o\text{-}C_6H_4CHCH_3O)H$.

Ph_3Si-C≡C-D. A 1.6 M solution of n-BuLi (37.5 mL, 60 mmoles) was slowly added to a stirring ether solution (80 mL) of Ph_3Si-C≡C-H (15.5 g, 55 mmoles) while under an argon atmosphere. After allowing the reaction mixture to stir for 30 min at room temperature, D_2O (1.1 mL, 60 mmoles) was slowly added dropwise. The reaction mixture was filtered in air and the solvent removed at aspirator pressure. The ^1H NMR spectrum indicated that there was ≤1% residual proton in the final product (13.5 g, 87% yield).

trans-**Ph_3SiCD=CHD.** Cold (-78°C) methylene chloride (300 mL) was transferred into a large Schlenk flask containing $Cp_2Zr(D)Cl$ (15.5 g, 60 mmoles) and Ph_3Si-C≡C-D (15.5 g 54 mmoles). The reaction mixture became a clear orange solution upon warming to room temperature with stirring. Removal of the solvent under vacuum followed by several petroleum ether (500 mL total) washings results in a nice yellow powder, presumably *trans*-$Cp_2Zr(CD{=}CDSiPh_3)Cl$. The yellow powder was dissolved in Et_2O (200 mL) and cooled to 0°C followed by slow addition of 1.5 mL (80 mmoles) of H_2O. The reaction flask was left open to a bubbler and evolution of some gas was observed. The white $[Cp_2ZrCl]_2O$ precipitate was filtered off in air and washed with Et_2O. The Et_2O solution was dried over $MgSO_4$ and the solvent removed under vacuum. The product was purified by addition of charcoal to a pentane solution of the crude off-white solid, followed by gravity filtration and flash chromatography on Florisil (pentane eluant). The fractions were concentrated and cooled to -10°C to induce formation of beautiful white crystals (11 g, 71% yield) of *trans*-Ph_3SiCD=CHD.

cis-**Ph_3SiCD=CDH.** The procedure followed was analogous to the *trans* isomer with the following exceptions. $Cp_2Zr(D)Cl$ (16 g, 62 mmoles) was reacted with Ph_3Si-C≡C-H (17 g, 60 mmoles), followed by addition of D_2O (1.5 mL) resulting in *cis*-Ph_3CD=CDH (16 g, 94% crude yield). Recrystallization from pentane gave 13 g (76% yield) of *cis*-Ph_3CD=CDH.

trans-**$Ph_3SiCDCHDO$.** *Trans*-Ph_3SiCD=CHD (10 g, 35 mmoles) was added as a solid to a slurry of 50% MCPBA (18 g, 52 mmoles) in $CHCl_3$ (75 mL) in air. The reaction mixture became

very hot and was solid after two hours. Chloroform was added to break up the solid followed by filtration and generous washings with chloroform. The $CHCl_3$ solution was ectracted five times with 5% $NaHCO_3$, two times with 5% $NaHSO_3$ and two times with 5% $NaHCO_3$. Drying over $MgSO_4$ and removal of the solvent under vacuum gave a yellow oil. The ^1H NMR spectrum of this oil indicated it was 50% starting material and 50% the desired product. The oil was dissolved in petroleum ether and then pumped on to remove the $CHCl_3$. This was repeated several times and resulted in a white solid that was insoluble in petroleum ether (as long as there was no $CHCl_3$ present) and a petroleum ether soluble portion (starting material). The mixture was loaded onto a flash column (Florisil) and eluted with generous quantities of petroleum ether and then $CHCl_3$. The petroleum ether fractions contained *trans*-$Ph_3SiCD{=}CHD$, which could be easily recovered by reducing the volume of the solvent and inducing crystallization by cooling. The final product, *trans*-$Ph_3SiCDCHDO$, was obtained removal of the $CHCl_3$ solvent under vacuum, several petroleum ether triterations and recrystallization from hot petroleum ether.

***cis*-Ph_3Si-CDCDHO.** The procedure followed was analogous to the procedure described above for the *trans* isomer with the following modifications. Solid *cis*-$Ph_3SiCD{=}CDH$ (15 g, 52 mmoles) was added to a stirring slurry of 50% MCPBA (38 g, 75 mmoles) in 75 mL of $CHCl_3$. Similar workup gave 8 g (90% yield based on starting material consumed) of *cis*-$Ph_3SiCDCDHO$.

***trans*-ethylene oxide-d_2.** A 50 mL heavy walled glass reaction vessel (with Kontes valve) was charged with *trans*-$Ph_3CDCHDO$ (1.3 g, 4 mmoles), $Et_4NF \cdot xH_2O$ (0.7 g, 4 mmoles) and DMSO (10 mL). After stirring at room temperature for 2 hours the reaction mixture was frozen to -196°C and the flask evacuated. The gaseous product (88% yield) was collected by Toepler pump (through two -78°C cold traps) as the reaction flask warmed to room

temperature. The gas phase IR spectrum (10 cm path) was recorded and is included in Appendix 2 because it is significantly different than reported in the literature.[27]

***cis*-ethyleneoxide-d_2.** The same procedure as described above for the *trans* isomer was followed. The product was collected *via* Toepler pump in 77% yield. The IR spectrum is significantly different than reported in the literature and is thus included in Appendix 2.

Deoxygenation of labeled ethyleneoxides. Approximately 5 mL of toluene was vacuum transerred in a 25 mL glass reaction vessel equipped with a Kontes valve containing [$Cp^*_2TaCH_2C_6H_5$] (500 mg, 1 mmole). *Trans*-ethyleneoxide-d_2 (125 mm, 0.16 atm, 0.7 mmoles) was admitted to an evacuated volumetric (104 mL) gas bulb and then condensed into the reaction flask at -196°C. To insure complete reaction the mixture was stirred at room temperature for 5 days. The reaction flask was cooled to -196°C again and the gaseous product collected *via* Toepler pump, through two cold traps at -78°C and -115°C (10:1 EtOH:MeOH), as the reaction mixture warmed to room temperature. When transfer of the toluene into the -78°C trap was complete ≥99% (by IR, *vide supra*) *trans*-ethylene-d_2 (85% yield) had been collected.

The same procedure was followed for the *cis* isomer and resulted in ≥95% (by IR) *cis*-ethylene-d_2 in a similar yield.

REFERENCES

1. (a) Sharpless, K.B.; Teranishi, A.Y.; Backvall, J.E. *J. Am. Chem. Soc.* **1977**, *99*, 3120. (b) Groves, J.T.; Ahn, K.H.; Quinn, R. *J. Am. Chem. Soc.* **1988**, *110*, 4217. (c) Groves, J.T.; Stern, M.K. *J. Am. Chem. Soc.* **1988**, *110*, 8628. (d) Groves, J.T.; Nemo, T.E. *J. Am. Chem. Soc.* **1983**, *105*, 5786. (e) Groves, J.T.; Myers, R.S. *J. Am. Chem. Soc.* **1983**, *105*, 5791. (f) Garrison, J. M.; Bruice, T.J. *J. Am. Chem. Soc.* **1989**, *111*, 191. (g) Garrison, J. M.; Ostovic, D.; Bruice, T.J. *J. Am. Chem. Soc.* **1989**, *111*, 4960. (h) Ostovic, D.; Bruice, T.J. *J. Am. Chem. Soc.* **1989**, *111*, 6511. (i) Castellino, A.J.; Bruice, T.C. *J. Am. Chem. Soc.* **1988**, *110*, 158. (j) Castellino, A.J.; Bruice, T.C. *J. Am. Chem. Soc.* **1988**, *110*, 7512. (k) Collman, J.P.; Kodadek, T.; Raybuck, S.A.; Brauman, J.I.; Papazian, L.M. *J. Am. Chem. Soc.* **1985**, *107*, 4343. (l) Groves, J.T.; Ahn, K.H.; Quinn, R. *J. Am. Chem. Soc.* **1988**, *110*, 4217. (m) Samsel, E.G.; Srinivasan, K.; Kochi, J.K. *J. Am. Chem. Soc.* **1985**, *107*, 7606. (n) Kinneary, J.F.; Albert, J.S.; Burrows, C.J. *J. Am. Chem. Soc.* **1988**, *110*, 6124. (o) Collman, J.P.; Kodadek, T.; Brauman, J.I.; *J. Am. Chem. Soc.* **1986**, *108*, 2588. (p) Collman, J.P.; Brauman, J.I.; Meunier, B.; Hayashi, T.; Kodadek, T.; Raybuck, S.A. *J. Am. Chem. Soc.* **1985**, *107*, 2000. (q) Collman, J.P.; Brauman, J.I.; Meunier, B.; Raybuck, S.A.; Kodadek, T. *Proc. Natl. Acad. Sci. USA* **1984**, *81*, 3245. (r) Traylor, T.G.; Miksztal, A.R. *J. Am. Chem. Soc.* **1987**, *109*, 2770. (s) Hill, C.L.; Brown, R.B. *J. Am. Chem. Soc.* **1986**, *108*, 536. (t) Collman, J.P.; Hampton, P.D.; Brauman, J.I. *J. Am. Chem. Soc.* Sept. **1989**, *112*, 2977. (u) Bressan, M.; Morvillo, A. *Inorg. Chem.* **1989**, *28*, 950.

2. Rappe, A.K.; Goddard, W.A. *J. Am. Chem. Soc.* **1980**, *102*, 5114.

3. Nugent, W.A.; Mayer, J.M. "Metal-Ligand Multiple Bonds" Wiley-Interscience, New York, 1988.

4. Cundari, T.R.; Drago, R.S. *Inorg. Chem.* **1990**, *29*, 487.

5. Day, V.W.;Klemperer, W.G.; Lockledge, S.P.; Main, D.J. *J. Am. Chem. Soc.* **1990**, *112*, 2031.

6. (a) Klein, D.P.; Hayes, J.C.; Bergman, R.G. *J. Am. Chem. Soc.* **1988**, *110*, 3704. (b) Klein, D.P.; Bergman, R.G. *J. Am. Chem. Soc.* **1989**, *111*, 3079.

7. Hartwig, J.F.; Bergman, R.G.; Andersen, R.A. *J. Am. Chem. Soc.* **1990**, *112*, 3234.

8. Kafafi, Z.H.; Hauge, R.H.; Billups, W.E.; Margrave, J.L. *J. Am. Chem. Soc.* **1987**, *109*, 4775.

9. Ho, S.C.; Hentges, S.; Grubbs, R.H. *Organometallics* **1988**, *7*, 780.

10. Bazan, G.B.; Schrock, R.R.; O'Regan, M.B. private communication.

11. (a) Gibson, V.C.; Bercaw, J.E.; Bruton, W.J.; Sanner, R.D. *Organometallics* **1986**, *5*, 976. (b) van Asselt, A.; Burger, B.J.; Gibson, V.C.; Bercaw, J.E. *J. Am. Chem. Soc.***1986**, *108*, 5347.

12. (a) Doherty, N.M.; Bercaw, J.E. *J. Am. Chem. Soc.* **1985**, *107*, 2670. (b) Burger, B.J.; Santarsiero, B.D.; Trimmer, M.S.; Bercaw, J.E. *J. Am. Chem. Soc.* **1988**, *110*, 3134.

13. (a) Parkin, G; Bunel, E.; Burger, B.J.; Trimmer, M.S.; van Asselt, A.; Bercaw, J.E. *J. Mol. Catal.* **1987**, *41*, 21. (b) Gibson, V.C.; Parkin, G.; Bercaw, J.E. manuscript in preparation.

14. (a) Tebbe, F.N.; Parshall, G.W.; Reddy, G.S. *J. Am. Chem. Soc.* **1978**, *100*, 3611. (b) Pine, S.H.; Zahler, R.; Evans, D.A.; Grubbs, R.H. *J. Am. Chem. Soc.* **1980**, *102*, 3270. (c) Buchwald, S.L.; Grubbs, R.H. *J. Am. Chem. Soc.* **1983**, *105*, 5490.

15. Collman, J.P.; Hegedus, L.S.; Norton, J.R.; Finke, R.G. "Principles and Applications of Organotransition Metal Chemistry" University Science Books, Mill Valley, California, 1987.

16. Hammond, G.S. *J. Am. Chem. Soc.* **1955**, *77*, 334.

17. Lee, J.J.; Ott, K.C.; Grubbs, R.H. *J. Am. Chem. Soc.* **1982**, *104*, 7491.

18. Schobert, R. *Angew. Chem. Int. Ed., Eng.* **1988**, *27*, 855.

19. Wheeler, D.R. Ph.D. Thesis, California Institute of Technology, June, 1990.

20. Dr. Dave Wheeler is gratefully acknowledged for the generous gift of *trans*-styreneoxide-d_1.

21. Dervan, P.B.; Dougherty "Diradicals" Borden, Weston Thatcher, ed., John-Wiley & Sons, Inc. 1982, New York, New York.

22. Lowry, T.H.; Richardson, K.S. "Mechanism and Theory in Organic Chemistry" second edition, Harper and Row, Publishers, New York, 1981.

23. Wheeler, D.R. private communication, Atheneaum, April 1989.

24. (a) Labinger, J.A. "Hydrozirconation of C=C and C≡C, and Hydrometallation by Other Metals." In *Comprehensive Organic Synthesis* (B.M. Trost and I. Flemming, Eds.), Pergammon Press, London, in press. (b) Buchwald, S.L.; LaMaire, S.J.; Nielsen, R.B.; Watson, B.T.; King, S.M. *Tetrahedron Lett.* **1987**, *28*, 3895.

25. Schwartz, N.N.; Blumbergs, J.H. *J. Org. Chem.* **1969**, *29*, 1976.

26. Chan, T.H.; Lau, P.W.K.; Li, M.P. *Tetrahedron Lett.* **1976**, *31*, 2667.

27. Price, C.C.; Spector, R. *J. Am. Chem. Soc.* **1966**, *88*, 4171.

28. It is also possible that the *trans*-ethylene oxide-d_2 was removed from the system when the reaction with the *cis*-ethylene oxide-d_2 was started. If this is the case, we would have to suggest that the small peak at 987 cm^{-1}, in the spectrum of the ethylene produced from the deoxygenation of *cis*-ethylene oxide-d_2 is actually a resonance of the *cis*-ethylene-d_2 for the reaction with the higher (98 *vs* 95%) retention of stereochemistry (also observed in the commercially obtained sample). There is a small peak at 728 cm^{-1} in the spectrum of *cis*-ethylene-d_2 which is coincidental with the other diagnostic resonance of *trans*-ethylene-d_2.

29. The concerted "suck-off" mechanism was first described by Mark Trimmer, private communication.

30. Trimmer, M.S. Ph.D. Thesis, California Institute of Technology, June 1989.

31. See Chapter 2.

32. International Tables for X-ray Crystallography, Vol. IV, p. 71, p. 149; Birmingham, Kynoch Press, 1974.

Appendix 1. X-ray crystal structure data for O-*exo*-$Cp^*_2Ta(OCH(C_6H_5)CH_2)CH_3$.

Table 6. Crystal and Intensity Collection Data for O-*exo*-$Cp^*_2Ta(OCH(C_6H_5)CH_2)CH_3$.

Formula: $TaOC_{29}H_{41}$	Formula weight: 586.59
Crystal color: Colorless	Habit: Irregular
Crystal size: $0.15 \times 0.23 \times 0.39$ mm	
Space group: $P2_1/c$ #14	Absences: $0k0, k$ odd; $h0l, l$ odd
$a = 15.677(10)$Å	
$b = 9.502(4)$Å	$\beta = 110.81(7)°$
$c = 18.315(18)$Å	
$V = 2550.3(32)$Å^3	$Z = 4$
$\mu = 45.62$ cm^{-1} ($\mu r_{max} = 1.09$)	$\rho_{calc} = 1.528$ g cm^{-3}
CAD-4 diffractometer	ω scan
$\lambda = 0.71073$ Å	Graphite monochromator
2θ range: 2°–40°	Octants collected: $-h, k, \pm l$
$T = 295$°K	

Number of reflections measured: 2795

Number of independent reflections: 2368

Number with $F_o^2 > 0$: 2153

Number with $F_o^2 > 3\sigma(F_o^2)$: 1694

Number of reflections used in refinement: 2368

Final R-index: 0.0544 for 2153 reflections with $F_o^2 > 0$

Final R-index: 0.0370 for 1694 reflections with $F_o^2 > 3\sigma(F_o^2)$

Final goodness of fit: 1.47 for 280 parameters and all 2368 reflections

Table 7. Final Non-Hydrogen Parameters for O-*exo*-$Cp^*_2Ta(OCH(C_6H_5)CH_2)CH_3$.

x, y, z and $U_{eq}{}^a \times 10^4$

Atom	x	y	z	U_{eq}
Ta	7857(.4)	−2218(.5)	7835(.3)	407(1)
C1	9407(8)	−2145(13)	8292(6)	650(37)
O	6903(5)	−3597(8)	7142(5)	573(26)
C2	8375(9)	−4123(13)	7407(8)	696(52)
C3	7455(10)	−4821(14)	7187(9)	696(46)
C4	7071(11)	−5727(13)	6420(8)	593(43)
C5	7637(11)	−6637(15)	6231(8)	753(48)
C6	7286(15)	−7598(15)	5621(10)	912(58)
C7	6380(16)	−7601(19)	5191(10)	1114(65)
C8	5821(12)	−6670(19)	5379(10)	1075(61)
C9	6161(11)	−5734(14)	5980(9)	765(50)
Cp1	8133(11)	247(12)	7511(8)	539(48)
Cp2	7215(12)	209(13)	7364(9)	584(45)
Cp3	6792(10)	−777(14)	6788(8)	601(48)
Cp4	7444(11)	−1252(14)	6491(7)	581(50)
Cp5	8276(10)	−647(13)	6908(8)	585(42)
Me1	8837(12)	1253(14)	7997(9)	993(57)
Me2	6743(13)	1282(14)	7698(10)	1139(63)
Me3	5796(10)	−1073(15)	6438(9)	1005(61)
Me4	7246(11)	−2187(16)	5772(7)	949(51)
Me5	9121(12)	−721(17)	6669(10)	1107(56)
Cp6	7799(14)	−1411(14)	9106(8)	644(49)
Cp7	8485(11)	−2347(16)	9314(7)	630(45)

Table 7. (Cont.)

Atom	x	y	z	U_{eq}
Cp8	8130(10)	−3693(14)	9057(8)	569(46)
Cp9	7179(11)	−3559(16)	8696(8)	627(45)
Cp10	6978(10)	−2114(19)	8723(7)	636(42)
Me6	7869(14)	53(16)	9468(8)	1198(62)
Me7	9433(10)	−2056(16)	9909(8)	1075(56)
Me8	8661(11)	−5036(15)	9253(8)	877(50)
Me9	6468(11)	−4708(16)	8449(8)	959(53)
Me10	6011(12)	−1592(18)	8530(10)	1261(60)

[a] $U_{eq} = \frac{1}{3}\sum_i \sum_j [U_{ij}(a_i^* a_j^*)(\vec{a}_i \cdot \vec{a}_j)]$

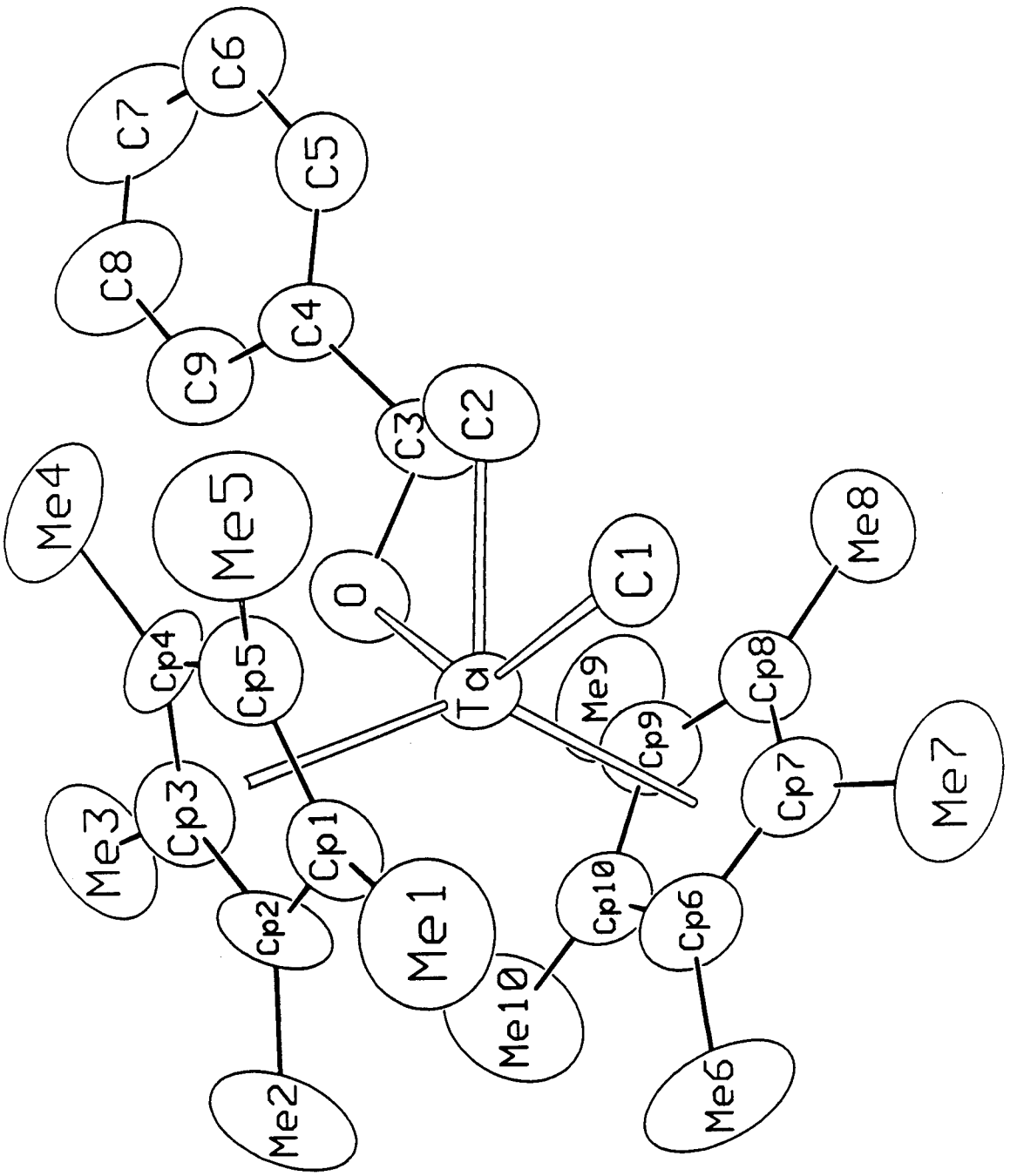

Figure 9. ORTEP drawing with atom labels of O-*exo*-$Cp^*_2Ta(OCH(C_6H_5)CH_2)CH_3$.

Table 8. Anisotropic Thermal Displacement Parameters x10^4 for

O-*exo*-Cp*$_2$Ta(OCH(C$_6$H$_5$)CH$_2$)CH$_3$.

Atom	U_{11}	U_{22}	U_{33}	U_{12}	U_{13}	U_{23}
Ta	426(3)	411(3)	429(3)	−33(4)	208(2)	−39(3)
C1	672(93)	743(87)	461(75)	31(82)	111(71)	45(72)
O	393(64)	601(54)	737(61)	−20(44)	215(54)	31(47)
C2	343(96)	755(100)	897(121)	−18(78)	107(90)	−162(82)
C3	761(138)	539(91)	780(109)	171(86)	264(108)	−43(82)
C4	655(119)	543(98)	573(99)	40(85)	207(95)	−137(76)
C5	1093(137)	546(96)	609(100)	99(96)	288(102)	77(81)
C6	1484(175)	573(113)	734(114)	74(117)	462(119)	44(96)
C7	1448(189)	1010(154)	925(137)	−457(149)	472(143)	−517(117)
C8	1007(149)	1249(153)	864(129)	−353(128)	202(115)	−568(115)
C9	655(127)	831(112)	768(114)	−65(94)	203(102)	−148(93)
Cp1	608(120)	266(78)	576(95)	−87(76)	4(86)	−31(68)
Cp2	653(118)	372(87)	876(134)	164(88)	456(110)	113(79)
Cp3	420(106)	593(100)	644(104)	−106(81)	8(89)	−57(80)
Cp4	644(116)	857(107)	246(81)	9(95)	164(85)	−21(72)
Cp5	571(113)	586(97)	634(102)	−55(80)	259(96)	98(77)
Me1	1378(162)	609(104)	988(129)	−267(107)	417(123)	147(91)
Me2	1696(186)	566(104)	1454(160)	450(115)	929(149)	340(102)
Me3	610(119)	963(122)	1087(133)	81(98)	−135(106)	177(97)
Me4	1192(136)	1230(124)	495(88)	−201(118)	387(92)	99(96)
Me5	1024(148)	1270(141)	1306(150)	−127(113)	757(130)	185(115)
Cp6	962(149)	442(101)	562(101)	−127(106)	311(102)	−56(80)
Cp7	974(130)	453(103)	521(88)	−92(102)	337(92)	35(79)
Cp8	507(118)	628(124)	561(95)	25(86)	177(87)	4(77)
Cp9	743(129)	550(109)	685(107)	−84(95)	373(98)	37(79)
Cp10	774(124)	812(122)	543(92)	101(114)	504(91)	131(92)
Me6	2048(218)	853(118)	902(122)	−195(126)	780(141)	−328(98)
Me7	830(120)	1424(142)	722(102)	−342(120)	−32(98)	−64(106)
Me8	970(139)	868(115)	798(113)	162(102)	319(106)	233(90)
Me9	1004(144)	1112(128)	771(112)	−348(111)	329(109)	−47(94)
Me10	1173(161)	1558(163)	1523(168)	425(132)	1058(142)	550(131)

The form of the displacement factor is:

$$\exp -2\pi^2(U_{11}h^2a^{*2} + U_{22}k^2b^{*2} + U_{33}\ell^2c^{*2} + 2U_{12}hka^*b^* + 2U_{13}h\ell a^*c^* + 2U_{23}k\ell b^*c^*)$$

Table 9. Assigned Hydrogen Parameters for O-*exo*-$Cp^*_2Ta(OCH(C_6H_5)CH_2)CH_3$.

x, y and $z \times 10^4$

Atom	x	y	z	B
H1C1	9625	−2741	8737	5.6
H2C1	9593	−1204	8429	5.6
H3C1	9610	−2471	7894	5.6
H1C2	8507	−3809	6953	6.4
H2C2	8918	−4720	7661	6.4
HC3	7474	−5525	7565	6.4
HC5	8289	−6592	6510	7.3
HC6	7655	−8302	5505	8.1
HC7	6151	−8261	4802	9.5
HC8	5187	−6644	5044	9.9
HC9	5768	−5061	6103	7.2
H1M1	8941	1073	8529	8.9
H2M1	8616	2177	7857	8.9
H3M1	9382	1106	7887	8.9
H1M2	6365	795	7919	9.5
H2M2	6390	1876	7287	9.5
H3M2	7196	1805	8087	9.5
H1M3	5638	−1219	5892	9.3
H2M3	5474	−294	6532	9.3
H3M3	5672	−1898	6678	9.3
H1M4	7753	−2133	5607	8.4
H2M4	6712	−1828	5374	8.4
H3M4	7148	−3113	5906	8.4
H1M5	9641	−786	7122	10.8
H2M5	9133	114	6383	10.8
H3M5	9059	−1523	6343	10.8
H1M6	7927	−49	9998	9.9
H2M6	7355	575	9183	9.9
H3M6	8413	484	9441	9.9
H1M7	9867	−2497	9728	9.9
H2M7	9468	−2439	10396	9.9
H3M7	9525	−1071	9946	9.9
H1M8	9006	−5118	8919	8.4
H2M8	8247	−5792	9172	8.4
H3M8	9057	−4994	9782	8.4
H1M9	6211	−4713	7904	9.0
H2M9	6022	−4508	8678	9.0
H3M9	6764	−5575	8645	9.0
H1M0	6006	−1008	8954	11.2
H2M0	5627	−2384	8488	11.2
H3M0	5838	−1079	8063	11.2

Table 10. Complete Distances and Angles for O-*exo*-$Cp^*_2Ta(OCH(C_6H_5)CH_2)CH_3$.

Distance(Å)			Angle(°)			
Ta	-C1	2.271(12)	Ta	-C2	-C3	91.1(9)
Ta	-C2	2.236(14)	C2	-C3	-O	99.2(11)
Ta	-O	2.053(8)	C3	-O	-Ta	100.9(7)
Ta	-CpA	2.198	O	-Ta	-C2	62.8(4)
Ta	-CpB	2.220	CpA	-Ta	-CpB	135.8
Ta	-Cp1	2.492(14)	CpA	-Ta	-C1	99.2
Ta	-Cp2	2.542(15)	CpA	-Ta	-C2	113.0
Ta	-Cp3	2.463(15)	CpA	-Ta	-O	98.0
Ta	-Cp4	2.487(14)	CpB	-Ta	-C1	96.4
Ta	-Cp5	2.516(14)	CpB	-Ta	-C2	111.2
Ta	-Cp6	2.484(17)	CpB	-Ta	-O	100.1
Ta	-Cp7	2.535(15)	C1	-Ta	-C2	71.4(5)
Ta	-Cp8	2.546(14)	O	-Ta	-C1	134.2(4)
Ta	-Cp9	2.536(16)	C2	-C3	-O	99.2(11)
Ta	-Cp10	2.480(16)	C4	-C3	-O	111.2(11)
O	-C3	1.436(17)	C4	-C3	-C2	120.4(12)
C2	-C3	1.51(2)	C5	-C4	-C3	119.7(13)
C3	-C4	1.57(2)	C9	-C4	-C3	121.2(13)
C4	-C5	1.37(2)	C9	-C4	-C5	118.8(14)
C4	-C9	1.37(2)	C6	-C5	-C4	120.6(15)
C5	-C6	1.40(2)	C7	-C6	-C5	119.9(17)
C6	-C7	1.36(3)	C8	-C7	-C6	118.9(18)
C7	-C8	1.37(3)	C9	-C8	-C7	121.4(17)
C8	-C9	1.37(2)	C8	-C9	-C4	120.3(15)
Cp1	-Cp2	1.37(2)	Cp5	-Cp1	-Cp2	105.5(12)
Cp1	-Cp5	1.47(2)	Me1	-Cp1	-Cp2	129.6(13)
Cp1	-Me1	1.49(2)	Me1	-Cp1	-Cp5	122.7(13)
Cp2	-Cp3	1.39(2)	Cp3	-Cp2	-Cp1	110.6(13)
Cp2	-Me2	1.51(2)	Me2	-Cp2	-Cp1	122.4(14)
Cp3	-Cp4	1.39(2)	Me2	-Cp2	-Cp3	126.3(14)
Cp3	-Me3	1.49(2)	Cp4	-Cp3	-Cp2	107.2(13)
Cp4	-Cp5	1.38(2)	Me3	-Cp3	-Cp2	126.8(14)
Cp4	-Me4	1.53(2)	Me3	-Cp3	-Cp4	125.0(13)
Cp5	-Me5	1.54(2)	Cp5	-Cp4	-Cp3	109.2(13)
Cp6	-Cp7	1.34(2)	Me4	-Cp4	-Cp3	124.9(13)
Cp6	-Cp10	1.40(2)	Me4	-Cp4	-Cp5	125.6(13)
Cp6	-Me6	1.53(2)	Cp4	-Cp5	-Cp1	106.8(12)
Cp7	-Cp8	1.41(2)	Me5	-Cp5	-Cp1	128.0(13)
Cp7	-Me7	1.52(2)	Me5	-Cp5	-Cp4	124.3(13)
Cp8	-Cp9	1.41(2)	Cp10	-Cp6	-Cp7	109.2(15)
Cp8	-Me8	1.50(2)	Me6	-Cp6	-Cp7	123.6(15)
Cp9	-Cp10	1.41(2)	Me6	-Cp6	-Cp10	124.3(15)
Cp9	-Me9	1.51(2)	Cp8	-Cp7	-Cp6	109.0(14)
Cp10	-Me10	1.51(2)	Me7	-Cp7	-Cp6	124.2(14)

Table 10. (Cont.)

			Angle(°)
Me7	-Cp7	-Cp8	124.9(13)
Cp9	-Cp8	-Cp7	107.6(13)
Me8	-Cp8	-Cp7	125.1(13)
Me8	-Cp8	-Cp9	126.6(13)
Cp10	-Cp9	-Cp8	106.5(13)
Me9	-Cp9	-Cp8	128.5(14)
Me9	-Cp9	-Cp10	124.2(14)
Cp9	-Cp10	-Cp6	107.7(14)
Me10	-Cp10	-Cp6	128.9(15)
Me10	-Cp10	-Cp9	121.8(14)

Appendix 2. IR and mass spectral data for *cis* and *trans*-ethyleneoxide-d_2.

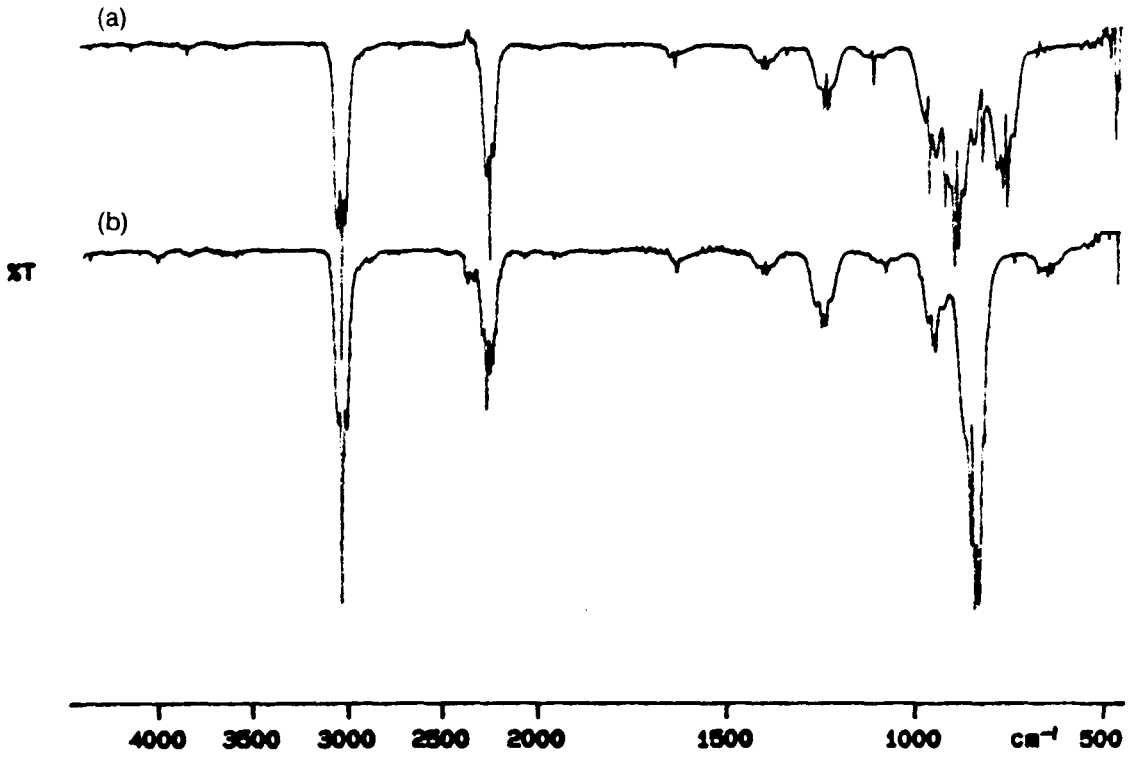

Figure 11. (a) Gas phase IR spectrum of *trans*-ethyleneoxide-d_2. (b) Gas phase IR spectrum of *cis*-ethyleneoxide-d_2.

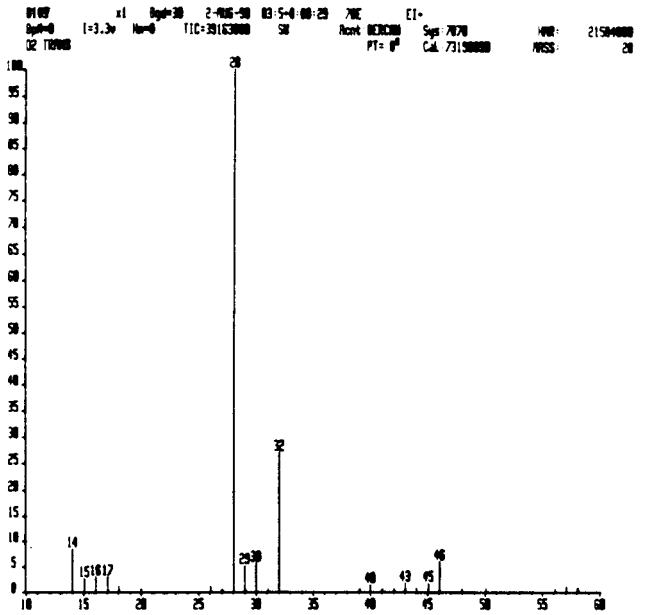

Figure 12. Mass spectrum of *trans*-ethyleneoxide-d_2 (m/z=46).

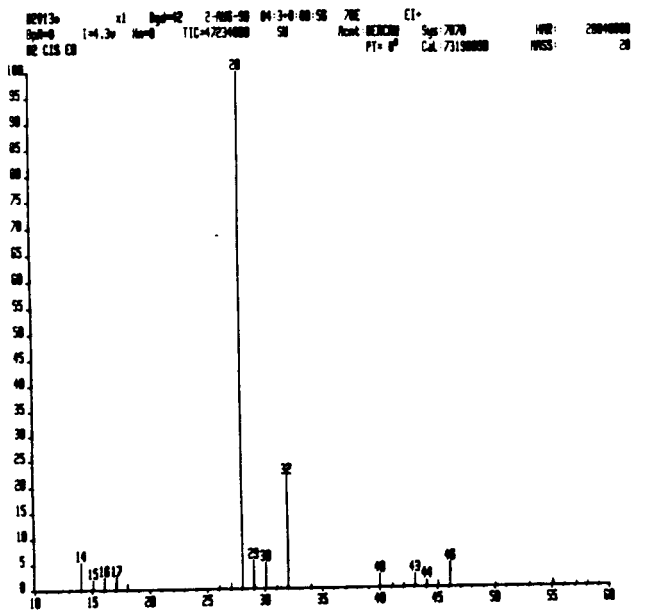

Figure 13. Mass spectrum of *cis*-ethyleneoxide-d_2 (m/z=46).

CHAPTER 2

Investigations of α-Migrations of Permethyltantalocene Alkylidene Hydrides and Alkylidene Alkyls

Abstract: Treatment of $Cp^*_2TaCl_2$ with a variety of substituted benzyl potassium reagents affords an equilibrium mixture of $Cp^*_2Ta(=CHC_6H_5)H$, **1**, and $Cp^*_2Ta(o\text{-}CH_2C_6H_4)H$, **2**, which interconvert presumably *via* the unstable 16 electron intermediate $[Cp^*_2Ta(CH_2C_6H_5)]$. Several derivatives substituted at the phenyl ring have been prepared to explore the effect of both sterics and electronics on the α-hydrogen migration equilibrium. Trapping of the benzyl intermediate by methylenetrialkylphosphoranes results in methylene transfer to give $Cp^*_2Ta(=CH_2)CH_2C_6H_5$. The substituted benzyl derivatives have provided a system to determine the influence of phenyl substituents on migratory aptitude of the benzyl group.

INTRODUCTION

Alpha and beta migrations are of fundamental importance to many stoichiometric and catalytic processes based on organometallic compounds. Although a great deal of work has been accomplished to determine the factors that influence β-migratory insertion processes, there are far fewer well-defined examples of α-migratory insertions. Alkylidene insertions are generally thought to be analogous to the well examined carbonyl insertions. However, there are still many unanswered questions related to the mechanism(s) operating in α-migratory insertion reactions.[1] One reason for the lack of clear cut examples of α-hydride migrations is the instability of either the starting alkylidene or the final alkyl product. Another reason is a stepwise α-hydride elimination followed by reductive elimination is very difficult to distinguish from a concerted 4-center α-hydrogen abstraction mechanism unless the alkylidene hydride species is directly observed.

The first example of a reversible α hydrogen elimination process was reported by Cooper and Green[2] in 1974. Loss of ethylene upon thermolysis of $[Cp_2W(CH_3)(CH_2CH_2PMe_2Ph)]PF_6$ permitted isolation and characterization of both a kinetic, $[Cp_2W(H)(CH_2PMe_2Ph)]PF_6$, and thermodynamic, $[Cp_2W(CH_3)(PMe_2Ph)]PF_6$, product. Labelling studies were in agreement with the two postulated, but unobserved, intermediates, $[Cp_2W(CH_3)]^+$ and $[Cp_2W(=CH_2)H]^+$, in a reversible equilibrium.

Schrock and co-workers[3] have reported a well defined example of a reversible α-hydride elimination on tantalum. In this example, magnetization transfer studies show the hydride resonance of $(PMe_3)_3TaI_2(=CHCMe_3)H$ exchanging with the alkylidene resonance in the ^1H NMR spectrum, indicating the two protons are equivalent at some point. It seems very reasonable that this alkylidene hydride species would be in a fast and reversible equilibrium with an unobserved alkyl species, $(PMe_3)_3TaI_2(CH_2CMe_3)$.

Methylidene insertion into a metal alkyl is invoked as the principal chain growth mechanism in Fischer-Tropsch Catalysis ($CO + H_2 \longrightarrow$ linear alkanes).[4] Although the pace of research in this area has diminished in recent years, investigation of Fischer-Tropsch Catalysis accounted for a high percentage of the organometallic research being done in both industry and academics only a decade ago. There are several apparent examples of well-defined alkyl to alkylidene migrations in the literature.[5] However, in each of these cases, the alkylidene alkyl species is generated in solution, and the alkyl then migrates to form an unsaturated (extended) alkyl complex, which is either trapped or undergoes a β-hydride elimination to form an olefin hydride complex.

We have previously shown that the permethyltantalocene fragment is very useful in stabilizing normally very reactive combinations of ligands (*e.g.*, benzyne-hydride, alkylidene-hydrides, alkylidene-alkyls, oxo-hydride and peroxo-alkyls)[6] permitting some detailed mechanistic work to be performed. Although transmetallation reactions involving "Gibson's Reagent," $Cp^*_2TaCl_2$, are sensitive to the nature of the Grignard, alkyllithium, or alkylpotassium, solvent, temperature and reaction time, a clean reaction can often be obtained. Shown below (Figure 1) is a summary of the alkylation chemistry that our research group has established for Gibson's Reagent. It should be noted that if a beta hydride elimination pathway is available, an olefin hydride complex will be obtained. As is usually the case in organometallic chemistry, lack of β-hydrogens or severe steric interactions are required to observe α-hydride elimination or *ortho*-metallation products.

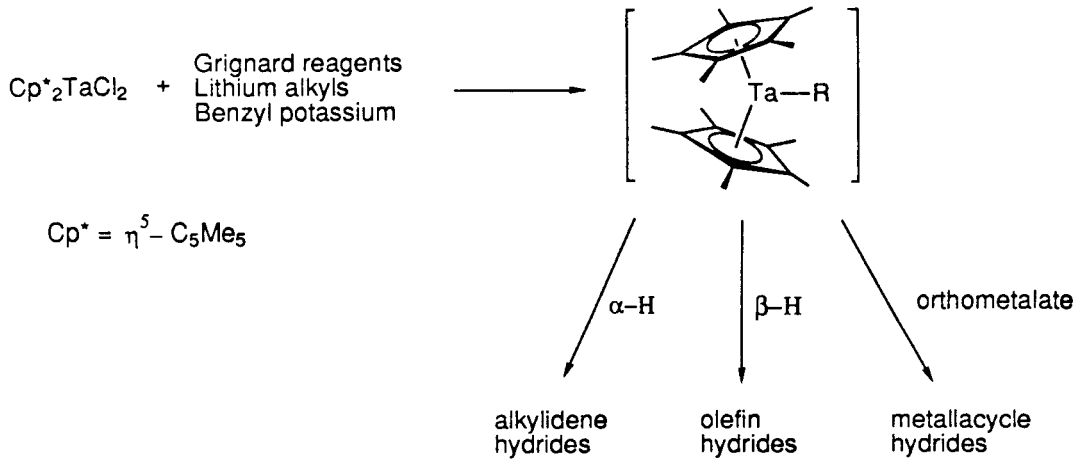

Figure 1. Alkylation chemistry of $Cp^*_2TaCl_2$

Discussed in the following chapter are some studies which have been designed to probe the effect of substituents on the phenyl ring of $Cp^*_2Ta(=CHC_6H_4X)H$ (**1**) on the rate of hydride migration. The effect of steric constraints on the equilibrium between $Cp^*_2Ta(=CHC_6H_4X)H$ (**1**) and $Cp^*_2Ta(o\text{-}CH_2C_6H_3X)H$ (**2**) is also investigated. The influence of phenyl substituents of $Cp^*_2Ta(=CH_2)CH_2C_6H_4X$ on the migratory aptitude of the benzyl group has also been examined.

RESULTS AND DISCUSSION

Preparation and Characterization of 1 and 2. The equilibrium mixture of **1** and **2**, as shown in Figure 2, is obtained upon mixing $Cp^*_2TaCl_2$ with excess, highly reactive and pyrophoric benzyl potassium. We generally think of this reaction proceeding *via* $[Cp^*_2TaCl]$ from reduction by the first equivalent of benzyl potassium followed quickly by metathesis to $[Cp^*_2TaCH_2C_6H_5]$. This 16 electron benzyl intermediate, $[Cp^*_2TaCH_2C_6H_5]$, has not been observed but is thought to be in reversible equilibrium with $Cp^*_2Ta(=CHC_6H_5)H$ (**1**) and $Cp^*_2Ta(o\text{-}CH_2C_6H_4)H$ (**2**). Tantalum=CHPh π-bonding directs the phenyl group toward one of the Cp*'s of **1**. One would expect this to raise the energy level of the ground state. We suggest

this destabilization of the ground state of 1 is responsible for the generation of substantial amounts of the strained tantalabenzocyclobutene hydride (2).

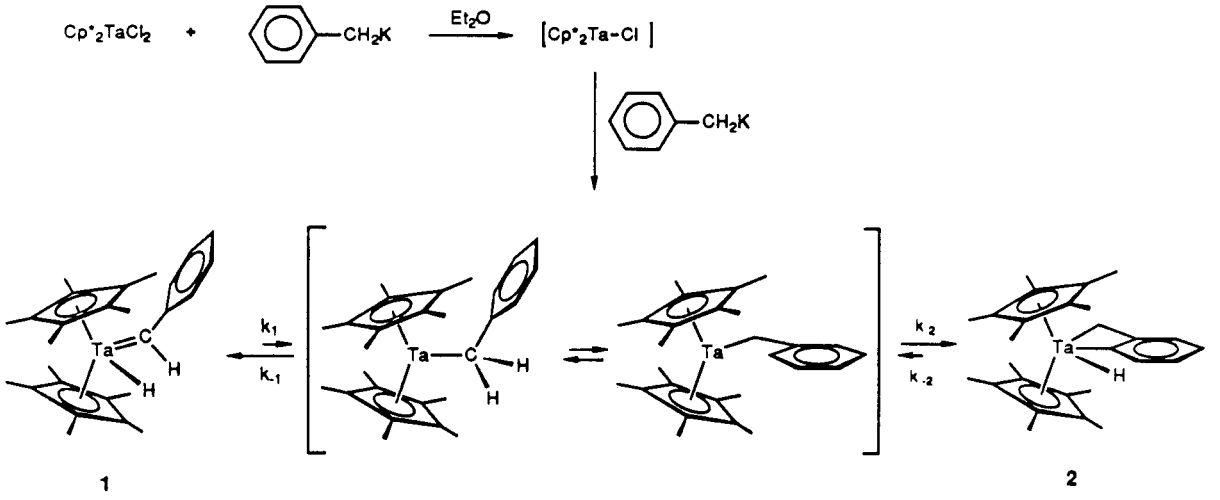

Figure 2. Synthesis of the reversible equilibrium mixture of 1 and 2.

Hoffmann and co-workers[7] theoretical orbital description of the bent metallocene complexes is generally accepted and in very good agreement with experiment. The generally most useful conclusion from Hoffmann's paper is that there are three frontier orbitals of accessible energy located in the equatorial wedge of bent metallocenes. This obrital description helps to explain the observation of two Cp* resonances for the benzylidene hydride, 1, in the low temperature ^{1}H NMR spectrum (<30°C, 400 MHz) of the equilibrium mixture. The p-orbital of the benzylidene carbon has to be in the plane of the wedge to overlap with the third metal orbital to form the π-bond resulting in the phenyl ring being directed at one of the Cp*'s and the hydrogen directed at the other one, and thus, the observed inequivalence of the Cp*'s.

At room temperature, however, only one resonance is observed in the ^{1}H and ^{13}C NMR spectrum for the Cp*'s of 1. Presumably there is a fast exchange process occurring at room

temperature that equilibrates the Cp*'s. This observation can be easily explained by either rotation around the Ta=C bond or a reversible α-H migratory insertion to give the benzyl intermediate with equivalent benzyl hydrogens. We favor the second explaination for the following reasons (1) magnetization transfer between $Cp^*_2Ta(=C\underline{H}C_6H_5)H$ and $Cp^*_2Ta(=CHC_6H_5)\underline{H}$ is observed, (2) $[Cp^*_2Ta(CH_2C_6H_5)]$ may be trapped with CO, $CNCH_3$ or N_2O to yield $Cp^*_2Ta(L)(CH_2C_6H_5)$ (L = CO, $CNCH_3$, O) and (3) the metallacycle, **2**, observed in equilibrium with **1** likely arises from *ortho*-metallation of $[Cp^*_2Ta(CH_2C_6H_5)]$. Magnetization transfer between the protons of the two Cp* resonances of the benzylidene hydride (**1**) and the tantalabenzocyclobutene (**2**) is also observed at room temperature (Figure 3). Exchange between the hydride resonance of **2** and a down field doublet, assigned to an ortho proton on the phenyl ring of the benzylidene (**1**) was indicated by selective irradiation experiments. Magnetization transfer was also observed between the hydride of **1** and methylene of the metallacycle (**2**).

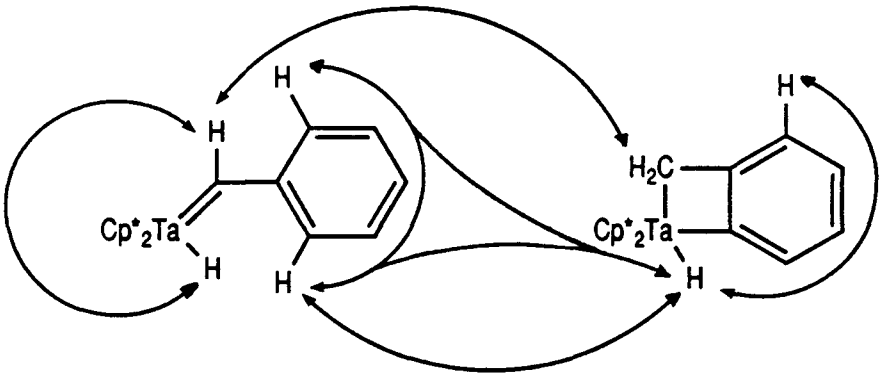

Figure 3. Magnetization transfer observations.

The effect of temperature on the equilibrium was examined by ^{1}H NMR spectroscopy. The data, obtained over a temperature range of -30°C to 60°C, is listed in Table 1. There is a slight curve[8] in the Van't Hoff Plot (Figure 4) which we have not been able to explain. Ignoring this curvature results in a $\Delta S°$ = 2.1(2) e.u., $\Delta H°$ = 1.0(1) kcal·mol^{-1} and $\Delta G°_{50°C}$ = 0.5(1) kcal·mol^{-1}.

Table 1. Temperature dependence of the equilibrium between **1** and **2** in the ^{1}H-NMR.

T(°C)	1/T	K_{eq}	ln[K_{eq}]
-30(1)	4.12x10^{-3}(2)	0.32(2)	-6.64(7)
-10(1)	3.80x10^{-3}(2)	0.36(2)	-6.61(7)
0(1)	3.66x10^{-3}(1)	0.38(2)	-6.58(6)
10(1)	3.53x10^{-3}(1)	0.40(2)	-6.56(5)
20(1)	3.41x10^{-3}(1)	0.43(2)	-6.52(4)
30(1)	3.30x10^{-3}(1)	0.46(2)	-6.48(4)
40(1)	3.19x10^{-3}(1)	0.50(2)	-6.45(5)
50(1)	3.10x10^{-3}(1)	0.53(2)	-6.41(4)
60(1)	3.00x10^{-3}(1)	0.59(2)	-6.34(4)

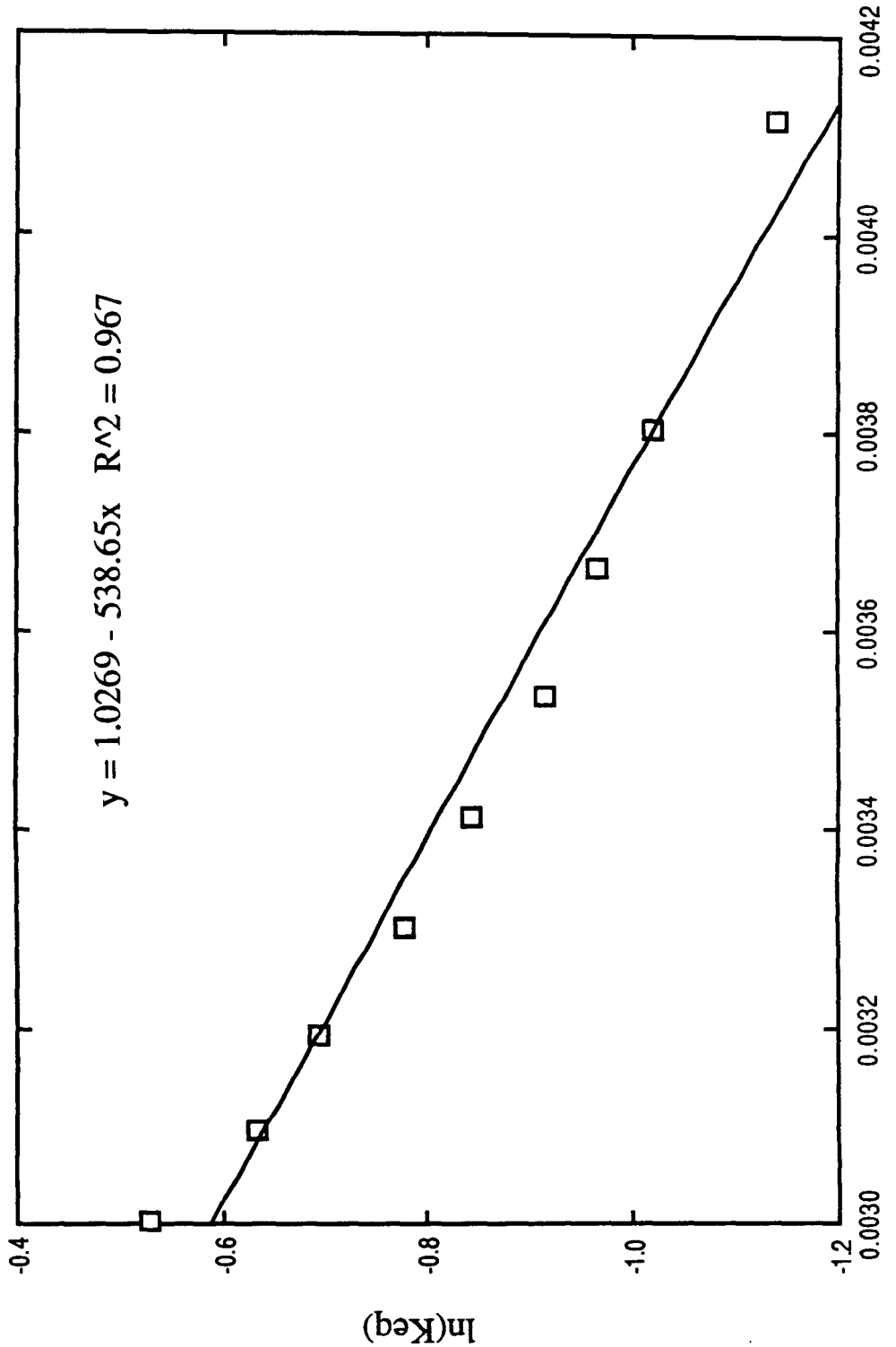

Figure 4. Van't Hoff plot for equilibrium mixture of 1 and 2.

In an attempt to observe the benzyl intermediate (which should have permitted us to map out the energy profile for the equilibrium between **1** and **2**) the low temperature photolysis of $Cp^*_2Ta(CO)CH_2C_6H_5$ was conducted. The aim of this experiment was to induce carbonyl loss at low temperature (-78°C) and record the spectrum before α-hydrogen elimination or *ortho*-metallation could occur. Unfortunately, no change was observed in the ^1H NMR spectrum upon photolysis.

Investigation of Electronic and Steric Effects on the Equilibrium Between 1 and 2. In an attempt to investigate the effect of varying electronics and sterics on the equilibrium between **1** and **2**, several related complexes with different substituents were prepared by treating $Cp^*_2TaCl_2$ with the appropriately substituted benzyl potassium reagent. The generality of these syntheses are limited by the nature of the benzyl potassium reagents that can be prepared. *Meta*-methoxy is the only electron-withdrawing substituent for which the benzyl potassium salt was prepared successfully. The benzyl potassium reagents with other electron withdrawing groups (NO_2, F, CF_3 and CN) are extremely unstable and often explosive. Moreover, permethyltantalocene alkylidene hydrides (*vide infra*) have been shown to react with alkyl and aryl halides to give the corresponding alkylidene halides, further limiting the number of benzyl derivatives that could be used in this study.

Substituted benzyl potassium reagents successfully prepared include: $X\text{-}C_6H_4CH_2K$ (X = H, p-CH_3, m-CH_3, p-OCH_3, m-OCH_3, p-$N(CH_3)_2$, m-$N(CH_3)_2$ and p-$C(CH_3)_3$), 3,5-$(CH_3)_2C_6H_3CH_2K$, $C_6H_5CH(CH_3)K$, $C_6H_5C(CH_3)_2K$ and $(CH_3)_5C_6CH_2K$. The equilibrium constants for each of the monosubstituted derivatives were determined (coalesence) and are listed in Table 2.

Table 2. Equilibrium constants, K_{eq}, for substituted derivatives of **1** and **2**.

Substituent*	%1	%2	K_{eq}(28°C)
H	72	28	0.40
m-CH_3	37	63	1.67
p-CH_3	56	44	0.79
m-OCH_3	20	80	4.00
p-OCH_3	84	16	0.20
m-$N(CH_3)_2$	23	77	3.29
p-$N(CH_3)_2$	33	67	2.03
p-$C(CH_3)_3$	60	40	0.67
3,5-dimethyl	60	40	

**meta* and *para* designations refer to the substitution pattern of the benzylidene.

As shown in Equation 1, a *para* substituent of $Cp^*_2Ta(=CHC_6H_4X)H$ becomes a *meta* substituent of $Cp^*_2Ta(o\text{-}CH_2C_6H_3X)H$, relative to the metallated position of the phenyl ring. However, a *meta* substituent (Eqn. 2) of $Cp^*_2Ta(=CHC_6H_4X)H$ can be either *ortho* or *para* to the metallated position in the metallacycle, $Cp^*_2Ta(o\text{-}CH_2C_6H_3X)H$. Surprisingly, we observed both **2a** and **2b** (Eqn. 2) in approximately equal amounts for several of the *meta* substituted metallacycles in the low temperature ^1H NMR spectrum (<-40°C, 400 MHz). The relative amounts of **2a** and **2b** present at low temperature in toluene-d_8 is dependent upon the substituent. Unless there is a dominating effect from one of the substitution patterns, a straightforward correlation between electron donating/accepting ability of the substituent and the equilibrium constant should not be expected.

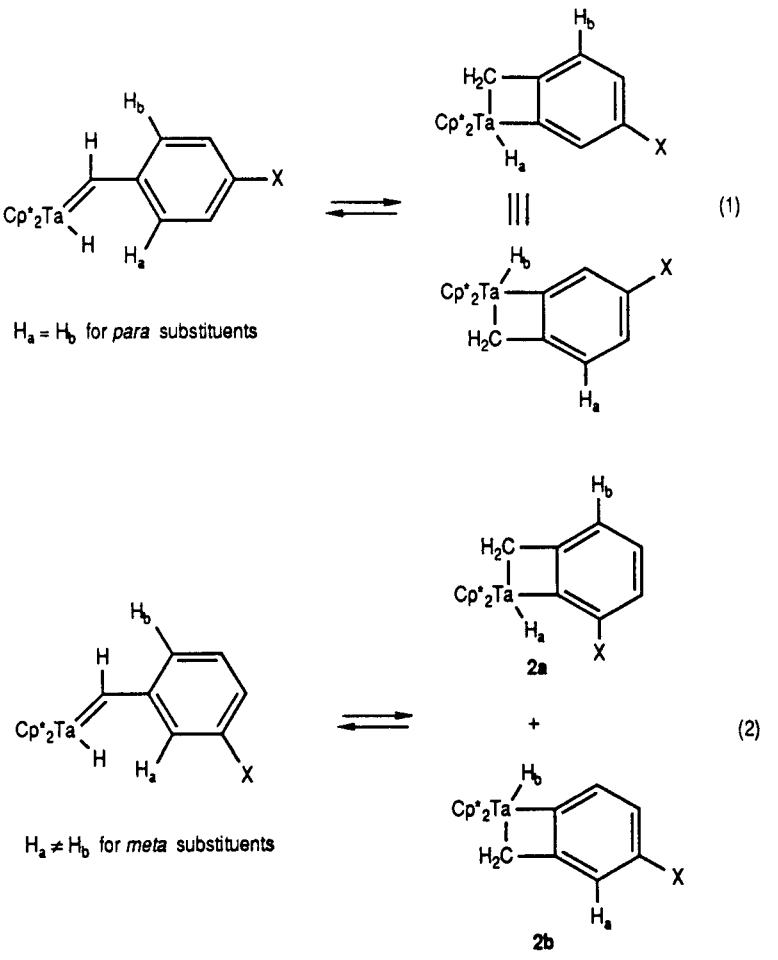

Several substituted derivatives of **1** and **2** were prepared with the anticipation they would shed some light on the role (if any) sterics play in shifting the equilibrium between these tautomers. The symmetrical 3,5-dimethylbenzyl derivative can result in only one isomer for the metallacycle **2**. If steric interactions were significant between the methyl group directed toward the hydride and the hydride, as we expected prior to observing both **2a** and **2b**, a shift of the equilibrium toward the benzylidene would be expected. As shown in Figure 5, K_{eq} of the 3,5-dimethyl derivative is virtually identical to the K_{eq} for the *meta*-methyl derivative, indicating

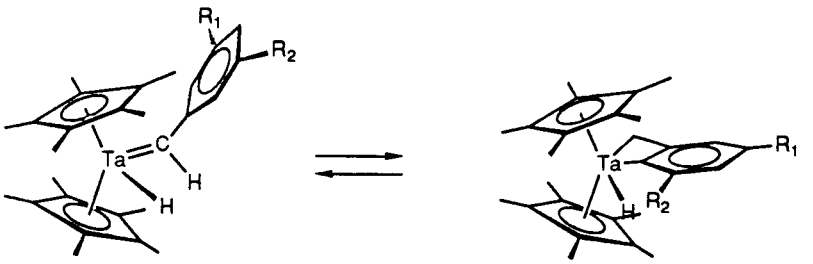

1 2

R_1	R_2	%1	%2
Me	Me	60	40
Me	H	63	37

Figure 5. The effect of 3,5-dimethyl *vs* m-Me substituents on the equilibrium between **1** and **2** at 25°C.

One would expect steric interactions in the plane of the wedge (metallacycle) to be much less than when the phenyl ring and substituent are directed at a Cp* (benzylidene). Thus, based on steric effects only, a bulky substituent on the phenyl ring would shift the equilibrium toward the metallacycle. Surprizingly, the *p*-CMe_3 substituent shifted the equilibrium toward the benzylidene (**1**:**2** = 60:40), relative to the *p*-Me substituent (**1**:**2** = 44:56), Figure 6, although the effect is very small. The results of the *p*-CMe_3 case indicate electronic effects must override the effects due to sterics. One explanation why steric interactions might not be as severe as initially thought is that substituents in the *para* position are located beyond the methyl groups of the Cp* rings.

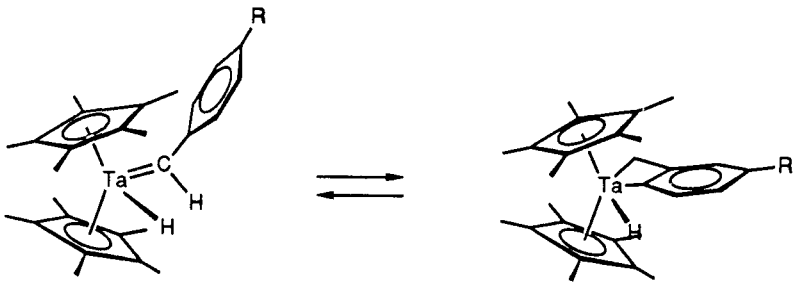

1 2

R	%1	%2
Me	44	56
CMe_3	60	40

Figure 6. The effect of *p*-CMe_3 *vs* p-Me substituents on the equilibrium between **1** and **2** at 25°C

In an attempt to shift the equilibrium completely to the benzylidene, a derivative with the *ortho* positions blocked, thus, preventing *ortho*-metallation, was prepared. No evidence for a benzylidene species was obtained in the reaction of the benzyl potassium salt of hexamethylbenzene, $(CH_3)_5C_6CH_2K$, with $Cp^*_2TaCl_2$. Instead, a very clean C-H activation of an *ortho*-methyl C-H bond, affording tantalabenzocyclopentene hydride (Equation 3) was observed. This is very similar to the niobium complex $(\eta^5\text{-}C_5H_4Si(CH_3)_3)_2Nb(o\text{-}CH_2C_6H_4CH_2)H$ reported by Lappert and co-workers.[9]

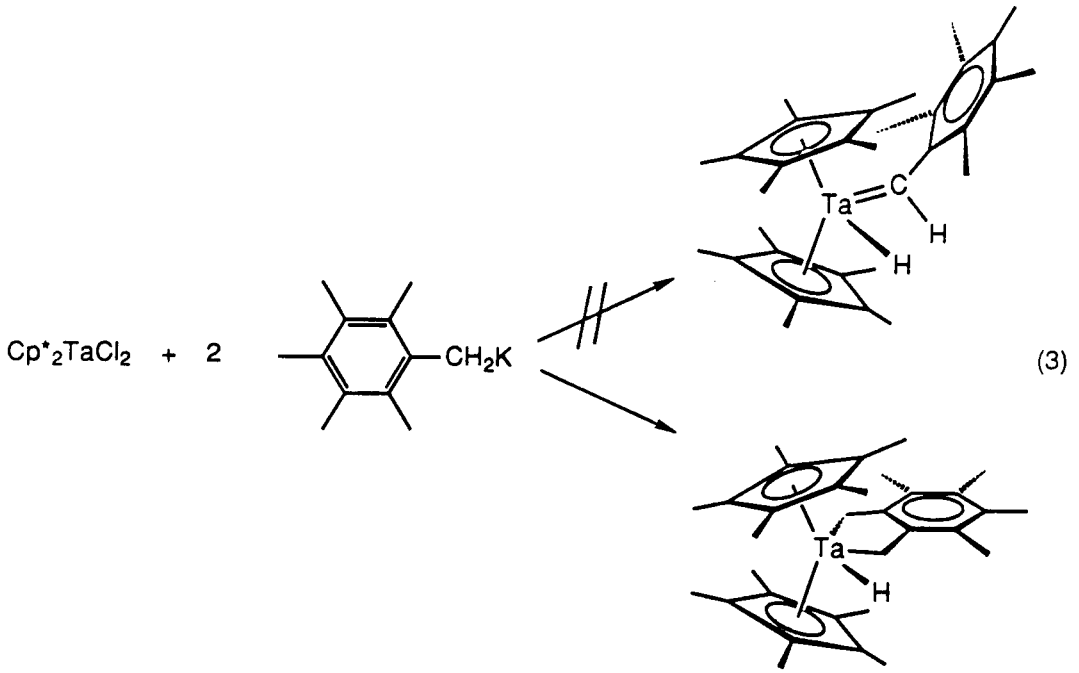

(3)

Methyl substitution on the α-carbon of the benzyl intermediate introduces β-hydrogen elimination as a possible reaction pathway. Treatment of $Cp^*_2TaCl_2$ with at least two equivalents of $C_6H_5CH(CH_3)K$ results in an inseparable mixture of *exo*-$Cp^*_2Ta(CH_2{=}CHC_6H_5)H$ and an unidentified compound (Eqn. 45). Although an equilibrium mixture of both *exo* and *endo* isomers are obtained in the preparation of normal ring niobocene and tantalocene styrene hydrides,[10] only *endo*-$Cp^*_2Ta(C_6H_5CH{=}CH_2)H$ is observed upon reaction of excess styrene with $Cp^*_2TaH_3$ at 120°C.[6b] The benzyl potassium synthetic route described here results in the first *exo* olefin hydride complex of a permethylmetallocene. Also shown in Equation 4 is the thermolysis of the *exo*-$Cp^*_2Ta(CH_2{=}CHC_6H_5)H$ to give the *endo* isomer. The unidentified compound also in solution remains unchanged throughout the thermolysis of the *exo* to *endo* isomerization, indicating it is not in equilibrium with the styrene hydride complex. Several attempts were made to isolate *exo*-$Cp^*_2Ta(CH_2{=}CHC_6H_5)H$ free of the contaminant, but without success. Due to these problems, the mechanism of this isomerization was not further pursued.

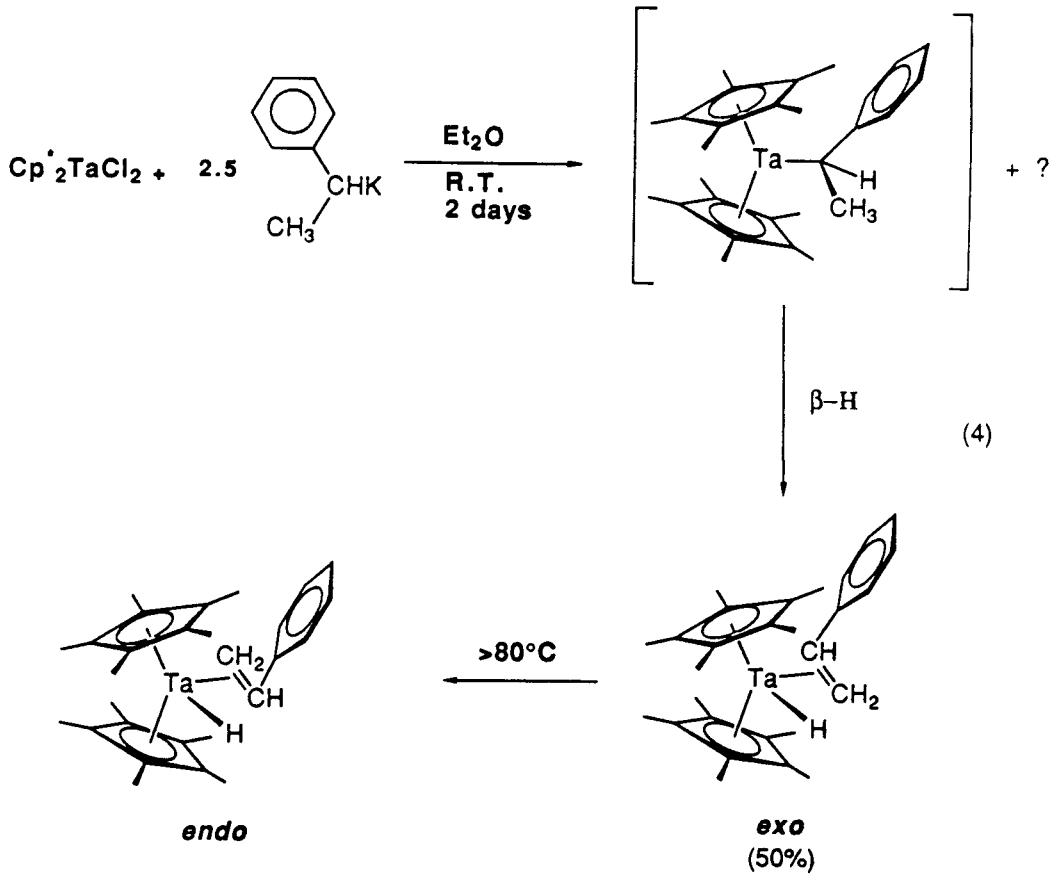

The equilibrium mixture of **1** and **2** is thermally stable up to approximately 80°C in a solution of toluene-d_8. Above this temperature the mixture decomposes to the "tuck-in" complexes shown in Figure 7. This equilibrium mixture of "tuck-ins" was observed previously by our research group[6f] from the thermolysis of $Cp^*_2Ta(=CH_2)H$. The mechanism is believed to involve the oxidative addition of one C-H bond of a Cp* ligand to the benzyl intermediate, followed by the reductive elimination of toluene and activation of another C-H bond of a second Cp* methyl group.

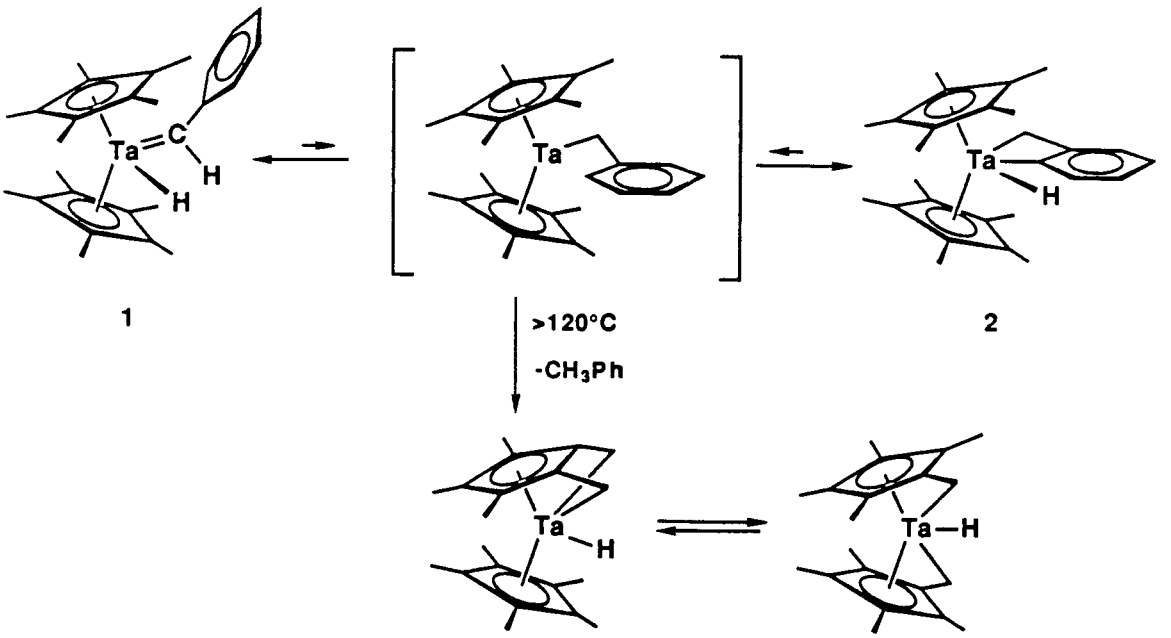

Figure 7. Thermolysis of **1** and **2**.

Minor efforts were directed at obtaining the unsubstituted cyclopentadienyl (η^5-C_5H_5) analogs of **1** and **2**. If steric interactions between the phenyl ring and the methyl groups of the Cp*'s are responsible for the destabilization of the ground state (and thus the observation of the metallacycle (**2**)), we would anticipate that benzylidene hydride, $Cp_2Ta(=CHC_6H_5)H$, would dominate such that no metallacycle hydride would be observed. When Cp_2TaCl_2 is treated with either $C_6H_5CH_2K$ or $C_6H_5CH_2MgCl$ several products are observed. Attempts to purify these mixtures were unsuccessful, and these compounds were not pursued further.

Substituent Effect on the Rate of α-Hydrogen Migration to Benzylidene. The rate of hydrogen migration to benzylidene, k_1 (Figure 2), was determined by coalescence of the Cp* resonance of the benzylidene hydride **1** in the ^1H NMR spectra at 90, 400 and 500 MHz field strengths, since the temperature at which coalescence occurs is dependent upon the strength

of the magnetic field. Coalescence at different field strengths can then be used to determine the $\Delta H^{\ddagger}$ and $\Delta S^{\ddagger}$ for the hydrogen migration. The $\Delta G^{\ddagger}_{50\,^{\circ}C}$ can also be extrapolated from this data to compare these values with similar migrations at the same temperature. The frequency shift difference for the two peaks, $\Delta\nu$, in the frozen out (slow exchange limit) spectra and the temperature at which the coalescence occurs, T_c, were used to generate a $\ln(k/T_c)$ *vs* $1/T_c$ plot. The rate constant, k, was determined at each of these different field strengths by using the equation $k = \Delta\nu\pi(2)^{-1/2}$. This slope and intercept resulted in $\Delta G^{\ddagger}_{50\,^{\circ}C}$ = 14.6(2) kcal · mol^{-1}, $\Delta H^{\ddagger}$ = 11.0(2) kcal · mol^{-1} and $\Delta S^{\ddagger}$ = -11(2) e.u.

Rate constants and values for $\Delta G^{\ddagger}_{50\,^{\circ}C}$ for α-hydride migratory insertions of permethyltantalocene alkylidene hydrides are listed in Table 3. The slightly lower value of $\Delta G^{\ddagger}_{50\,^{\circ}C}$ for the benzylidene hydride compared to the methylidene hydride and vinylidene hydride could be due to the previously discussed steric interaction between the phenyl ring and the Cp* methyl groups resulting in a higher ground state energy for the benzylidene hydride (1). The steric differences among these three will also result in different transition states; however, models suggest ground state energy differences should dominate.

Table 3. Relative α-hydride insertion barriers ($\Delta G^{\ddagger}_{50\,^{\circ}C}$) and rates (k) for various permethyltantalocene alkylidene hydride derivatives.

	$\Delta G^{\ddagger}_{50\,^{\circ}C}$(kcal · mol^{-1})	$k_{50\,^{\circ}C}$(sec^{-1})
$Cp^*_2Ta(=CHC_6H_5)H$[a]	14.6(2)	10^4
$Cp^*_2Ta(=CH_2)H$[b]	16.2(5)	10^2
$Cp^*_2Ta(=C=CH_2)H$[b]	17(1)	10^1

(a) this work. (b) from ref 5(f).

To probe the effect of electronics on the rate of α-hydride migratory insertions, we conducted the low temperature coalescence of the Cp* resonance of several substituted derivatives of 1 (see Table 4). The general trend from these data is that electron-donating substituents on the phenyl group result in a decrease in the rate of α-hydride migration. The best fit of the Hammet plot (Figure 8) resulted in ρ = 1.1. The decrease in rate can be accounted for by either a ground state argument (electron-donating substituents lowering the ground state of the benzylidene hydride), a transition state argument (electron-donating substituents raise the energy level of the transition state) or a combination of both. Early transition metal unstabilized alkylidenes are generally thought of as nucleophillic in character, *i.e.*, their polarity is $M^{\delta+}=C^{\delta-}R_2$. Indeed, as discussed in Chapter 1, $Cp^*_2Ta(=CH_2)CH_3$ reacts very readily with benzaldehyde, as expected for a nucleophillic alkylidene. Thus, ground state arguments do not account for the decrease in rate of hydrogen migration, since electron donating substituents would be expected to destabilize the ground state of a nucleophillic carbene and increase the rate of migration. The predicted destabilization of the ground state must be more than compensated for by the transition state destabilization.

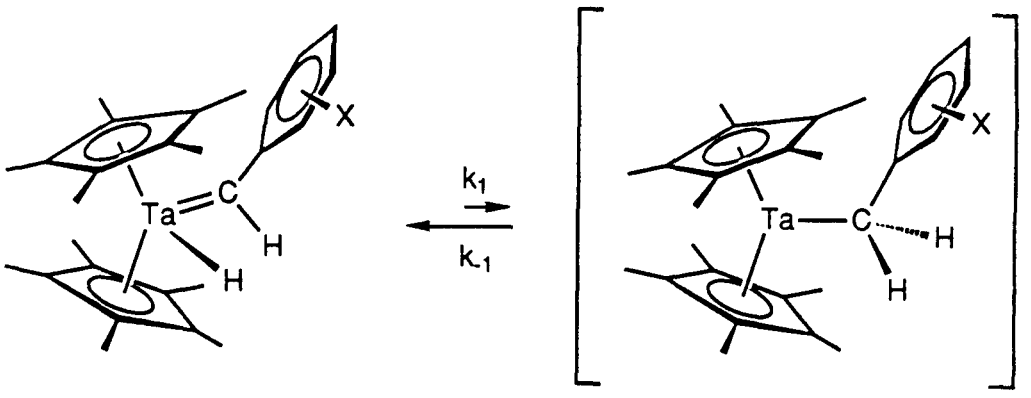

1

Table 4. Substituent effects on the rate of hydrogen migration shown above.

X	σ	k_1(-15°C) (x10^2 sec-1)	ΔG‡(-15°C)
m-OMe	0.12	11(3)	11.5(2)
H	0.00	5.0(5)	11.8(1)
m-CH_3	-0.07	4.6(9)	11.9(2)
p-CH_3	-0.17	4.0(9)	12.0(2)
m-NMe_2	-0.21	4.3(9)	11.9(2)
p-NMe_2	-0.60	1.4(4)	12.5(2)

Figure 8. Hammett Plot of Hydrogen Migration to Benzylidene

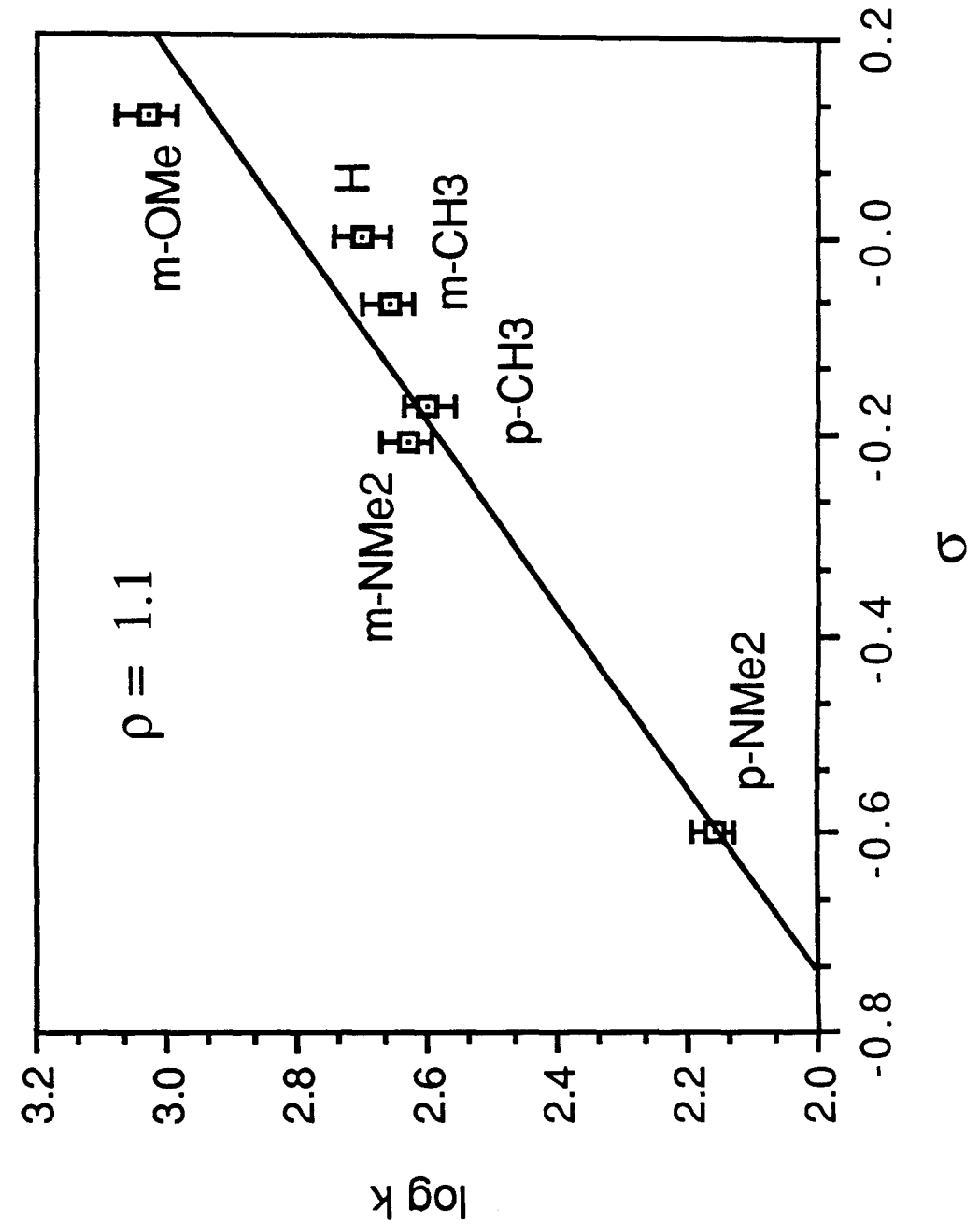

Substituent Effects on Migratory Aptitude of α-Benzyl to Methylidene. The equilibrium mixture of **1** and **2** reacts cleanly with methylenetrialkylphosphoranes to afford $Cp^*_2Ta(=CH_2)CH_2C_6H_5$ and trialkylphosphine, presumably by a simple trapping reaction with methylene transfer and phosphine dissociation (Equation 5). No intermediates in the formation of the methylene complex have been observed. Although alkylidene transfer directly to a metal center has not always been well established in organometallic chemistry, several recent examples have been reported.[11]

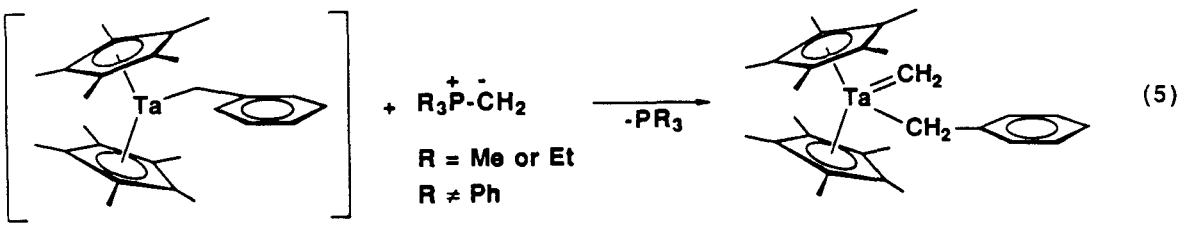

(5)

X-ray quality crystals were obtained upon cooling a petroleum ether solution of $Cp^*_2Ta(=CH_2)CH_2C_6H_5$ and the structure determined by Lawrence Henling. The ORTEP drawing is shown in Figure 9 and significant distances and angles are listed in Table 5. The molecule crystallizes in the triclinic system, in space group P1 (#2), with a = 8.514(3), b = 10.049(4), c = 15.491(12) Å, α = 95.14(4)°, β = 95.12(4)°, γ = 113.03(2)°, V = 1203.6(11)Å^3, z = 2 and density = 1.536 gm · cm^{-3}.

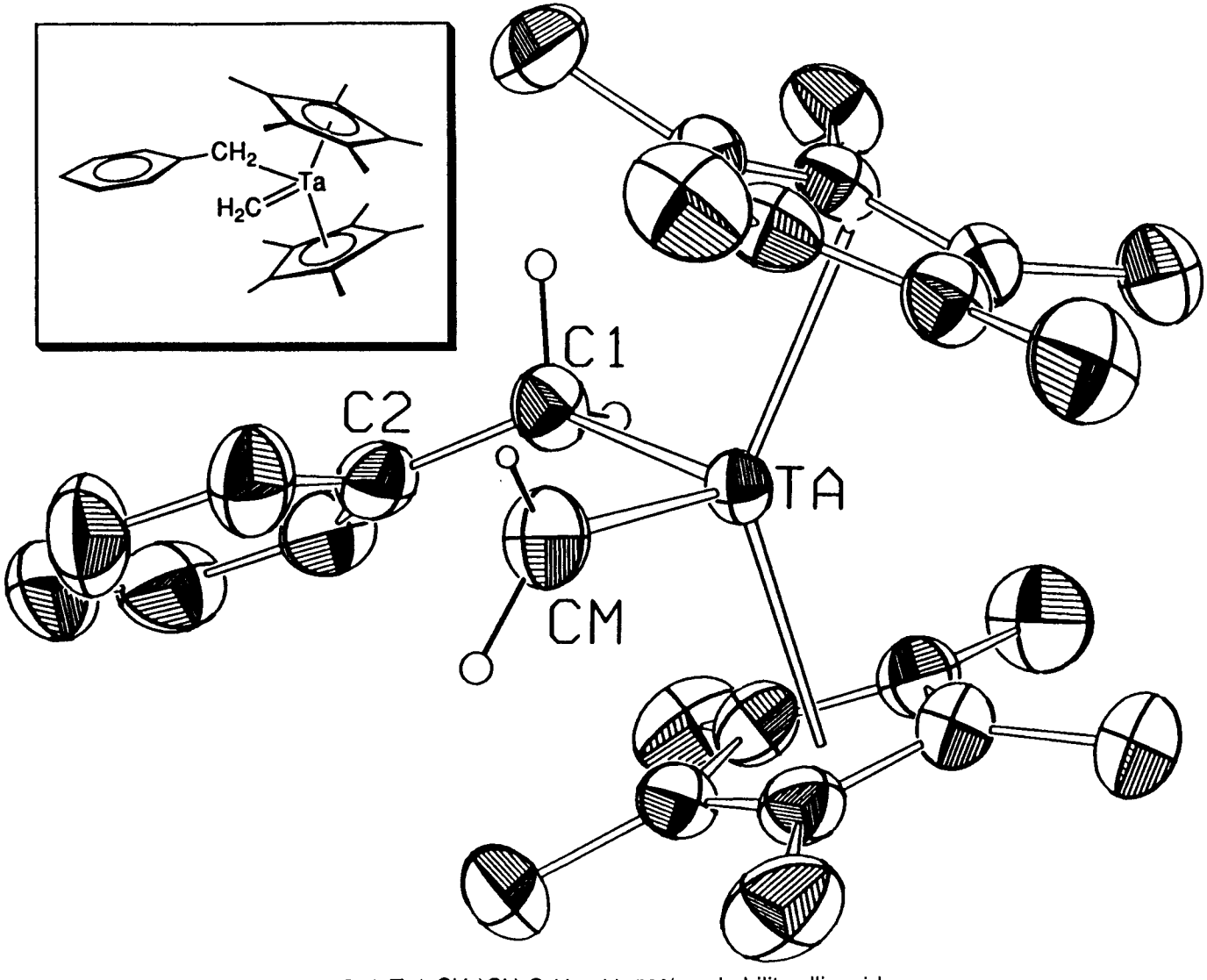

Figure 9. ORTEP drawing of $Cp^*_2Ta(=CH_2)CH_2C_6H_5$ with 50% probability ellipsoids.

Table 5. Distances and angles obtained from the X-ray crystal determination of $Cp^*_2Ta(=CH_2)CH_2C_6H_5$.

Distance(Å)			Angle(°)			
Ta	-CM	1.985(5)	Cp*A	-Ta	-CM	103.6
Ta	-C1	2.299(5)	Cp*B	-Ta	-CM	104.2
Ta	-Cp1	2.464(5)	Cp*B	-Ta	-C1	104.1
Ta	-Cp2	2.472(5)	Cp*A	-Ta	-C1	102.8
Ta	-Cp3	2.500(5)	Cp*A	-Ta	-Cp*B	139.7
Ta	-Cp4	2.485(5)	CM	-Ta	-C1	93.3(2)
Ta	-Cp5	2.492(5)	Ta	-C1	-C2	124.4(3)
Ta	-Cp6	2.472(5)	Cp5	-Cp1	-Cp2	107.9(4)
Ta	-Cp7	2.510(5)	Me1	-Cp1	-Cp2	126.1(4)
Ta	-Cp8	2.475(5)	Me1	-Cp1	-Cp5	125.4(4)
Ta	-Cp9	2.446(5)	Cp3	-Cp2	-Cp1	108.1(4)
Ta	-Cp10	2.444(5)	Me2	-Cp2	-Cp1	127.0(4)
Ta	-Cp*A	2.172	Me2	-Cp2	-Cp3	124.0(4)
Ta	-Cp*B	2.159	Cp4	-Cp3	-Cp2	108.6(4)
Cp1	-Cp2	1.421(6)	Me3	-Cp3	-Cp2	127.7(5)
Cp1	-Cp5	1.413(6)	Me3	-Cp3	-Cp4	122.9(5)
Cp1	-Me1	1.499(7)	Cp5	-Cp4	-Cp3	108.0(4)
Cp2	-Cp3	1.400(7)	Me4	-Cp4	-Cp3	123.7(5)
Cp2	-Me2	1.500(7)	Me4	-Cp4	-Cp5	126.8(5)
Cp3	-Cp4	1.405(7)	Cp4	-Cp5	-Cp1	107.5(4)
Cp3	-Me3	1.498(8)	Me5	-Cp5	-Cp1	125.3(4)
Cp4	-Cp5	1.425(7)	Me5	-Cp5	-Cp4	125.6(4)
Cp4	-Me4	1.500(8)	Cp10	-Cp6	-Cp7	107.4(4)
Cp5	-Me5	1.498(7)	Me6	-Cp6	-Cp7	125.1(4)
Cp6	-Cp7	1.420(7)	Me6	-Cp6	-Cp10	126.6(4)
Cp6	-Cp10	1.413(7)	Cp8	-Cp7	-Cp6	108.3(4)
Cp6	-Me6	1.506(7)	Me7	-Cp7	-Cp6	125.3(5)
Cp7	-Cp8	1.386(7)	Me7	-Cp7	-Cp8	125.3(5)
Cp7	-Me7	1.500(8)	Cp9	-Cp8	-Cp7	108.7(4)
Cp8	-Cp9	1.419(7)	Me8	-Cp8	-Cp7	123.3(5)
Cp8	-Me8	1.513(8)	Me8	-Cp8	-Cp9	127.1(5)
Cp9	-Cp10	1.411(7)	Cp10	-Cp9	-Cp8	107.3(4)
Cp9	-Me9	1.500(8)	Me9	-Cp9	-Cp8	126.6(5)
Cp10	-Me10	1.508(8)	Me9	-Cp9	-Cp10	123.9(5)
C1	-C2	1.512(7)	Cp9	-Cp10	-Cp6	108.2(4)
C2	-C3	1.383(8)	Me10	-Cp10	-Cp6	125.9(5)
C2	-C7	1.392(7)	Me10	-Cp10	-Cp9	125.4(5)
C3	-C4	1.378(9)	C3	-C2	-C1	122.1(4)
C4	-C5	1.362(10)	C7	-C2	-C1	121.3(4)
C5	-C6	1.363(10)	C7	-C2	-C3	116.4(5)
C6	-C7	1.393(9)	C4	-C3	-C2	122.0(5)
			C5	-C4	-C3	120.9(6)
			C6	-C5	-C4	118.7(7)
			C7	-C6	-C5	120.9(6)
			C6	-C7	-C2	121.0(5)

Bonded to the tantalum atom in the plane bisecting the Cp* rings are the methylidene carbon, CM, at 1.985(5) Å and the C1 carbon of the benzyl group at 2.299(5) Å. The plane containing the methylidene carbon and hydrogen atoms is approximately perpendicular (93(7)°) to the equitorial plane and the hydrogen-carbon-hydrogen angle is 107(4)°. All internal benzyl parameters are normal. The ring of the benzyl group is rotated 37(4)° out of the Ta-C1-CM plane. The Ta-C1-C2 angle is 124.5(3)°, in agreement with an angle of 124.2(6)° for the previously reported compound $Cp^*_2Ta(O_2)CH_2C_6H_5$.[6d] The angle between the two metal carbon bonds is 93.3(2)°.

Thermolysis of $Cp^*_2Ta(=CH_2)CH_2C_6H_5$ cleanly yields *endo*-$Cp^*_2Ta(CH_2=CHC_6H_5)H$, presumably *via* the 16 electron phenethyl intermediate which subsequently undergoes a β-hydrogen elimination, as shown in Equation 6. The rate of disappearance of $Cp^*_2Ta(=CH_2)CH_2C_6H_5$ is cleanly first order, and example is shown in Figure 10. The rate of α-benzyl migration to methylidene in $Cp^*_2Ta(=CH_2)CH_2C_6H_5$ has been determined at six temperatures over a 37°C range (see Eyring plot, Figure 11). Data from the temperature dependence on the rate of benzyl migration lead to a $\Delta H^{\ddagger}$ = 25.6(2) kcal · mol^{-1}, $\Delta S^{\ddagger}$ = -11(4) e.u. and from extrapolation to 50°C $\Delta G^{\ddagger}$ = 29.2(2) kcal · mol^{-1}.

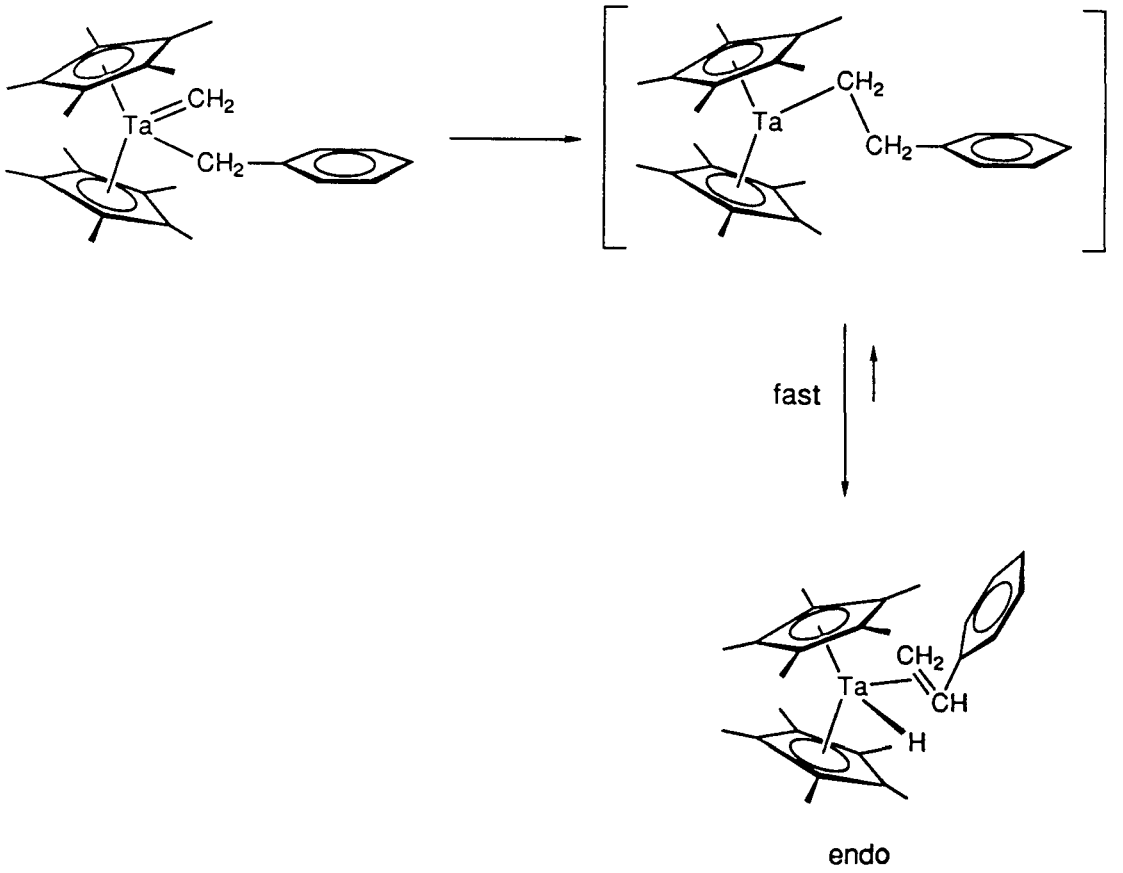

endo

(6)

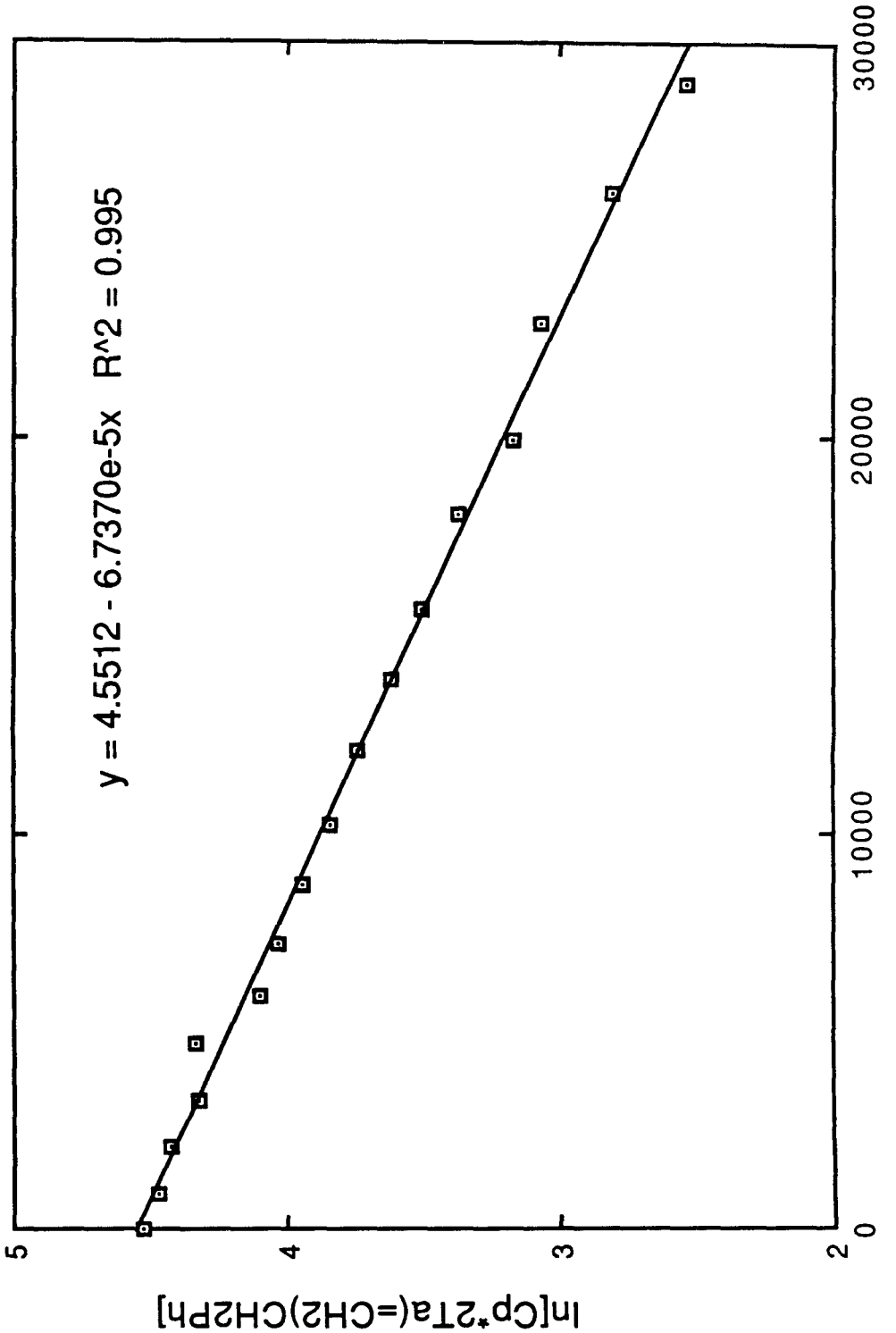

Figure 10. First order plot for rate of decomposition of Cp*2Ta(=CH2)CH2Ph at 115°C.

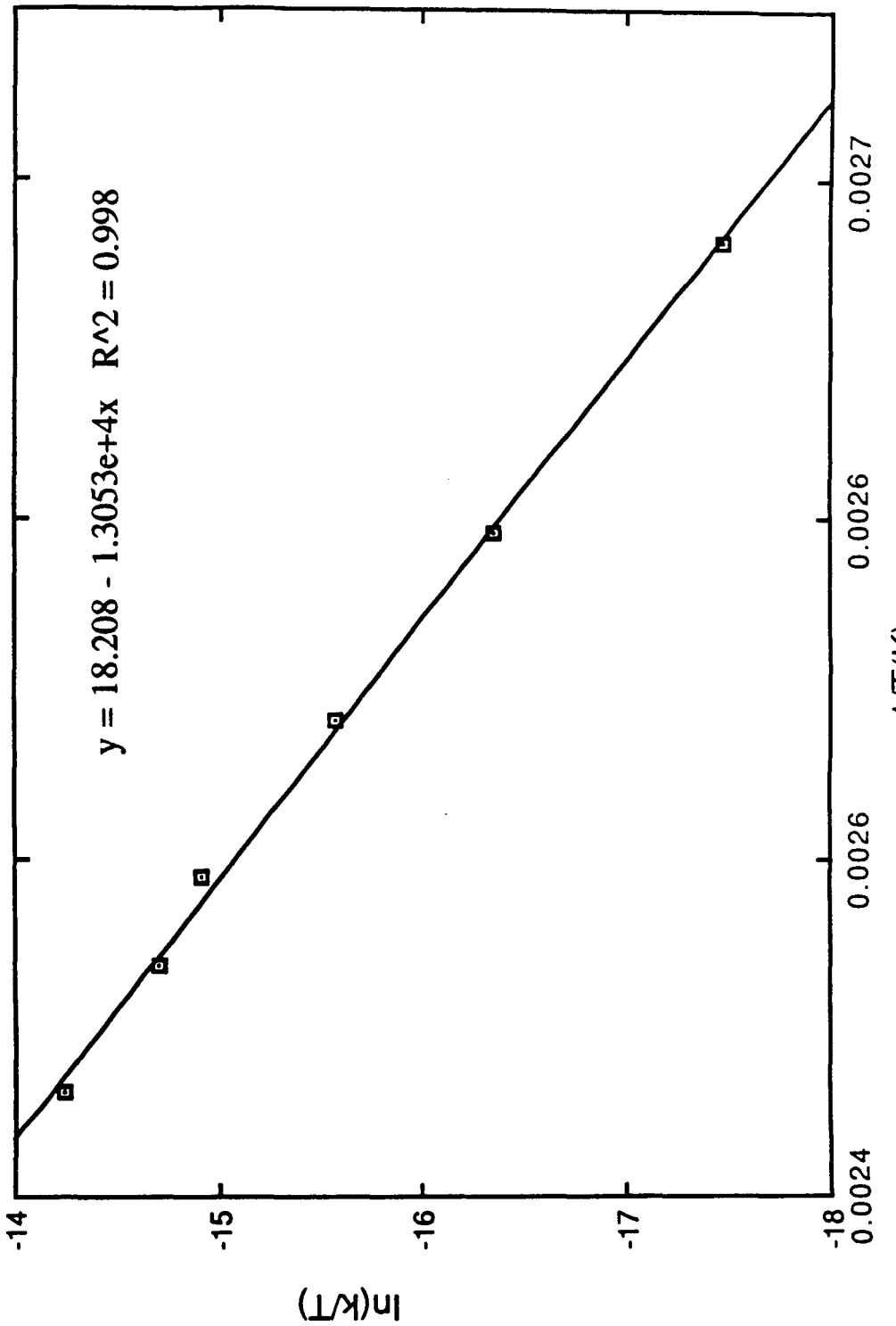

Figure 11. Eyring plot of benzyl migration to methylidene.

Comparison of the rate constants and activation free energies at 50°C for α-benzyl to methylidene migration with other α migrations in the permethyltantalocene system is shown in Table 6. Benzyl and methyl have approximately the same migratory aptitude toward methylidene. Hydride, however, migrates much more readily (and also reversibly) than alkyls or aryls. The larger rate of α-hydride migration is most likely due to the fact that the hydrogen orbital is spherically symmetric, whereas the alkyl and aryl carbon orbitals are directional. Thus, the bridged transition state is more bonding, lower in energy, for hydride. Phenyl migration is much slower than methyl or benzyl migration to methylidene in the permethyltantalocene system for at least two reasons: (1) metal-aryl bond strengths are generally stronger than metal-alkyl bonds and (2) the phenyl ring must rotate 90° prior to migration to achieve a favorable bridging transition state.[11] In contrast, the rate of phenyl migration to CO for $(CO)_5MnR$ is approximately the same as the rate of alkyl migrations to CO.[12] In this classic organometallic example of migratory insertion, it is generally accepted that the ground state stabilization, from the stronger metal-aryl bond strength, is offset by the transition state stabilization obtained with the bridging phenyl group.

Table 6. Relative hydrogen and alkyl α-migratory insertion barriers ($\Delta G^{\ddagger}_{50\,°C}$) and rates ($k_{50\,°C}$) for various permethyltantalocene methylidene hydrides and alkyls.

	$\Delta G^{\ddagger}_{50\,°C}$(kcal · mol^{-1})	$k_{50\,°C}$(sec^{-1})
$Cp^*_2Ta(=CH_2)H$[b]	16.2(5)	10^{2}
$Cp^*_2Ta(=CH_2)CH_2C_6H_5$[a]	29.9(2)	10^{-7}
$Cp^*_2Ta(=CH_2)CH_3$[b]	30.3	10^{-8}
$Cp^*_2Ta(=CH_2)C_6H_5$[c]	34	10^{-11}

(a) this work. (b) from ref 5(f). (c) Trimmer, M.S. Ph.D. Thesis, California Institute of Technology, 1989.

In the previous section we described the effect alkylidene substituents impart on the rate of hydride α migratory insertion. In this section we examine the effect of benzyl group substituents on the rate of benzyl α migratory insertion to methylene. The availability of several substituted benzyl derivatives and the generality of the reaction sequence shown in Equations 5 and 6 resulted in a convenient system to examine the effect of varying the electronic characteristics of the migrating group.

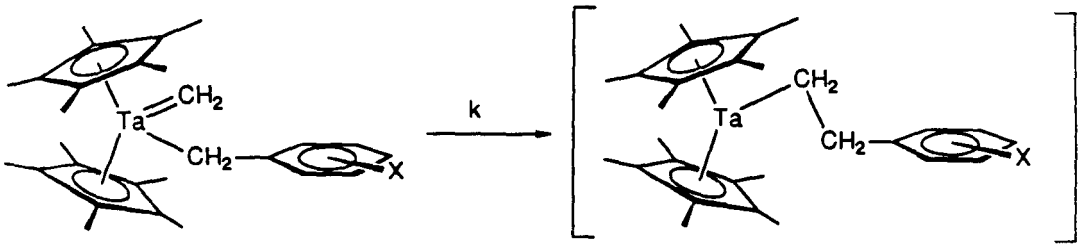

Table 7. Substituent effects on the rate of benzyl migration to methylidene.

X	σ	k(115°C) (x10-5 sec-1)	$\Delta G^{\ddagger}$(115°C)
m-OMe	0.12	6.21(37)	30.4(2)
H	0.00	8.45(2)	30.1(2)
m-CH3	-0.07	7.90(16)	30.2(2)
p-CH3	-0.17	7.90(3)	30.2(2)
m-NMe2	-0.21	7.97(20)	30.2(2)
p-OMe	-0.27	8.97(18)	30.1(2)
p-NMe2	-0.60	14.4(3)	29.7(2)

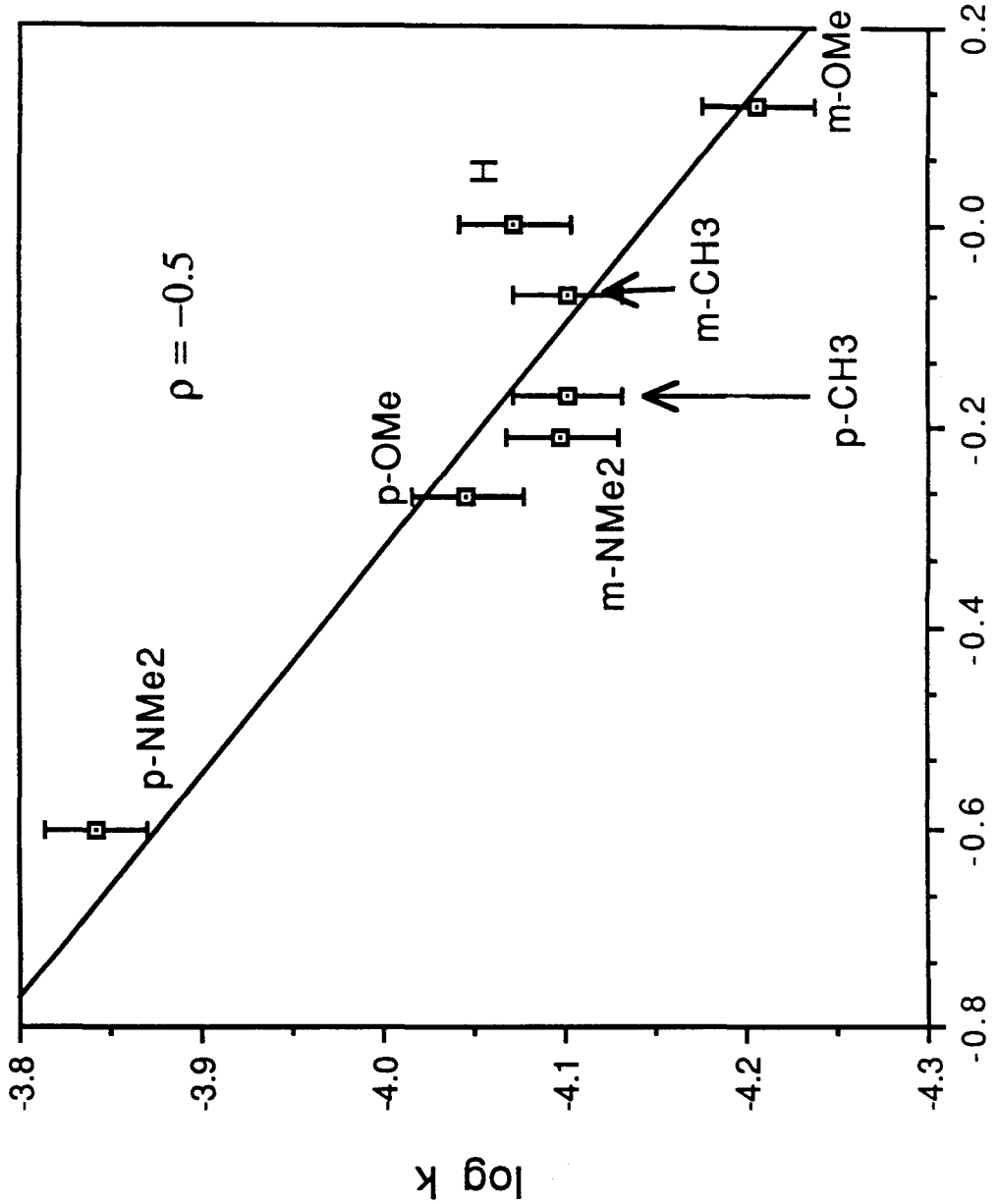

Figure 12. Hammett Plot of Benzyl Migration to Methylidene

The observed trend in the data, shown in Table 7, is that electron-donating substituents on the phenyl ring increase the rate of α-benzyl migration to methylidene. The magnitude of the effect is relatively small (ρ = -0.5, Figure 12), indicating a relatively low polarity for the transition state. Since the effect of the substituents is so small, we cannot say anything conclusive about the relative ground and transition states.

A related system that may have exhibited a larger difference in rates is the phenyl to methylidene migration previously studied by Mark Trimmer,[10] shown in Equation 7. The phenyl migration might have been expected to have a larger effect on the rate of migration because there is one less bond that the electronics would have to be transmitted through, (compared to the benzyl case). Unfortunately, the only derivatives of the benzyne hydride precursor, $Cp^*_2Ta(C_6H_3\text{-}X)H$, that have been prepared successfully are *para* and *meta*-methyl. The corresponding *para* and *meta*-methyl phenyl methylidene complexes have not been prepared, thus their migratory aptitudes have not been determined.

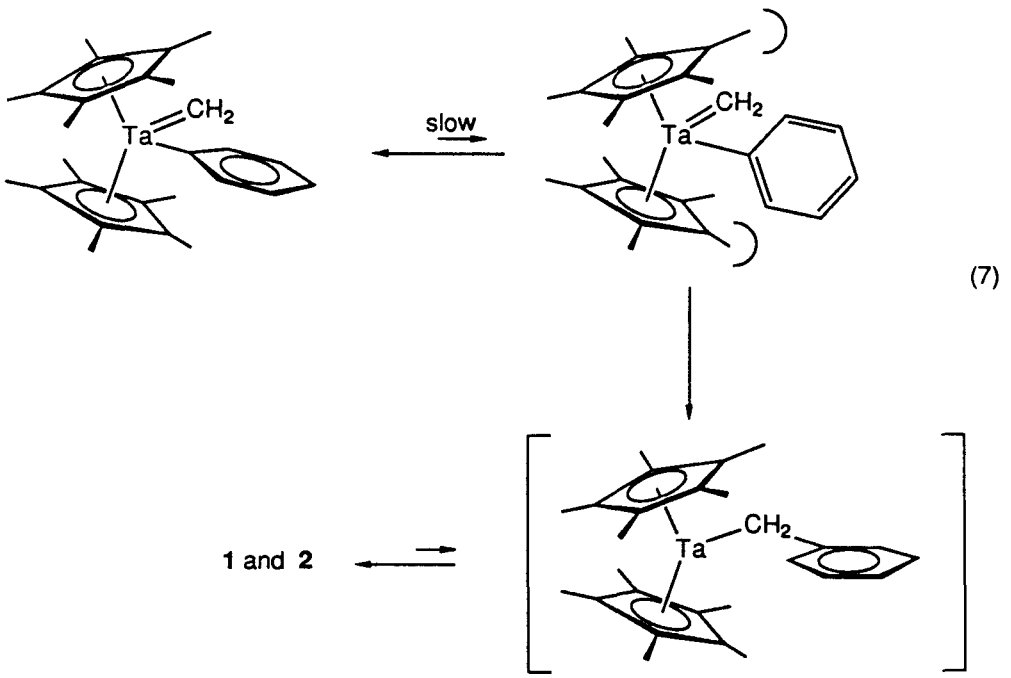

(7)

The isolation of $Cp^*_2Ta(=CHC_6H_5)CH_3$ would have been interesting for several reasons. It may have been instructional to compare the rate of methyl to benzylidene migration with the other α migrations discussed previously. This complex would also present the possibility of another way to make *exo*-$Cp^*_2Ta(CH_2=CHC_6H_5)H$ as shown in Equation 8. The synthetic strategy used in attempting to prepare $Cp^*_2Ta(=CHC_6H_5)CH_3$ involved making a benzylidene halide complex, $Cp^*_2Ta(=CHC_6H_5)X$, followed by a transmetallation reaction with MeLi, MeMgCl or Me_2Zn. The equilibrium mixture of **1** and **2** reacts with CH_3I quickly and quantitatively (by ^1H NMR) to yield $Cp^*_2Ta(=CHC_6H_5)I$. It was also discovered later that chlorobenzene, bromobenzene and iodobenzene react with $Cp^*_2Ta(=CH_2)H$ in a similar fashion to yield $Cp^*_2Ta(=CH_2)Cl$, $Cp^*_2Ta(=CH_2)Br$ and $Cp^*_2Ta(=CH_2)I$. Unfortunately, the products obtained from the alkylation reactions of $Cp^*_2Ta(=CHC_6H_5)I$ were generally impure and did not contain any of the desired $Cp^*_2Ta(=CHC_6H_5)CH_3$.

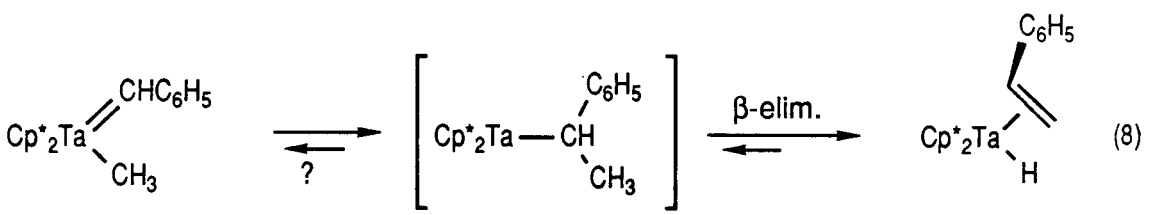

(8)

CONCLUSION

We have made a fairly detailed study of α migrations on the permethyltantalocene fragment. The modest effect of electronics (ρ = 1.1) on the rate of α hydrogen migratory insertions indicates the transition state is only slightly polarized. This decrease in rate of hydrogen migration to benzylidene substituted with electron-donating groups has forced us to formulate the transition state with a partial positive charge on the migrating hydrogen. This is contrary to how migratory insertion reactions are usually envisioned.[6f,13,14] Obviously, a closer look at other α migrations is required to determine the generality of the results discussed here.

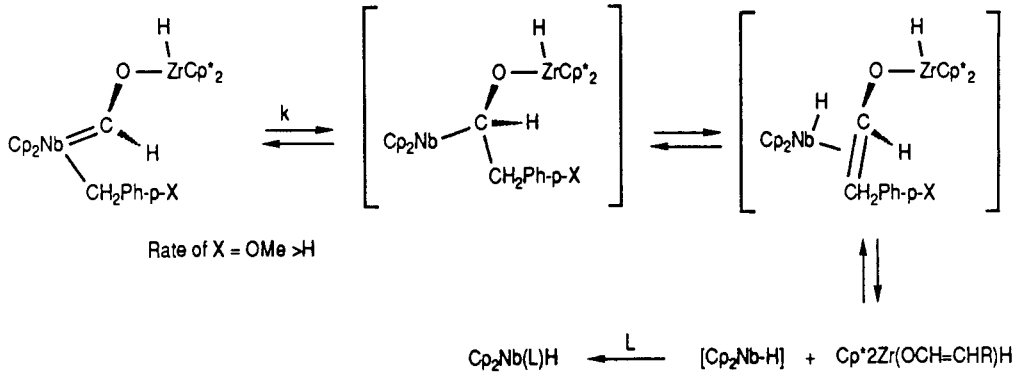

(9)

Rich Threlkel in our research group has previously reported the results of an α-hydrgen and α-alkyl migration to a zirconoxy carbene. The niobocene system he examined is shown in Equation 9. Threlkel suggests the migration is observed because the carbene is electrophillic in character (Fischer type). The qualitative results of the effect of electron-donating substituents on the migrating group slightly accelerating the rate of α migration in the niobocene and permethyltantalocene systems are similar. But, the tantalum-carbene is a nucleophillic alkylidene (Schrock-type) and might be expected to display the opposite substituent effect as an electrophillic carbene. These results question the validity of considering the niobocene

carbene as an electrophillic. Three resonance structures of the niobocene zirconoxy carbene are depicted in Figure 13. Resonance structures A and B are the usual forms considered for Fischer-type carbenes (with B dominating). However, the zirconium's ability to π-bond with the oxygen offers another resonance form (C). Furthermore, we suggest, due to the strong zirconium-oxygen interaction, the niobocene zirconoxy carbene is actually more nucleophillic in character.

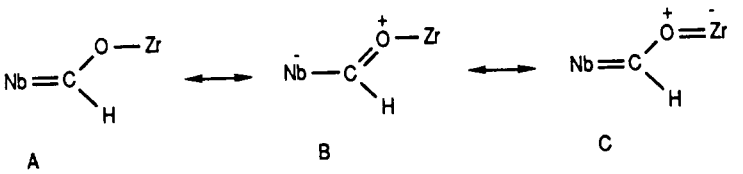

Figure 13. Resonance structures for niobocene zirconoxy carbene.

Table 8. ^{1}H and ^{13}C NMR data recorded at room temperature in benzene-d_6 on a JOEL GX400Q (^{1}H, 399.78 MHz; ^{13}C, 100.38 MHz) unless otherwise noted.

Compound	assignments	^{1}H(ppm)	^{13}C(ppm)	$^{1}J_{CH}$(Hz)
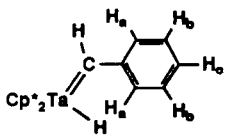 1	$C_5(CH_3)_5$	1.90(s)	12.3(q)	127
	$C_5(CH_3)_5$		108.9(s)	
	Ta=CH	10.67(s)	249.0(d)	112
	Ta-H	2.81(s)		
	C_6H_5:H_a	7.11(d)	124-129[b]	
	H_b	7.25(t)		
	H_c	6.97(t)		
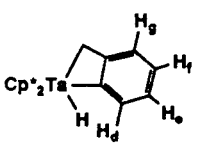 2	$C_5(CH_3)_5$	1.60(s)	11.3(q)	127
	$C_5(CH_3)_5$		107.2(s)	
	CH_2	0.58(s)	4.2(t)	126
	Ta-H	3.79(s)		
	C_6H_4:$H_{d(g)}$	7.61(dt)	124-129[b]	
	$H_{g(d)}$	6.87(d)		
	$H_{e(f)}$	7.18(t)		
	$H_{f(e)}$	7.30(t)		
1-m-CH_3	$C_5(CH_3)_5$	1.92(s)		
	Ta=CH	10.78(s)		
	Ta-H	2.79(s)		
	C_6H_4	6.5-7.5[a]		
	CH_3	2.37(s)		
2-m-CH_3	$C_5(CH_3)_5$	1.62(s)		
	CH_2	0.69(s)		
	Ta-H	3.78(s)		
	C_6H_3	6.5-7.5[a]		
	CH_3	2.30(s)		
1-p-CH_3	$C_5(CH_3)_5$	1.93(s)		
	Ta=CH	10.78(s)		
	Ta-H	2.85(s)		
	C_6H_4	6.5-7.5[a]		
	CH_3	2.29(s)		
2-p-CH_3	$C_5(CH_3)_5$	1.62(s)		
	CH_2	0.63(s)		
	Ta-H	3.84(s)		
	C_6H_3	6.5-7.5[a]		
	CH_3	2.36(s)		

	$C_5(CH_3)_5$	1.94(s)
	Ta=CH	10.65(s)
1-m-OCH_3	Ta-H	2.78(s)
	C_6H_4	6.5-7.5[a]
	OCH_3	[b]
	$C_5(CH_3)_5$	1.63(s)
	CH_2	0.66(s)
2-m-OCH_3	Ta-H	3.59(s)
	C_6H_3	6.5-7.5[a]
	OCH_3	[b]
	$C_5(CH_3)_5$	1.93(s)
	Ta=CH	[c]
1-p-OCH_3	Ta-H	[c]
	C_6H_4	6.5-7.5[a]
	OCH_3	[b]
	$C_5(CH_3)_5$	1.55(s)
	CH_2	0.65(s)
2-p-OCH_3	Ta-H	3.35(s)
	C_6H_3	6.5-7.[a]
	OCH_3	[b]
	$C_5(CH_3)_5$	1.94(s)
	Ta=CH	10.85(s)
1-m-$N(CH_3)_2$	Ta-H	2.85(s)
	C_6H_4	6.5-7.5[a]
	$N(CH_3)_2$	1.85(s)
	$C_5(CH_3)_5$	1.66(s)
	CH_2	0.65(s)
2-m-$N(CH_3)_2$	Ta-H	3.95(s)
	C_6H_3	6.5-7.5[a]
	$N(CH_3)_2$	1.75(s)
	$C_5(CH_3)_5$	1.94(s)
	Ta=CH	10.83(s)
1-p-$N(CH_3)_2$	Ta-H	2.90(s)
	C_6H_4	6.5-7.5[a]
	$N(CH_3)_2$	[b]
	$C_5(CH_3)_5$	1.66(s)
	CH_2	0.60(s)
2-p-$N(CH_3)_2$	Ta-H	3.80(s)
	C_6H_3	6.5-7.5[a]
	$N(CH_3)_2$	[b]

	$C_5(CH_3)_5$	1.93(s)		
	Ta=CH	10.75(s)		
1-m-$C(CH_3)_3$	Ta-H	2.82(s)		
	C_6H_4	6.5-7.5[a]		
	$C(CH_3)_3$	1.23(s)		
	$C_5(CH_3)_5$	1.62(s)		
	CH_2	0.60(s)		
2-m-$C(CH_3)_3$	Ta-H	3.780(s)		
	C_6H_3	6.5-7.5[a]		
	$C(CH_3)_3$	1.34(s)		
	$C_5(CH_3)_5$	1.92(s)		
	Ta=CH	10.78(s)		
1-mesityl	Ta-H	2.82(s)		
	C_6H_4	6.5-7.5[a]		
	$2CH_3$'s	[b]		
	$C_5(CH_3)_5$	1.62(s)		
	CH_2	0.60(s)		
2-mesityl	Ta-H	3.80(s)		
	C_6H_3	6.5-7.5[a]		
	$2CH_3$'s	[b]		
	$C_5(CH_3)_5$	2.11(s)	11.0(q)	127
	$C_5(CH_3)_5$		107.0(s)	
	CH_2(inner)	0.58[a]	26.04(d of t)	122
				$^2J_{CH}$=17
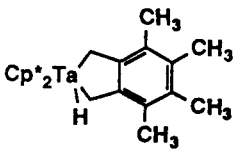	CH_2(outer)	2.22[a]	39.0(t)	122
	Ta-H	[b]		
	$C_6(CH_3)_4$		105-135[b]	
	$C_6(CH_3)_4$	≈1.6[b]	11.1(q)	127
			11.2(q)	127
			11.6(q)	127
			11.8(q)	127
	$C_5(CH_3)_5$	1.73(s)		
	$C_5(CH_3)_5$	1.53(s)		
exo-$Cp^*_2Ta(CH_2{=}CHC_6H_5)(H)$	$=CH_2$	[b]		
	=CH	[b]		
	Ta-H	-1.46(s)		
	C_6H_5	6.5-7.5[a]		
	$C_5(CH_3)_5$	1.67(s)		
	$C_5(CH_3)_5$	1.53(s)		
endo-$Cp^*_2Ta(C_6H_5CH{=}CH_2)(H)$	$=CH_2$	[b]		
	=CH	[b]		
	Ta-H	-1.26(s)		
	C_6H_5	7.6(d)		
		7.2(t)		
		6.9(t)		

	$C_5(CH_3)_5$	1.58(s)	10.8	
	$C_5(CH_3)_5$		100.5	
	CH_2	1.40(s)	18.1	
$Cp^*_2Ta(CO)bz$	CO		274	
	C_6H_5	6.5-7.5[a]	156	
			132	
			127	
			122	
	$C_5(CH_3)_5$	1.67(s)		
	CH_2	1.40(s)		
$Cp^*_2Ta(CNMe)bz$	N-CH_3	3.34(s)		
	C_6H_5	7.60(d)		
		7.27(t)		
		7.05(t)		
	$C_5(CH_3)_5$	1.85(s)		
$Cp^*_2Ta(=O)bz$	CH_2	2.30(s)		
	C_6H_5	6.5-7.5[a]		
	$C_5(CH_3)_5$	1.80(s)		
	CH_2	1.55(s)		
$Cp^*_2Ta(=CH_2)bz$	$=CH_2$	10.0(s)		
	C_6H_5	7.45(d)		
		7.30(t)		
		6.30(t)		
	[d]$C_5(CH_3)_5$	1.71(s)		
	CH_2	1.60(s)		
$Cp^*_2Ta(=CH_2)bz$	$=CH_2$	9.83(s)		
m-Me	CH_3	2.28(s)		
	C_6H_5	[a]		
	[d]$C_5(CH_3)_5$	1.70(s)	[e]11.6(q)	128
	$C_5(CH_3)_5$		110.2(s)	
	CH_2	1.35(s)		
$Cp^*_2Ta(=CH_2)bz$	$=CH_2$	9.80(s)	239.5(t)	130
p-Me	CH_3	2.28(s)		
	C_6H_5	[a]	150.4(s)	
			140.0(s)	
			131.5(d)	
			129.4(d)	
			128.9(d)	
			127.4(d)	
	[d]$C_5(CH_3)_5$	1.72(s)		
	CH_2	[b]		
$Cp^*_2Ta(=CH_2)bz$	$=CH_2$	9.80(s)		
m-OMe	OCH_3	3.60(s)		
	C_6H_5	[a]		

	[d]$C_5(CH_3)_5$	1.77(s)	[e]11.6(q)	
	$C_5(CH_3)_5$		110.2(s)	
	CH_2	1.42(s)	[b]	
$Cp^*_2Ta(=CH_2)bz$	$=CH_2$	9.82(s)	239.5(t)	131
p-OMe	OCH_3	[b]	6.6(q)	128
	C_6H_5	[a]	[a]	
	[d]$C_5(CH_3)_5$	1.72(s)		
	CH_2	1.42(s)		
$Cp^*_2Ta(=CH_2)bz$	$=CH_2$	9.80(s)		
m-NMe_2	$N(CH_3)_2$	[b]		
	C_6H_5	[a]		
	[d]$C_5(CH_3)_5$	1.72(s)		
	CH_2	1.48(s)		
$Cp^*_2Ta(=CH_2)bz$	$=CH_2$	9.87(s)		
p-NMe_2	$N(CH_3)_2$	2.66(s)		
	C_6H_5	[a]		
	$C_5(CH_3)_5$	1.97(s)	13.7(q)	127
	$C_5(CH_3)_5$	1.77(s)	13.4(q)	127
	$C_5(CH_3)_5$		113.4(s)	
	$C_5(CH_3)_5$		112.4(s)	
$Cp^*_2Ta(=bz)I$	$=CH$	10.82(s)	254.6(d)	123
	C_6H_5	6.5-7.5[a]	155.5(s)	
			129.5(d)	
			126.9(d)	
			123.8(d)	
	$C_5(CH_3)_5$	1.83(s)		
$Cp^*_2Ta(=CH_2)Cl$	$=CH_2$	9.83(s)		
	$C_5(CH_3)_5$	1.85(s)		
$Cp^*_2Ta(=CH_2)Br$	$=CH_2$	10.15(s)		
	$C_5(CH_3)_5$	1.91(s)		
$Cp^*_2Ta(=CH_2)I$	$=CH_2$	10.56(s)		

[a]complex. [b]individual assignments were not made. [c]not observed because of small concentration in equilibrium mixture. [d]recorded on an EM390 spectrometer in toluene-d_8. [e]^{13}C spectrum recorded in dioxane-d_8.

EXPERIMENTAL

General Considerations. All reactions were carried out under an atmosphere of prepurified (passed thru an activated column of molecular sieves and a column of MnO on vermiculite) nitrogen or argon (except where noted) using standard Schlenk,[15] high vacuum line[16] or glove box techniques. "Titanocene" was prepared as described in the literature[17] and stored at -40°C in the nitrogen filled glove box. Ethylene, methylbromide, and carbon monoxide were used as obtained from Matheson Gas Co. Benzene-d_6 (99.5+%) and toluene-d_8 (99.5+%), obtained from Aldrich Chemical Co., were dried over activated 3Å molecular sieves for several hours and degassed by at least three freeze pump thaw cycles and then stored over titanocene until needed. THF-d_8, obtained from Aldrich Chemical Co., was dried and stored over Na/benzophenone. All of the substituted toluenes were used as obtained from Aldrich Chemical Co., except for *p*-xylene which was obtained from MCB Reagents. The potassium-*t*-butoxide was used as obtained from MCB Reagents. Reagent grade petroleum ether (bp 35-60°C), obtained from J.T. Baker Chemical Co., was refluxed over calcium hydride under a nitrogen atmosphere before being collected and degassed. Anhydrous diethyl ether, obtained from J.T. Baker Chemical Co., was stored over $LiAlH_4$ for at least one week before being collected by vacuum transfer. THF and benzene were refluxed over Na/benzophenone until a deep blue color was observed. Reagent grade toluene, obtained from EM Science, was dried by refluxing over Na/K. All other chemicals were used as obtained from Aldrich Chemical Co. Bu_3SnCp^*,[18] $(CH_3)_3P$[19], $(CH_3)_3P{=}CH_2$[20], $(CH_3CH_2)_3P{=}CH_2$[20], $(CH_3)_2Zn$[21], $Cp^*_2TaCl_2$[6b] and Cp_2TaCl_2[22] were prepared according to previously reported procedures. Solvents for reactions carried out using high vacuum techniques were stored over titanocene.

^{1}H-NMR spectra were obtained on either a Bruker WM500 (^{1}H, 500 MHz), a JEOL GLX400 (^{1}H, 399.78MHz; ^{13}C, 100.38 MHz), a JEOL FX90Q (^{1}H, 89.56MHz) or a Varian EM390 (^{1}H, 90 MHz) spectrometer. All ^{13}C-NMR spectra were obtained on the JEOL GLX400. IR

spectra were run on a Beckman 4240 inrfared spectraphotometer. Elemental analyses were provided by the Caltech microanalytical service.

$C_6H_5CH_2K$. A 3 neck round bottom flask equipped with a swivel frit, an addition funnel and a large stirbar was charged with 4.3 g (38 mmoles) of CMe_3OK and ≈35 mL (excess) of dry toluene. After degassing the system, 24 mL (38 mmoles) of n-BuLi (1.6 M in hexane) was added to the addition funnel and slowly added to the stirring suspension. Approximately 15 minutes after the addition of the n-BuLi was complete, the orange solid was collected on the frit. The solvent was removed and petroleum ether was vacuum transferred in and was used to wash the solid several times. 4.7 g (95% yield) of $C_6H_5CH_2K$ was obtained. This product is pyrophoric and also decomposes in the absence of air at room temperature over several weeks.

All of the substituted benzyl potassium reagents in this report were prepared using the same method as described for the parent above. The substituents that were prepared include: *p*-CH_3, *m*-CH_3, *p*-OCH_3, *m*-OCH_3, *p*-$N(CH_3)_2$, *m*-$N(CH_3)_2$, *p*-^{t}Bu, 2,4-dimethyl, 2,3,4,5,6-pentamethyl, α-CH_3, and α-$(CH_3)_2$. The substituents that were attempted to be prepared but were unsuccessful include: *p*-CN, *m*-CN, *m*-F, *p*-NO_2, *m*-NO_2, *p*-CF_3, and *m*-CF_3. Some of these substituents reacted violently upon addition of the *n*-BuLi and care should be taken if future attempts are made.

Equilibrium Mixture of 1 and 2. A mixture of $Cp^*_2TaCl_2$ (2.0 g, 3.8 mmoles) and $C_6H_5CH_2K$ (1.25 g, 9.6 mmoles) in ≈50 mL of diethyl ether was stirred for 2 days before the solvent was removed under vacuum. Petroleum ether was then transferred onto the solid residue, stirred and then removed under vacuum. This was to get rid of any remaining diethyl ether. More petroleum ether was added and the orange solution was filtered away from the insoluble salt through a filter stick into another Schlenk flask. The solvent was removed and the resulting solid was pumped on for several hours at ≈60°C to sublime out the organic bibenzyl, $C_6H_5CH_2CH_2C_6H_5$, that is also formed in this reaction. The orange solid was then recrystallized

from petroleum ether to give 1.5 g (73% yield) of the equilibrium mixture of **1** and **2**. Anal. Calcd. for $C_{27}H_{37}Ta$ (MW=542.95): C, 59.76; H, 6.89. Found: C, 59.76; H, 6.83.

All of the substituted benzyl potassium reagents discussed above were treated with $Cp^*_2TaCl_2$ in the same manner as the parent and their elemental analyses are listed below.

Table 11. Elemental analyses of substituted derivatives of **1** and **2**.

		Theoretical			Observed		
Substituent	Formula(MW)	%C	%H	%N	%C	%H	%N
m-CH_3	$C_{28}H_{39}Ta$(556.98)	60.38	7.07		60.85	7.07	
p-CH_3	$C_{28}H_{39}Ta$(556.98)	60.38	7.07		61.80	7.28	
m-OCH_3	$C_{28}H_{39}OTa$(572.98)	58.69	6.87		61.75	6.73	
p-OCH_3	$C_{28}H_{39}OTa$(572.98)	58.69	6.87		53.04	6.55	
m-$N(CH_3)_2$	$C_{29}H_{42}NTa$(586.02)	59.43	7.24	2.39	59.71	7.19	3.33
p-$N(CH_3)_2$	$C_{28}H_{42}NTa$(586.02)	59.43	7.24	2.39	59.34	7.16	2.29

$Cp^*_2Ta[o\text{-}CH_2C_6(CH_3)_4CH_2](H)$. The same procedure was used as described in the synthesis of **1** and **2** except that $(CH_3)_5C_6CH_2K$ was added to $Cp^*_2TaCl_2$ in diethyl ether.

exo-$Cp^*_2Ta(CH_2{=}CHC_6H_5)(H)$. The same procedure was used as described in the synthesis of **1** and **2** except that $C_6H_5CH(CH_3)K$ was added to $Cp^*_2TaCl_2$ in diethyl ether. Only an impure red oil (at room temperature) was ever obtained as the result of this synthesis. The impurity in this reaction has not been identified at this time.

endo-$Cp^*_2Ta(C_6H_5CH{=}CH_2)(H)$. This compound was not isolated and was only observed in the ^{1}H-NMR upon heating a sample of the exo isomer prepared as discussed above. This *endo* isomer is also obtained upon thermolysis of $Cp^*_2Ta(=CH_2)CH_2C_6H_5$ or as described in the literature.[6b]

$Cp^*_2Ta(CH_2C_6H_5)(CO)$. Excess CO was reacted with a stirring solution of the equilibrium mixture of **1** and **2** in petroleum ether. The solution immediately turned green and

after ≈10 minutes the volume of the solution was reduced and the green precipitate $Cp^*_2Ta(CH_2C_6H_5)(CO)$ was collected. This reaction is quantitative by ^{1}H-NMR. Anal. Calcd. for $C_{28}H_{37}OTa$ (MW=570.55): C, 58.94; H, 6.55. Found: C, 58.43; H, 6.58.

$Cp^*_2Ta(CH_2C_6H_5)(CNCH_3)$. Excess $CNCH_3$ was vacuum transferred into a sealable NMR tube containing ≈30 mg of the equilibrium mixture of **1** and **2** in benzene-d_6 (or toluene-d_8). The color of the solution changed from orange to red.

$Cp^*_2Ta(CH_2C_6H_5)(=O)$. An excess of styreneoxide (9 μl, 0.75 mmoles) was added *via* syringe to a septum capped NMR tube containing the equilibrium mixture (27 mg, 0.05 mmoles) in ≈0.5 mL of benzene-d_6. The reaction was monitored by ^{1}H NMR and was complete after 3 hours producing $Cp^*_2Ta(=O)CH_2C_6H_5$ and styrene. The product was not isolated, but was spectroscopically identical to an independently prepared sample (by Mark Trimmer) from the reaction of **1** and **2** with N_2O.

$Cp^*_2Ta(CH_2C_6H_5)(=CH_2)$. A slight excess of $(CH_3)_3P=CH_2$ or $(CH_3CH_2)_3P=CH_2$ was added to a solution of the equilibrium mixture of **1** and **2** in petroleum ether. After approximately 8 hours the ^{1}H-NMR spectrum shows that the reaction has gone to completion (quantitative by ^{1}H-NMR). The volatiles are removed under vacuum and the orange product $Cp^*_2Ta(CH_2C_6H_5)(=CH_2)$ is recrystallized from petroleum ether. Anal. Calcd. for $C_{28}H_{39}Ta$ (MW=556.62): C, 60.38; H, 7.07. Found: C, 54.54; H, 6.43.

All of the substituted benzyl derivatives of $Cp^*_2Ta(CH_2C_6H_5)(=CH_2)$ were prepared in a manner directly analogous to the procedure described for the parent.

Reaction of 1 and 2 with $Ph_3P=CH_2$. A sealable NMR tube was charged with 25 mg (0.046 mmoles) of the equilibrium mixture of **1** and **2** and 19 mg (0.069 mmoles) of $Ph_3P=CH_2$ in toluene-d_8 (and Cp_2Fe as an internal reference). After 10 hours at room temperature only a very small amount of $Cp^*_2Ta(CH_2C_6H_5)(=CH_2)$ was observed in the ^{1}H-NMR

spectrum. Heating the sample to 50°C resulted in many products being formed, but only very little of the desired product.

$Cp^*_2Ta(=CHC_6H_5)(I)$. A slight excess of CH_3I was admitted to a Schlenk flask containing 0.5 g (0.92 mmoles) of the equilibrium mixture of **1** and **2** in ≈30 mL of petroleum ether. After several minutes a precipitate formed and 0.43 g of $Cp^*_2Ta(=CHC_6H_5)(I)$ was collected (72% yield). Anal. Calcd. for $C_{27}H_{36}ITa$ (MW=668.84): C, 48.48; H, 5.44. Found: C, 48.69; H, 5.44.

$Cp^*_2Ta(=CH_2)Cl$. $Cp^*_2Ta(=CH_2)H$ (30 mg, 0.6 mmoles) was dissolved in C_6D_6 an NMR tube in the glovebox. Chlorobenzene (6.6 μl, 0.6 mmoles) was added *via* syringe through the septum capped tube. The reaction was monitored by ^1H NMR and was complete within 2 hours at room temperature.

$Cp^*_2Ta(=CH_2)Br$ and $Cp^*_2Ta(=CH_2)I$ were prepared by a procedure directly analogous to $Cp^*_2Ta(=CH_2)Cl$ described above and were not isolated.

Reaction of Cp_2TaCl_2 with $C_6H_5CH_2K$. Cp_2TaCl_2 (100 mg, 0.26 mmoles) was reacted with $C_6H_5CH_2K$ (85 mg, 0.65 mmoles) in diethyl ether for 3 days (the reaction looked the same after three days as it did after 3 hours). The solvent was removed under vacuum and toluene was transferred in. The orange solution was filtered through a filter stick away from the insoluble precipitate. The volume of the solution was reduced and the flask was placed in the -78°C freezer to induce precipitation. Unfortunately, no precipitate was observed, so the remaining solvent was removed and the ^1H-NMR spectrum recorded. Only a small amount of something that might have been an alkylidene product was observed.

Reaction of Cp_2TaCl_2 with $C_6H_5CH_2MgCl$. 0.33 mL (0.65 mmoles) of $C_6H_5CH_2MgCl$ (2.0 M in THF) was syringed into a Schlenk flask containing a stirring suspension of 100 mg (0.26 mmoles) of Cp_2TaCl_2 in ≈20 mL of diethyl ether. The solvent was removed after 1 hour.

Toluene was transferred onto the solid and the resulting orange solid was filtered through a filter stick into another Schlenk flask where the volume of the solution was reduced. 21 mg of a microcrystalline red-brown solid was obtained. The ^{1}H-NMR spectrum of this solid showed resonances due to the residual solvent and TMS only.

Low Temperature Coalescence. A sealable NMR tube containing ≈30 mg of the equilibrium mixture of 1 and **2** and ≈0.5 mL of toluene-d_8 was cooled down to -70 °C in the NMR probe and the spectrum recorded. On all three field strengths -70 °C was used as the slow exchange limit spectra and the difference (in hertz) between the singlets of the Cp^* resonances of 1 was used as $\Delta\nu$. The sample was slowly warmed in the probe until coalescence of the Cp^* resonance of 1 was observed. At this point, the sample containing 1 and **2** was removed and a sample containing methanol was placed in the probe. The methanol was given only one pulse and the spectrum recorded. The difference (in hertz) between the two resonances of methanol was used to calculate the temperature of the probe.

Monitoring Temperature Dependance in the ^{1}H-NMR. The same sample used to obtain the coalescence temperature was used to monitor the temperature dependence of the equilibrium. The spectrum was recorded every 10 degrees from -60 °C to 80 °C. Spectra below -30 °C and above 60 °C could not be used in calculating the equilibrium constant because the peaks were too broad.

Monitoring Kinetics of Benzyl Migration By ^{1}H-NMR. In a typical experiment, a slight excess of $(CH_3)_3P{=}CH_2$ was added to a solution of 25 mg (0.046 mmoles) of the equilibrium mixture of 1 and **2** and 17 mg (0.092 mmoles) of Cp_2Fe (as an internal standard) in ≈0.5 mL of C_6D_6 in a sealable NMR tube. After 8 hours at room temperature (or 1 hour at 60 °C) the volatiles were removed from the reaction mixture. Toluene-d_8 was condensed in and the ^{1}H-NMR spectrum recorded. The NMR tube was then placed in a constant temperature bath for

a measured period of time the ^{1}H-NMR spectrum recorded. The reaction was monitored over at least 3 half-lives and between 11 and 24 data points were taken.

Low Temperature Photolyses. A sealed NMR tube containing $Cp^*_2Ta(CH_2C_6H_5)(CO)$ in toluene-d_8 and a separate tube containing the equilibrium mixture of **1** and **2** in toluene-d_8 was placed in a Pyrex dewar filled with dry ice/acetone. These samples were irradiated for 2 hours and then transferred to a dewar at -196°C. The samples were removed from the l-N_2 and immediately placed in the probe which was at -75°C. The ^{1}H-NMR spectra were recorded and no change was observed for either sample.

REFERENCES

1. Collman, J.; Hegedus, L.; Norton, J.; Finke, R. *Principles and Applications of Organotransition Metal Chemistry*; University Science Books:Mill Valley, California, 1987.

2. (a) Cooper, N.J.; Green, M.L.H. *J. Chem. Soc., Chem. Commun.* **1974**, 208. (b) Cooper, N.J.; Green, M.L.H. *J. Chem. Soc., Chem. Commun.* **1974**, 761. (b) Cooper, N.J.; Green, M.L.H. *J. C. S. Dalton Trans.* **1979**, 1121.

3. Turner, H.; Schrock, R.; Fellmann, J.; Holmes, S. *J. Am. Chem. Soc.* **1983**, *105*, 4942; and references therein.

4. Herrmann, W. *Angew. Chem., Int. Ed. Engl.* **1982**, *21*, 117.

5. (a) Kleitzein, H.; Werner, H.; Serhadli, P.; Ziegler, M. *Angew. Chem., Int. Ed. Engl.* **1983**, *22*, 46. (b) Jernakoff, P.; Cooper, N. *J. Am. Chem. Soc.* **1984**, *106*, 3026. (c) Thorn, D.; Tulip, T. *J. Am. Chem. Soc.* **1981**, *103*, 5984.

6. (a) Trimmer, M. Ph.D. Thesis, California Institute of Technology, 1989. (b) Gibson, V.; Bercaw, J.; Bruton, W.; Sanner, R. *Organometallics* **1986**, *5*, 976. (c) Parkin, G.; van Asselt, A.; Leahey, D.; Whinnery, L.; Hua, N.; Schaefer, W.; Marsh, R.; Santarsiero, B.; Bercaw, J. to be submitted to *Inorg. Chem.* (d) van Asselt, A.; Trimmer, M.; Henling, L.; Bercaw, J. *J. Am. Chem. Soc.* **1988**, *110*, 8254. (e) van Asselt, A.; Burger, B.; Gibson, V.; Bercaw, J. *J. Am. Chem. Soc.* **1986**, *108*, 5342.

7. Lauher, J.; Hoffmann, R. *J. Am. Chem. Soc.* **1976**, *98*, 1729.

8. Changing the value of the temperature by 20K in either direction did not increase the correlation to an appreciable extent.

9. Hitchcock, P.; Lappert, M.; Milne,C. *J. Chem. Soc., Dalton Trans.* **1981**, 180.

10. Trimmer, M. Ph.D. Thesis, California Institute of Technology, 1989.

11. (a)Johnson, L.; Grubbs, R. private communication. (b) Gibson, V.; Bercaw, J.; Bruton, W.; Sanner, R. *Organometallics* **1986**, *5*, 976.

12. Collman, J.; Hegedus, L.; Norton, J.; Finke, R. *Principles and Applications of Organotransition Metal Chemistry*; University Science Books:Mill Valley, California, 1987.

13. Threlkel, R.S.;Bercaw, J.E. *J. Am. Chem. Soc.* **1981**, *103*, 2650.

14. (a) Doherty, N.; Bercaw, J. *J. Am. Chem. Soc.* **1985**, *107*, 2670. (b) Burger, B.; Santarsiero, B.; Trimmer, M.; Bercaw, J. *J. Am. Chem. Soc.* **1988**, *110*, 3134.

15. Shriver, D. "The Manipulation of Air-Sensitive Materials"; McGraw-Hill Book Company: New York, New York, **1969**.

16. Burger, B.; Bercaw, J. "New Developments in the Synthesis, Manipulations and Characterization of Organometallic Compounds"; *ACS Symp. Ser.*, in press.

17. Marvich, R.; Brintzinger, H. *J. Am. Chem. Soc.* **1971**, *93*, 2046.

18. Sanner, R.; Carter, S.; Bruton, W. *J. Organomet. Chem.* **1982**, *240*, 157.

19. Sharp, P. *Organometallics* **1984**, *3*, 1217.

20. Wolfsberger, W.; Schmidbauer, H. *Synth. React. Inorg. Met-Org. Chem.* **1974**, *4*, 149.

21. Moore, E.J. Ph.D. Thesis, California Institute of Technology, **1984.**

22. Cp_2TaCl_2 Prep.

Appendix 3. X-ray crystal structure data for $Cp^*_2Ta(=CH_2)CH_2C_6H_5$.

Table 10. Crystal and intensity collection data for $Cp^*_2Ta(=CH_2)CH_2C_6H_5$.

Formula: $TaC_{28}H_{39}$	Formula Weight: 556.56
Crystal Color: orange	Habit: tabular
$a = 8.514(3)$ Å	$\alpha = 95.14(4)°$
$b = 10.049(4)$ Å	$\beta = 95.12(4)°$
$c = 15.491(12)$ Å	$\gamma = 113.03(2)°$
$v = 1203.6(11)$ Å^3	$z = 2$
$\lambda = 0.7107$ Å	Density 1.536 gm cm^{-3}
Graphite monochromator	T: 21°
Space group: P1	Absences: none
Crystal Size: $0.11 \times 0.31 \times 0.64$ mm	$\mu = 48.25$ cm^{-1} ($\mu r_{max} = 1.74$)
$P2_1$ Diffractometer	θ-2θ scan
2θ range: 2°-50°	Octants collected: $\pm h, \pm k, \pm l$

Number reflections measured: 9142

Number of independent reflections: 4132

Number with $F_o^2 > 0$: 4075

Number with $F_o^2 > 3\sigma(F_o^2)$: 3794

Goodness of fit for merging data: 1.19

Final R-index: 0.0274 (0.0249 for $F_o^2 > 3\sigma(F_o^2)$)

Final goodness of fit: 2.12

Table 11. Final parameters for $Cp^*_2Ta(=CH_2)CH_2C_6H_5$.

x, y, z and U_{eq}[a] $\times 10^4$

Atom	x	y	z	U_{eq}
Ta	224(.2)	1971(.2)	2630(.1)	291(.4)
Cp1	2419(5)	2806(5)	1639(3)	399(10)
Cp2	1017(6)	3123(5)	1300(3)	402(10)
Cp3	905(6)	4208(5)	1893(3)	455(10)
Cp4	2193(6)	4557(5)	2610(3)	443(11)
Cp5	3170(5)	3710(5)	2446(3)	411(10)
Me1	3152(7)	1863(6)	1165(4)	572(12)
Me2	19(7)	2619(6)	398(3)	604(15)
Me3	−155(7)	5080(6)	1754(4)	652(14)
Me4	2675(8)	5849(6)	3299(4)	685(16)
Me5	4908(6)	3994(6)	2917(4)	616(15)
Cp6	−1351(5)	396(5)	3675(3)	416(10)
Cp7	−11(6)	−60(5)	3512(3)	442(10)
Cp8	1553(6)	1094(6)	3815(3)	463(11)
Cp9	1231(6)	2286(5)	4194(3)	456(11)
Cp10	−572(6)	1844(5)	4107(3)	420(10)
Me6	−3240(6)	−588(6)	3555(4)	614(14)
Me7	−249(9)	−1602(6)	3231(4)	669(15)
Me8	3262(7)	950(7)	3871(4)	736(16)
Me9	2486(7)	3595(7)	4799(4)	724(17)
Me10	−1495(8)	2699(7)	4514(4)	685(15)
CM	−2000(6)	2179(5)	2433(3)	463(10)
C1	−667(6)	−56(5)	1595(3)	426(10)
C2	−2507(6)	−1167(5)	1372(3)	442(11)
C3	−3855(7)	−770(6)	1145(4)	612(14)
C4	−5509(7)	−1790(8)	872(4)	785(19)
C5	−5886(8)	−3245(8)	826(4)	842(21)
C6	−4586(10)	−3678(6)	1032(4)	810(21)
C7	−2904(7)	−2658(5)	1300(4)	576(14)

[a] $U_{eq} = \frac{1}{3}\sum_i \sum_j [U_{ij}(a_i^* a_j^*)(\vec{a}_i \cdot \vec{a}_j)]$

Table 12. Anisotropic displacement factors x 10^4 for $Cp^*_2Ta(=CH_2)CH_2C_6H_5$.

Atom	U_{11}	U_{22}	U_{33}	U_{12}	U_{13}	U_{23}
Ta	265(1)	294(1)	312(1)	120(1)	37(1)	2(1)
Cp1	385(22)	351(22)	448(26)	113(19)	168(19)	50(19)
Cp2	398(23)	369(22)	401(25)	116(19)	47(19)	44(19)
Cp3	471(25)	405(24)	571(31)	220(21)	186(22)	156(22)
Cp4	461(25)	347(23)	482(28)	125(20)	98(21)	−3(20)
Cp5	343(22)	426(24)	413(26)	106(19)	50(19)	34(20)
Me1	558(29)	532(29)	662(35)	239(25)	264(26)	−5(25)
Me2	709(35)	630(33)	388(29)	179(28)	−7(24)	149(25)
Me3	670(35)	541(31)	898(45)	353(28)	193(31)	269(30)
Me4	814(39)	390(27)	721(41)	145(27)	117(31)	−132(26)
Me5	331(24)	816(38)	635(36)	158(25)	33(23)	140(30)
Cp6	371(23)	499(26)	390(25)	166(20)	98(19)	110(21)
Cp7	541(27)	457(25)	389(26)	269(22)	27(21)	73(20)
Cp8	390(24)	632(30)	428(27)	258(23)	69(20)	115(23)
Cp9	418(24)	493(26)	386(26)	125(21)	20(19)	20(21)
Cp10	445(24)	510(26)	340(24)	225(21)	97(19)	31(20)
Me6	404(26)	662(34)	672(37)	76(25)	105(24)	184(28)
Me7	1017(45)	538(31)	598(36)	457(32)	80(31)	166(27)
Me8	553(32)	1067(48)	820(44)	532(35)	102(30)	313(37)
Me9	615(34)	819(41)	465(33)	53(30)	−40(26)	−58(29)
Me10	822(40)	906(43)	494(33)	534(36)	174(29)	−28(30)
CM	419(24)	490(26)	537(30)	253(22)	17(21)	66(22)
C1	418(23)	360(22)	453(27)	125(19)	61(20)	−28(20)
C2	512(26)	396(24)	330(24)	104(21)	55(20)	−23(19)
C3	555(31)	566(32)	603(35)	172(26)	−49(25)	−100(26)
C4	484(31)	930(49)	709(43)	134(32)	−62(28)	−193(36)
C5	605(38)	824(47)	648(42)	−153(35)	57(31)	−42(35)
C6	978(51)	456(32)	641(41)	−97(33)	148(36)	71(28)
C7	743(35)	384(26)	483(31)	106(25)	91(26)	23(22)

The form of the displacement factor is:

$$\exp -2\pi^2(U_{11}h^2a^{*2} + U_{22}k^2b^{*2} + U_{33}\ell^2c^{*2} + 2U_{12}hka^*b^* + 2U_{13}h\ell a^*c^* + 2U_{23}k\ell b^*c^*)$$

Table 13. Hydrogen parameters for $Cp^*_2Ta(=CH_2)CH_2C_6H_5$.

x, y and $z \times 10^4$

Atom	x	y	z	B
H1C1	−242(63)	475(53)	1002(33)	4.8(11)
H2C1	163(63)	−592(54)	1726(33)	4.9(12)
HC3	−3688(69)	280(58)	1239(36)	5.6(13)
HC4	−6447(84)	−1463(73)	685(43)	8.3(18)
HC5	−7111(116)	−3882(99)	551(59)	13.6(29)
HC6	−4724(77)	−4609(65)	989(40)	7.2(16)
HC7	−1961(54)	−2966(46)	1484(28)	3.3(9)
H1M1	3966(92)	2283(77)	963(48)	8.9(19)
H2M1	2315(76)	1040(64)	697(39)	6.5(15)
H3M1	3617(80)	1371(69)	1573(43)	7.3(16)
H1M2	208(74)	3282(60)	71(37)	6.2(14)
H2M2	−1284(79)	2196(66)	400(40)	7.0(15)
H3M2	−51(88)	1567(72)	85(46)	8.4(18)
H1M3	693(90)	6180(74)	1761(46)	8.5(18)
H2M3	−732(87)	5406(74)	2352(47)	8.5(19)
H3M3	−936(62)	4681(52)	1208(33)	4.7(11)
H1M4	3746(86)	5961(73)	3602(45)	8.6(19)
H2M4	1646(75)	5779(64)	3532(40)	6.9(15)
H3M4	2928(72)	6785(60)	2970(38)	6.2(14)
H1M5	5670(89)	4692(77)	2644(48)	9.1(20)
H2M5	5263(65)	3069(57)	2904(36)	5.3(12)
H3M5	5104(82)	4160(71)	3529(44)	7.9(17)
H1M6	−3594(102)	−1262(89)	4014(55)	11.0(24)
H2M6	−3679(84)	−1217(74)	3056(47)	8.4(18)
H3M6	−4003(94)	−140(81)	3501(50)	9.5(20)
H1M7	683(82)	−1544(67)	2811(42)	7.1(16)
H2M7	−1368(105)	−2235(85)	2913(54)	11.2(24)
H3M7	−285(87)	−2100(72)	3734(47)	8.1(18)
H1M8	4050(86)	1623(76)	4281(45)	8.6(18)
H2M8	3320(67)	518(57)	3243(36)	5.6(13)
H3M8	3126(76)	146(66)	4272(39)	6.9(15)
H1M9	3381(70)	3866(59)	4625(37)	6.0(13)
H2M9	2649(87)	3213(75)	5431(45)	8.5(18)
H3M9	1889(95)	4365(77)	4877(48)	9.3(20)
H1M0	−633(125)	3876(102)	4468(61)	13.7(30)
H2M0	−1369(95)	2665(81)	5106(50)	9.7(21)
H3M0	−2546(102)	2537(85)	4155(52)	10.4(23)
H1CM	−2195(45)	2773(38)	2087(24)	1.9(7)
H2CM	−3113(59)	1728(50)	2760(32)	4.3(11)

Appendix 4. LeRoy's complete packing list.

CLOTHING / GEAR

- ——— 2 Pair Wool Socks (or cotton)
- ——— 2 Pair polypropylene liners
- ——— Hat with rim / sunglasses
- ——— Gloves-optional
- ——— Ski Cap (for sleeping)
- ——— "Flannel" shirt-opt
- ——— Long Pants
- ——— Polypropylene thermalwear
- ——— Rain Garment(s)
- ——— Comfortable dayvear (2 shorts, 2 light shirts, 2 underwears)
- ——— Sleeping pad / Thermarest
- ——— Warm Jacket
- ——— Pillow Case (to make pillow)
- ——— Sleeping Bag with stuff sack
- ——— Towel (washcloth-opt)
- ——— Plastic trash bags(for trash and rain protection)
- ——— Bowl/cup/spoon/scoop cup
- ——— Share of Group Equipment
- ——— Sneakers
- ——— Daypack-opt
- ——— Extra Ziplock Bags
- ——— Bandana
- ——— **BOOZE** (≈500mL) + mixer
- ——— Deodorant
- ——— Replacement clips and pins
- ——— Fire Ribbon
- ——— Whistle
- ——— Money ($20-40) + change

MISCELLANEOUS (cont.)

- ——— 2 Flashlight 4 batteries + spare bulb)
- ——— Insect Repellent-DET
- ——— Iodine (for water purification)
- ——— 2 Pocket Knifes
- ——— Matches in Nalgene bottle
- ——— Topo Map(s)/Compass
- ——— Sunscreen (lots o'hν @ 10,000 ft)
- ——— Chapstick
- ——— 2-1Liter Water Bottles
- ——— **Toilet Paper** (full roll)
- ——— Toothbrush / paste
- ——— Campsoap (bring, but don't use)
- ——— Trowel
- ——— Rope (75 Ft)
- ——— **M + M's**
- ——— Wire
- ——— Fishing Gear (license)
- ——— Paperback Book
- ——— Needle/thread/safety pins
- ——— Trail description
- ——— Camera / film
- ——— Pack cover
- ——— Moleskin/Bandages/First Aid
- ——— Snacks
- ——— Candle
- ——— 1/2 ground cloth
- ——— 1 gallon poly jug
- ——— Pencil/paper
- ——— ID (drivers or fishing license)

NOTES

Rainproof everything

-All stuff sacks

-Pack cover

-Backpack

Put everything possible in a Ziplock

Kidney beans must be COMPLETELY cooked

Change of clothes for ride home

If renting tent assemble it before you leave

OBVIOUS THINGS

—— Backpack
—— Good Hiking Boots
—— Tent + poles
—— Stove/Fuel bottle(s)
—— Sleeping Bag
—— Cooking Pots
—— Water Filter
—— DET

GOOD SNACKS

—— M + M's
—— Nuts
—— Trail Mix (2 lbs/wk)
—— Raisins
—— Granola (bars)
—— Dried fruit (Apples, apricots, *etc.*)
—— Satrbursts
—— Carrots

GENERAL GROUP EQUIPMENT

—— Cooking oil (squeeze jiz)
—— **Coffee**
—— Sugar
—— Salt + pepper
—— Cooking pots
—— Stove (s) + fuel bottle(s)
—— Powdered milk
—— Water filter

LUNCH

—— Peanut Butter
—— Jelly
—— Cheese
—— Crackers
—— Bagels-opt
——

FIRST AID

—— Ace Bandage
—— Band-Aids
—— Thin (white) Moleskin
—— Second skin
—— Slip Tape
—— Kit (Antiseptic, bandages, smelling salts, alcohol, *etc.*)

BREAKFAST

——— Oatmeal (1 pkg/day)
——— Granola Bar
——— Coffee
——— Cereal/milk

MISC MEDICATIONS

——— Alergy meds.
——— Benedryl
——— Asthema med.
——— ROLAIDS
——— Pepto tabs
——— Synthroid
——— Tylenol
——— Vitamins

THE ALL BAG

——— Bunji cords
——— Straps
——— Duct tape
——— Matches
——— Batteries
——— Safety pins
——— Nail clippers
——— Wire
——— Carbener
——— Flashlight bulb
——— Needle + Thread
——— Extra knife